# Characterizing the Interaction of the ATP Binding Cassette Transporters (G subfamily) with the Intracellular Protein Lipid Environment

Sonia Gulati

Submitted in partial fulfillment of the requirements for the degree of Doctor of Philosophy under the Executive Committee of the Graduate School of Arts and Sciences

**Columbia University**

**2011**

## Abstract

### Characterizing the Interaction of the ATP Binding Cassette Transporters (G subfamily) with the Intracellular Protein Lipid Environment

Sonia Gulati

Cholesterol is an essential molecule that mediates a myriad of critical cellular processes, such as signal transduction in eukaryotes, membrane fluidity, and steroidogenesis. As such it is not surprising that cholesterol homeostasis is tightly regulated, striking a precise balance between endogenous synthesis and regulated uptake/efflux to and from extracellular acceptors. In mammalian cells, sterol efflux is a key component of the homeostatic equation and is mediated by members of the ATP binding cassette (ABC) transporter superfamily.

ATP-binding cassette (ABC) transporters represent a group of evolutionarily highly conserved cellular transmembrane proteins that mediate the ATP-dependent translocation of substrates across membranes. Members of this superfamily, ABCA1 and ABCG1, are key components of the reverse cholesterol transport pathway. ABCG1 acts in concert with ABCA1 to maximize the removal of excess cholesterol from cells by promoting cholesterol efflux onto mature and nascent HDL particles, respectively. To date, mammalian ABC transporters are exclusively associated with efflux of cholesterol. In *Saccharomyces cerevisiae*, we have demonstrated that the opposite (i.e inward) transport of sterol in yeast is also dependent on two ABC transporters (Aus1p and Pdr11p). This prompts the question what dictates directionality of sterol transport by ABC transporters. The main focus of this study is to define the parameters that result in sterol movement across membranes. The comparison between these contrasting states (outward v. inward transport of the same substrate) will allow us to dissect whether sterol transport across the plasma membrane is defined by the molecule (i.e. the ABC transporter) or by microenvironment (i.e. the status of other proteins and lipids) in which it resides.

We have developed the model eukaryote *Saccharomyces cerevisiae* as a tool to understand the mechanisms that influence ABC-transporter mediated

movement of sterols. Specifically, we expressed murine ABCG1 (mABCG1) in yeast and assessed how changes in the intracellular sterol environment affect movement of sterols by this transporter. We found that expression of mABCG1 is able to vary (both increase and decrease) the concentration of exogenous sterols in the cell in response to intracellular sterol changes. We also found that yeast members of the ABCG subfamily, Aus1p and Pdr11p are able to promote either influx of cholesterol or efflux of a cholesterol derivative depending on the sterol context of the cell. This is the first example of an ABC transporter mediating bi-directional transport. These data suggest that direction of transport is not a static property of the transporter but rather can adapt in response to changes in the intracellular microenvironment.

In addition to sterols we also found that proteins in the microenvironment may also influence direction of transport. Specifically, we found that the yeast sterol esterifying enzyme Are2p, physically interacts with the ABC transporters Aus1p and Pdr11p. Furthermore, all three proteins were found to co-localize to detergent resistant membrane microdomains. Deletion of either ABC transporter resulted in Are2p re-localization from DRMs to a detergent soluble fraction as well as a significant decrease in the percent of sterol esterified. This phenomenon is evolutionarily conserved in the murine lung where ABCG1 and ACAT1 were observed to co-localize with flotillin-1, a marker of DRMs. We propose that co-localization and complex formation of sterol esterification enzymes and ABC transporters in DRMs reflects a novel mechanism that directs membrane sterols to the esterification reaction.

The studies presented in this thesis provide evidence that direction of transport is not a static inherent property of the transporter, but rather that it is mutable and influenced by surrounding sterols and proteins. The data provided here offers further insight as to how ABC transporters move cholesterol from the membrane and therefore may provide a platform for innovative strategies to combat atherosclerosis.

## Table of Contents

**List of Tables and Figures**

**Chapter 1**



**Chapter 2**



**Chapter 3**

**Chapter 4**

List of Abbreviations

| | |
|---|---|
| ACAT | Acyl-CoA acyltransferases |
| ABC | ATP Binding Cassette |
| ARE | ACAT-related enzyme |
| ATP | Adenosine Triphosphate |
| BHK | Baby hamster kidney |
| Cdx2 | caudal type homeobox transcription factor 2 |
| Co-IP | Co-Immunoprecipitation |
| CSM | Complete Synthetic Medium |
| Cub | C-terminal Ubiquitin |
| DAmp | Decreased Abundance by mRNA Perturbation |
| DGAT | Diacylglycerol Acyltransferase |
| DRM | Detergent resistant microdomain |
| DSP | Dithiobis[succinimidyl propionate] |
| DUP | Duplicated gene family |
| ER | Endoplasmic Reticulum |
| GFP | Green Fluorescent Protein |
| HA | Human influenza hemagglutinin |
| HDL | High-density lipoprotein |
| HNF1$\alpha$ | Hepatocyte Nuclear Factor 1alpha |
| LDL | Low-density lipoprotein |
| LDLR | Low-density lipoprotein receptor |
| LXR | Liver X Receptor |
| MATLAB | Matrix Laboratory |
| Nub | N-terminal Ubiquitin |

| | |
|---|---|
| OD | Optical Density |
| PC | phosphotidylcholine |
| PBS | Phosphate Buffered Saline |
| PM | Plasma Membrane |
| PMSF | Phenylmethylsulphonylfluoride |
| SCD | Synthetic Complete Dextrose |
| SDS | Sodium Dodecyl Sulfate |
| SREBP | Sterol Regulatory Element Binding Proteins |
| SM | Sphingomyelin |
| TLC | Thin Layer Chromatography |
| UPC | Uptake Control |
| UPR | Unfolded Protein Response |
| VLDL | Very low-density lipoprotein |
| VPS | Vacuolar Protein Sorting |
| Y2H | Yeast Two Hybrid |
| YFP | Yellow Fluorescent Protein |
| X-Gal | 5-bromo-4-chloro-3-indolyl-ß-D-galactoside |
| YPD | Yeast extract, Peptone, and Dextrose |

**Acknowledgments**

I would like to thank the numerous people who not only contributed to my dissertation work but also my professional growth and education. First I would like to thank my mentor, Dr. Stephen Sturley for his immeasurable support and enthusiasm for science. He provided me with both the intellectual freedom to pursue my own scientific goals and the guidance to think critically about them. His kindness, generosity, and support were essential for my success during my tenure in his laboratory. I would also like to thank the members of the Sturley lab (Caryn, Andy, Kelly, Moneek, Aaron, Christine, James, and Matthew) for the endless laughs, their support, and friendship. I would like to especially thank Kelly Ruggles for helping me with Matlab analysis and Excel. I am also grateful for the support from the faculty and staff of the IHN. I appreciate the time and help they have provided in helping me to achieve this body of work.

Finally, I would like to thank my family for supporting all of my pursuits. They made me the person I am today. I would like to thank my parents for teaching me the value of hard work and a wonderful education. I would also like to thank my brother and sister-in-law whose love, support, and endless supply of cable TV got me through my graduate career. I would also like to thank my nephews, Devin and Currin, for being my greatest cheerleaders. Last I would like to thank my late mother, whose courage, love for her family, and tenacity have inspired me both personally and professionally.

# Chapter 1: An Overview of Sterol Homeostasis in Model Systems

## Preface

The origins of cholesterol research can be traced back to pre-revolutionary France where cholesterol was initially discovered in human gallstones and later purified in 1815 (1). Today, cholesterol has become a household word and easily one of the most studied endogenously synthesized molecules (1). The fascination with cholesterol stems from the fact that it is essential for life but if deregulated, instigates death. Dysregulation of cholesterol metabolism contributes to the pathogenesis of such potentially fatal diseases as atherosclerosis, diabetes, and Alzheimer's (1). Over the last two centuries great strides have been made in elucidating the biosynthesis, metabolism, and regulation of cholesterol (2). However, by no means is cholesterol research complete or depreciating, as many facets of cholesterol metabolism have yet to be illuminated. In this thesis I will expound on one of these facets by characterizing the energy dependent movement of cholesterol across the plasma membrane and its subsequent intracellular distribution.

## Cholesterol Structure and Significance

Cholesterol is an essential lipid present in the membranes of most eukaryotes. It is a seventeen-carbon polycyclic compound consisting of a four ring steroid structure with a hydroxyl group at C3 and a double bond at C5 and C6 (2). In the membrane bilayer, cholesterol is intercalated between the fatty acid chains of neighboring phospholipids, with its polar hydroxyl group adjacent to the phospholipid head groups (3). Cholesterol promotes a liquid ordered phase of the bilayer by modulating fluidity based on the degree of saturation of neighboring fatty acid chains (3). In addition to regulating membrane fluidity, cholesterol serves as an essential precursor for physiologically important metabolites, such as bile acids, steroid hormones, and vitamin D (2).

**Cholesterol in Membranes**

Cholesterol is heterogeneously disseminated across the membranes of the secretory system (4). In human fibroblasts approximately 85% of unesterified cholesterol is found in the plasma membrane, 10% in the endocytic pathway, and 0.5% in the endoplasmic reticulum (ER) (5). Within the plasma membrane cholesterol segregates into regions of membranes with strongly hydrated large head groups, like those found in sphingolipids, to form liquid-ordered membrane microdomains or lipid rafts (3). Lipid rafts are defined as small (10–200 nm), heterogeneous, highly dynamic, sterol- and sphingolipid-enriched domains that can sometimes be stabilized to form larger platforms through protein-protein and protein-lipid interactions (6). They represent as much as 30% of the plasma membrane and contain twice as much cholesterol and one and a half times the sphingolipids as the surrounding bilayer (7). The coalescence of these lipids into membrane micro-domains, likely functions to enhance the physical structure of the membrane as well as generate foci that integrate pathways such as lipid influx and efflux, protein trafficking, signal transduction, and even viral entry (8).

The concept of lipid rafts presented in 1997, transformed the field of membrane biology, in that it altered the perception that lipids in the bilayer were just structural passive solvents (9). Experimentally however, the study of lipid rafts stagnated due to the inability to define the specific components (lipids and proteins) of rafts or assess with certainty their existence. A major impediment to studying lipid rafts is that they have poorly defined morphology (unlike lipid bound organelles or caveolae) and are too small to resolve via conventional microscopy (10). As such the burden of proof for their existence has relied on the biochemical attributes of these complexes (9). The first working biochemical definition of lipid rafts was suggested by Brown and Rose who reported that cholesterol, sphingolipids, and GPI anchored proteins are insoluble in Triton X-100 at 4°C and floated to a characteristic density following equilibrium density gradient centrifugation (11). Detergent insolubility quickly became the governing principle in determining lipid and protein raft affinity. Although biophysical studies of model

membranes demonstrated that lipids in the liquid-ordered phase are resistant to detergent solubilization, they also showed that treatment of membranes with detergents can create artificial membrane domains (12). This latter point coupled with the observation that raft components may vary based on the concentration and type of detergent utilized became a point of contention in the lipid raft field. Detergent screens have shown that less efficient detergents such as the Brij series, Lubrol, and Tween-20 do produce a distinct, less temperature sensitive, and diminished cholesterol dependent subpopulation of the membrane (13-15). Despite its imperfections, detergent resistance remains the only biochemical means of isolating lipid rafts and has contributed to many breakthroughs in the field (6). Today, data provided by detergent resistance is being corroborated by the findings of such innovative techniques as stimulated emission depletion far-field fluorescence and fluorescence correlation spectroscopy that have been able to detect lipid rafts under physiological conditions (16,17).

**Cholesterol Synthesis and Trafficking**

An estimated 70% of total body cholesterol is derived from de novo synthesis. Cholesterol biosynthesis occurs in all mammalian cells, however this capacity is greatest in liver, adrenal cortex, and reproductive tissues (18). The synthesis of cholesterol is a multi-step process involving nearly 30 enzymes. The rate-limiting step of this pathway HMG-CoA reductase catalyses the formation of mevalonate and is also the target of cholesterol lowering pharmaceuticals such as the statins (2). Mevalonate is then subjected to a series of phosphorylations and a decarboxylation reaction to produce isopentenyl pyrophosphate, an activated isoprenoid molecule. IPP is subsequently converted to squalene, which undergoes cyclization to produce lanosterol. Ultimately, lanosterol is converted to cholesterol through 19 additional reactions (2). Cholesterol metabolism is transcriptionally regulated by sterol regulatory element binding proteins (SREBPs), a group of master regulators that control the feedback regulation of synthesis and uptake of many lipids, at many steps (19). Cleavage of the

membrane associated SREBP protein by two proteases in the Golgi complex releases a soluble amino-terminal transcription factor domain. The domain is then translocated to the nucleus where it activates the transcription of target genes (20). Numerous accessory proteins (SREBP cleavage activating protein SCAP and INSIGs 1 or 2) and proteases (S1p and S2p) mediate the sensing of membrane composition, fluidity, and the subsequent translocation and activation of the transcription factor (19). This process is repressed when cellular sterol concentrations peak; recent studies elegantly describe the manner in which ER cholesterol concentrations greater that 0.5 mol% are sufficient to block ER exit of SREBP and the cholesterol sensor, SCAP (21). Further fine-tuning of cholesterol biosynthesis via post-translational regulation of HMG-CoA reductase is achieved through INSIG1 dependent proteasomal degradation, which also responds to cholesterol levels in the ER (22,23).

Humans also obtain one-third of their total body cholesterol via their diet (24). Dietary cholesterol along with triglycerides are absorbed by enterocytes of the small intestine and packaged into chylomicrons (24). These lipoproteins enter the circulation where they adhere to the inner surface of capillaries of skeletal muscle and adipose tissue. At these tissues, triglyceride distribution occurs first via hydrolysis by lipoprotein lipase. The residual components (including cholesterol) of the chylomicron re-enter circulation and are subsequently taken up the by the liver (24). Like the intestines, the liver generates cholesterol transport carriers called very low-density lipoproteins (VLDL), which resemble chylomicrons both structurally and functionally. In circulation, VLDL undergoes a successive depletion of triglycerides transforming it into a cholesteryl ester-laden remnant particle, known as low-density lipoprotein (LDL). Cholesterol delivery to peripheral tissues is facilitated by the uptake of LDL via the LDL receptor (25). Excess cholesterol in extrahepatic tissues can be transported back to the liver by high-density lipoprotein (HDL) via the reverse cholesterol transport pathway (26). At the liver, cholesterol is secreted into bile (either as cholesterol or after it has

been metabolized to bile acids) that enters the small intestine, where it is either reabsorbed (enterohepatic cycle) or excreted into feces (27).

**Sterol Homeostasis**

A myriad of biological processes work in concert to impart cholesterol homeostasis, including transcriptional regulation of the biosynthetic pathways, translocation of the products between and within membranes, efflux to extracellular acceptors, and catabolism to inert but recoverable storage forms such as steryl esters (28). The following is an overview of some of the key cholesterol homeostatic events with a particular emphasis placed on those aspects (esterification and efflux) that I will explore in this thesis.

**Esterification of sterols**

The esterification of sterols by the acyl-coenzyme A:cholesterol acyl-transferases (ACATs) is a fundamental reaction in eukaryotic cells that is conserved throughout evolution (29). Cholesteryl esters, the products of this reaction can be packaged into lipoproteins or stored in cytosolic lipid droplets as a means to protect the cell from cholesterol toxicity (29). In mammalian cells, the ACAT gene family is tripartite, consisting of ACAT1, ACAT2 and DGAT1 (the latter enzyme esterifies diacylglycerol) (30-32).

ACAT1 Gene and Protein Structure

In humans, *Soat1* (the gene encoding for ACAT1) is located on two different chromosomes, chromosome 1 and 7, with each chromosome containing a distinct promoter. Promoter P1 (located on chromosome 1) is contiguous with exons 1-16 and promoter P7 (located on chromosome 7) is contiguous with the optional long exon, Xa (29,33). Of the known four human *Soat1* splice variants, the 2.8-kb and 3.6kb mRNA contain a short 5' untranslated region and constitute approximately 75% of the total *Soat1* mRNAs that are produced from the P1 promoter. These mRNAs are translated into a single 50 kDa protein band, which

is the major ACAT1 isoform observed in tissue (33). The 4.3-kb *Soat1* mRNA consists of exon Xa and is produced from two different chromosomes by a novel RNA recombination event. This splice variant of human *Acat1* can produce two isoforms, a 50 kDa protein and a minor 56 kDa protein with different enzymatic activities (34). Zhao et al. have shown that the presence of exon Xa, impairs the production of the major isoform of the ACAT1 protein by promoting its mRNA decay. This phenomenon appears to be human specific as the murine *Soat1* gene does not contain the optional exon Xa (34).

Although the exact structure of ACAT1 is unknown, data by Guo et al. suggests that it contains nine transmembrane domains, with the amino terminus located in the cytosol and the carboxyl terminus embedded in the ER lumen (34). ACAT1 is comprised of two putative N-terminal leucine zipper motifs located at aa 47–61 and aa 80–94. Deletion of the former putative leucine zipper results in a functional dimeric form with increased catalytic activity (30). It is unclear whether the latter putative leucine zipper motif participates in the homotetramerization of ACAT1 or if it mediates the interaction with other proteins. Transmembrane domains 7 and 8 contain coiled coil domains that have two distinct functions. One side of the domain promotes subunit interaction whereas the other side is involved in substrate binding and/or enzymatic catalysis (35). Sequences in transmembrane domains 1,2, and 4-6 are highly conserved amongst the ACATs but not the DGAT enzymes, suggesting that these regions may play a role in cholesterol binding (36). Conversely, the motif FYXDWWN (amino acids 403-409 of human ACAT1) and MK*XX*SF (amino acids 265–270 of human ACAT1) are highly conserved amongst all family members, the former maybe involved in fatty acyl-CoA binding and the latter, specifically the serine residue is required for ACAT activity (37). In addition, all members of this enzyme family have a potential tyrosine phosphorylation motif and at least one *N*-linked glycosylation site (38).

ACAT1 cellular and tissue distribution

ACAT1 is a homotetrameric enzyme primarily found in the ER (39). However, this localization is not static, as it changes with varying cell condition. In nonadherent mouse macrophages, 10–15% of ACAT1 immunoreactivity was localized to the cell surface (40). In cholesterol-loaded human macrophages, 20–40% of ACAT1 immunoreactivity was found in small vesicles, observed near the trans-Golgi network and the endocytosis recycling compartment (41).

ACAT1 mRNA is ubiquitously expressed in mammalian tissues with the highest expression levels occurring in the adrenal glands, macrophages, and sebaceous glands, all of which store cholesteryl esters in cytoplasmic droplet (42). Human ACAT1 protein is also found in hepatocytes and Kupffer cells of the liver, neurons, and atherosclerotic lesions (41). Immunodepletion experiments in human tissues have suggested that human ACAT1 accounts for nearly all of the ACAT activity in the liver, adrenal gland, macrophages, and kidney, but only about 20% of the activity in small intestine (43). Murine distribution of ACAT1 is similar to that of the human enzyme, except that it is not the major ACAT isoform in the liver (38).

Biological activity and regulation of ACAT1

ACAT1 catalyzes the formation of an ester bond between the carboxylate group of a fatty acid and the hydroxyl group of cholesterol. In extrahepatic cells, cholesteryl esters generated by ACAT1 are shuttled out of the ER and into cytoplasmic lipid droplets. In hepatocytes, cholesteryl esters are recruited to the ER lumen where they are packaged into the neutral core of a VLDL particle (38). ACAT1 activity accounts for more than 80% of the total ACAT enzyme activity in vitro. ACAT1 is primarily allosterically regulated by its substrates, cholesterol and oxysterols (38). In cholesterol-loaded cells, esterification increased without a concomitant change in expression level of ACAT1 mRNA or protein (44). Allosteric regulation allows ACAT1 to respond rapidly to changes in intracellular

cholesterol levels, suggesting that cholesteryl esterification may be a first-line defense in preventing cholesterol toxicity (29).

Although ACAT1 is mainly regulated allosterically, evidence for transcriptional regulation began to emerge from a study examining how *glucocorticoids* increase the incidence of atherosclerosis (45). This study found that dexamethasone treatment resulted in a 60% increase in ACAT1 activity as well as an increase in *hSoat1* mRNA (45). Consistent with these results it was later found that the *hSoat1* P1 promoter possesses a glucocorticoid response element (29). Other proatherogenic molecules such as the cytokine, interferon-$\gamma$ and the hormone Urotensin-II have also been found to upregulate *hSoat1* expression in macrophages. In addition, atheroprotective agents such as adiponectin and adipocytokine downregulate *hSoat1* expression (29). In the liver, *Soat*1 mRNA expression increased 2-3 fold when mice or rabbits were fed a diet rich in fat and cholesterol (46). The modulation of *hSoat1* mRNA by atherogenic molecules and presence of the ACAT1 protein in atherosclerotic lesions suggests that it may conduce the initiation of athersclerosis (38).

In vivo function of ACAT1

ACAT1 null mice were generated in order to further elucidate the physiological role of ACAT1 and its contribution to the development of atherosclerosis. ACAT1-deficient ($ACAT1^{-/-}$) mice are healthy with normal serum cholesterol, intestinal cholesterol absorption, and hepatic ACAT activity (40). The most profound effects of ACAT1 deficiency was observed in the adrenal gland, testis, and ovary, where ACAT activity was reduced by more than 95% (38). Furthermore, cholesteryl esters were nearly undetectable in the adrenal cortex, ovaries (47), and cultured peritoneal macrophages (38). Despite the loss of ACAT activity and depletion of cholesteryl esters in the adrenal gland, corticosterone synthesis was normal, suggesting a functional redundancy in pathways providing cholesterol for steroidogenesis(38). In addition, cholesteryl

esters were depleted in the meibomian glands resulting in dry eye and a narrowing of the eye opening by age 3-4 weeks, a physical hallmark of ACAT1 deficient mice (47).

To test the hypothesis that ACAT1 activity in macrophages promotes the pathogenesis of atherosclerosis, ACAT1$^{-/-}$mice were crossed with two strains of mice that are susceptible to atherosclerosis: low density lipoprotein receptor-deficient (LDLR$^{-/-}$) mice and apoE-deficient (apoE$^{-/-}$) mice. ACAT1 deficiency in both backgrounds resulted in a significant increase in the deposition of free cholesterol in the skin and in the brain (47). However, the effect of ACAT1 deficiency on the development of atherosclerosis was inconclusive. A study performed by Chiwata et al. found that ACAT1 deficiency was associated with an estimated 50% reduction in aortic root lesions in LDLR$^{-/-}$ mice and did not decrease serum cholesterol levels (48). Conversely, Fazio *et al.* showed that LDLR$^{-/-}$ mice reconstituted with ACAT1$^{-/-}$ macrophages had increased atherosclerotic lesions that contained more free cholesterol and fewer macrophages than control lesions (49). The differences in results may in part be due to different strain background and varying methodology. However, further studies are necessary to clearly delineate if ACAT1 has pathological role in atherosclerosis.

## ACAT2

### ACAT2 gene and protein structure

The retention of normal hepatic ACAT activity in ACAT1$^{-/-}$ mice and the presence of two sterol esterifying ACAT-related enzymes in yeast, suggested that the esterification reaction in higher eukaryotes may also be catalyzed by multiple enzymes. In 1998, three laboratories cloned a gene encoding a second mammalian ACAT (31,50,51). The human ACAT2 gene, *SOAT2*, encodes for a 2.2 kb mRNA and produces a 60 kDA protein, which is 43% identical to ACAT1 (29). In addition to this major isoform, Yao et al have found two human ACAT2

mRNA splice variants, ACAT2b and ACAT2c. Comparable amounts of the alternatively spliced ACAT2 mRNA variants and their corresponding proteins were detected in human liver and intestine cells (52). However, these isoenzymes exhibited a 25%-35% reduction in enzymatic activity as compared to the major isoform, which may attributed to the absence of a phosphorylation site SLLD, found in the major isoform (9).

ACAT2 has a high degree of sequence similarity with ACAT1 near the carboxy terminus and also possesses multiple transmembrane domains (50). However, the actual number of transmembrane domains remains controversial. Both ACAT enzymes share a number of motifs including, the MK*XX*SF consensus sequence, a potential tyrosine phosphorylation site, a leucine zipper motif, and two potential N-linked glycosylation sites (38). The consensus sequence (specifically the serine residue) is essential for ACAT activity and is located in the ER lumen for ACAT2 and in the cytoplasm for ACAT1. This suggests that the active sites of these enzymes reside on opposite sides of the ER membrane (29).

ACAT2 cellular and tissue distribution

ACAT2 is an integral membrane ER protein (50). It is predominantly expressed in the enterocytes of the small intestine and the fetal liver (51). In addition, ACAT2 is also expressed in the human adult liver, although the extent of its expression is contentious. Parini et al. showed that both ACAT1 and ACAT2 are present in hepatocytes and in 75% of the liver samples examined, ACAT2 was responsible for more than 50% of the total ACAT activity (53). Conversely, Smith et al., demonstrated that on average ACAT1 mRNA was nine-fold more abundant than ACAT2 mRNA in hepatocytes. They also found that ACAT1 mRNA levels were far more constant, whereas ACAT2 mRNA levels fluctuated (54). Additionally, elevated levels of ACAT2 mRNA have been observed in a subpopulation of patients with hepatocellular carcinoma. In contrast to humans, it is established that ACAT2 is the major isoform in murine liver (29).

Biological activity and regulation of ACAT2

ACAT2, like ACAT1, catalyzes the esterification of cholesterol with fatty acids. Specifically, in the small intestine, ACAT2 esterifies the cholesterol absorbed by the body so that it may be more efficiently packaged into apolipoprotein B-containing lipoproteins (50). Immunodepletion experiments have shown that ACAT2 accounts for 80-90% of activity in the adult small intestine and fetal liver, whereas it only accounts for 10% of ACAT activity in the human adult liver (38).

ACAT2 is allosterically regulated by cholesterol and transcriptionally by Cdx2 (caudal type homeobox transcription factor 2) and HNF1$\alpha$ (hepatocyte nuclear factor 1alpha). Both Cdx2 and HNF1$\alpha$ work synergistically to promote the expression of *hSOAT2 (29)*. HNF1$\alpha$ is expressed in a myriad of tissues including hepatocytes, kidney, and the intestinal epithelium. In contrast, Cdx2 is a largely an intestine specific transcription factor. Interestingly, in normal adult human liver, Cdx2 expression is virtually undetectable and consequently ACAT2 expression levels are very low as well (29). However, in certain models of hepatocellular carcinoma, Cdx2 and subsequently ACAT2 expression is significantly elevated. This observation may explain the conflicting data regarding ACAT2 expression and activity in the liver (55).

In vivo function of ACAT2

Further insight into the specific biological role of ACAT2 has been garnered from knockout models in mice. ACAT2$^{-/-}$ mice have nearly undetectable ACAT activity and lack cholesteryl esters in the liver and small intestine (56). ACAT2$^{-/-}$ mice exhibit a decreased ability to absorb dietary cholesterol, a resistance to diet induced hypercholesterolemia, and gallstone formation (56). These data suggests that murine ACAT2 plays a key role in regulating the response to dietary cholesterol (38).

To ascertain the contribution of ACAT2 to the development of atherosclerosis, ACAT2$^{-/-}$ mice were crossed with an atherosclerosis-susceptible strain, ApoE$^{-/-}$. These mice exhibited high levels of total plasma lipids and an increase in apolipoprotein-B particles that were rich in trigylcerides and void of any cholesteryl esters (57). Despite elevated levels of total plasma and apo-B particles, the ACAT2 deficient mice in the ApoE$^{-/-}$ background were almost completely protected from atherosclerosis (57). Willner et al suggested that the altered composition of the apoB particle in the double knockout mice made it less atherogenic. These data connote that cholesteryl esters catalyzed by ACAT2 contribute to the onset of atherosclerosis in mice and therefore may be a salient drug target in humans (57).

ACAT inhibitors

The discovery that the ACAT reaction contributes to the formation of both the macrophage "foam cell" and the atherogenic apolipoprotein B–containing lipoproteins, suggested that inhibiting this reaction maybe key in preventing or treating atherosclerosis (58). Several animal studies involving nonselective ACAT inhibitors showed a promising reduction of atherosclerotic plaques. Unfortunately, human trials proved to be disappointing, likely because generalized ACAT inhibition leads to an increase in free cholesterol levels, apoptosis, and destabilization of ATP binding cassette A1 (32). However, the finding that ACAT2 deficiency in a pro-atherogenic mouse model was athero-protective, suggested that ACAT2 specific inhibition may prove more fruitful (57). In fact, Bell et al. demonstrated that liver ACAT2 specific inhibition in atherosclerosis prone mice were resistant to diet-induced hypercholesterolemia and had fewer aortic atherosclerotic lesions (59). However, unlike in mice, ACAT2 is not the major isoform in human liver and therefore this may prove to be a confounding factor when translating these results to humans (60).

Cholesterol homeostasis is achieved by a myriad of pathways working contemporaneously. The esterification of sterols by the ACATs is one

indispensible component of homoestasis. The efflux of cholesterol by ATP binding cassette (ABC) transporters represents another fundamental arm of this system (4). Together the ACATs and ABC transporters help maintain optimal intracellular sterol levels for normal cell function (18).

**Cholesterol Efflux by ABC Transporters**

ABC transporters

ATP-binding cassette transporters harness the energy of ATP binding and/or hydrolysis to transport a diverse set of hydrophobic molecules across membranes. ABC transporters represent one of the largest transporter gene families that are evolutionarily conserved (61). These transporters have a canonical architecture that consists of two transmembrane domains and two nucleotide binding domains. These domains can either be found in tandem in a single molecule or allocated to separate proteins, which must dimerize to form a functional transporter. The transmembrane domains are comprised of alpha helices that are embedded in the membrane whereas the nucleotide binding domains extrude into the cytoplasm (62). The nucleotide binding domain contains a set of highly conserved motifs such as the Walker A, Walker B, and the ABC signature motif, which is the hallmark of this protein superfamily (63). Conversely, the transmembrane domains exhibit a significant amount of diversity both in sequence and architecture, reflecting the heterogeneity of this superfamily's substrates (63). *Human ABC transporters are classified into seven families (*six of which are also found in the *Saccharomyces cerevisiae* genome*), based on* similarity in gene structure (half *versus* full transporters), order of the domains, and on sequence similarity in the nucleotide binding and transmembrane domains (63). ABC transporters mediate the transport of various amphiphilic ligands including, sterols, phospholipids, and xenobiotics. As such, they participate in diverse biological processes such as cell signaling, drug resistance, stem cell development, lipid trafficking, and membrane homeostasis (63).

Cholesterol and lipid efflux by ABC transporters

Members of this superfamily were first implicated in lipid transport when the classical drug transporters, MDR1 and MDR3 were shown to mediate phospholipid efflux (64). This novel concept that would later define a subset of ABC transporters was substantiated when it was discovered that ABCA1 is a key regulator of HDL metabolism (65). In 1998, several groups discovered that mutations in ABCA1 are the underlying defect in Tangier disease, a disease characterized by the virtual absence of HDL cholesterol (66-68). Functional studies showed that ABCA1 promotes the efflux of cholesterol and phospholipids to apolipoprotein A1, a nascent HDL particle (69). As a result, ABCA1 is a major determinant of plasma HDL levels. To date, 20 ABC transporters have been shown to mediate lipid and/or cholesterol flux across membranes (Table 1) (70).

ABCG Subfamily of ABC Transporters

The mammalian ABCG subfamily consists of 6 transporters, a majority of which, play a pivotal role in sterol transport and metabolism. Mammalian members in this subfamily are half-transporters comprised of a single nucleotide binding domain and a single transmembrane domain (71). The hallmark of this particular subfamily is its characteristic topology, in which the nucleotide binding domain is located N-terminal to the transmembrane domain. These transporters are orthologs of the Drosophila gene White, which forms obligate heterodimers with Scarlet or Brown in order to mediate the uptake of eye pigment precursors (33). Similarly, mammalian members of this subfamily must also form homodimers or obligate heterodimers in order to become functionally active (33).

Below is an overview of the physiologic function and relevance of the five mammalian members (ABCG1, G2, G4, G5, and G8) of the ABCG subfamily. A particular emphasis is placed on ABCG1, as its specific biological role in maintaining cholesterol homeostasis is explored in my thesis.

ABCG2 and ABCG3

ABCG2 is a homodimer that localizes to the plasma membrane of epithelial cells in various tissues including the placenta, kidney, and intestine (72,73). In these tissues ABCG2 is thought to play a role in regulating the efflux, absorption and circulation of xenobiotics. ABCG2 is highly expressed in tumor cells where it mediates multi-drug resistance to various chemotherapeutic agents (72). Unlike other mammalian members of this subfamily, a lipid substrate for ABCG2 has not been identified. In order to better understand the physiological role of ABCG2, *abcg2-/-* mice were created (74,75). To date, these mice do not display a distinctive phenotype. However, they do have increased levels of a heme precursor, protoporphyrin IX in plasma and erythrocytes (75).

ABCG3 is 54% identical to ABCG2 and was identified as a result of a computer search of EST databases. ABCG3 is highly expressed in the thymus and spleen, however its function is unknown (76).

ABCG4

ABCG4 and ABCG1 are 82% identical and exhibit overlapping functions. Overexpression of either protein in HEK293 cells promotes the efflux of cholesterol to mature HDL particles (69,77). In order to become functionally active ABCG1 and ABCG4 must either homodimerize or heterodimerize with each other. Despite their high homology and shared function, ABCG1 and G4 exhibit a disparate tissue distribution and transcriptional regulation. ABCG4 unlike ABCG1 is not regulated by the liver X receptor (LXR) and possesses a more restricted expression profile (78). ABCG4 is predominantly expressed in various cell types of the central nervous system (78). However, abcg4-/- mice do not display any overt neurological phenotypes (33). In contrast, the brains of *Abcg1*$^{-/-}$*Abcg4*$^{-/-}$ mice exhibited a significant increase in both the cholesterol metabolite 27-hydroxycholesterol and in the levels of several intermediates of the cholesterol biosynthetic pathway (79). Additionally, astrocytes from these mice showed a signficiant decrease in the efflux of cholesterol and desmosterol to

HDL. These data suggest that ABCG1 and ABCG4 may work synergistically in astrocytes to promote the efflux of desmosterol and cholesterol to HDL like particles (79).

The cellular localization for both ABCG1 and ABCG4 remains elusive. Localization studies have produced discordant results, with one study proposing that both proteins co-localize to the plasma membrane and another study showing that they localize to endosomes (71). Additional studies are needed to more precisely define the subcellular localization and molecular role of ABCG4.

ABCG5 and ABCG8

Two tandemly aligned genes, ABCG5 and ABCG8, encode for proteins that act as obligate heterodimers to promote sterol efflux into bile and the intestinal lumen. ABCG5 and ABCG8 are coordinately expressed and induced following activation of LXR (71). Both transporters localize to the apical membranes of intestinal enterocytes and the canalicular membranes of hepatocytes. Deletion of either half transporter results in the retention of the other in the ER as a consequence of impaired translocation to the plasma membrane (80). Functional and structural studies demonstrated that the nucleotide binding domains of ABCG5 and ABCG8 are not functionally equivalent (80). These studies found that Walker A and Walker B motif from ABCG5 and the signature motif of ABCG8 were required for ATP binding and hydrolysis (80). Initial characterization of these transporters by Hobbs et al., demonstrated that mutations in ABCG5 or ABCG8 were the underlying cause for β-sitosterolemia, a rare autosomal recessive disorder.β-sitosterolemia is primarily characterized by a significant increase in plasma and tissue plant sterols. Patients may also present with other lipid abnormalities such as the deposition of sterols in the skin (xanthomas) and coronary arteries (81).

Analysis of *Abcg5*$^{-/-}$*Abcg8*$^{-/-}$ mice confirmed the role of these transporters in β-sitosterolemia, as these mice exhibited a 3-fold increase in dietary plant sterol fractional absorption, a 30% increase in plasma sitosterol levels, and a

reduction in biliary cholesterol levels (81). In addition, substrate specificity was gleaned from these studies as the double knockout mice exhibited low levels of biliary cholesterol only, not bile acids or phospholipids (82). By controlling sterol intestinal absorption and hepatic excretion, ABCG5 and ABCG8 effectively limit circulating sterols in plasma, suggesting that modulation of the activity of these transporters might be used as a novel therapeutic intervention in the treatment of hypercholesterolemias. Indeed, *Ldlr*$^{-/-}$ mice overexpressing both ABCG5 and ABCG8 showed a marked decrease in circulating cholesterol and reduced atherosclerotic lesions, compared to *Ldlr*$^{-/-}$ controls (83).

## ABCG1

### ABCG1 Gene and Protein Structure

In 1997, human *ABCG1* cDNA was identified and found to encode for a 74 kDa protein (678 amino acids) that exhibited 33% identity with the *Drospophila white* gene (84). *ABCG1* is comprised of 23 exons and is found on chromosome 21 as well as on the corresponding locus of murine chromosome 17 (84). Seven *ABCG1* splice variants have been identified and differ only at the amino terminus. In mice, $ABCG1_{678}$ is the predominant splice variant, however for humans the major transcript has yet to be established (85). Engel et al., investigated the expression patterns and functionality of a shorter splice variant $ACBG1_{666}$, an isoform in which 12 amino acids in the cytoplasmic domain (found between the transmembrane region and the ATP cassette) have been spliced (85,86). They demonstrated that $ABCG1_{666}$ localizes to the plasma membrane where it is able to promote cholesterol efflux and form a homodimer (85). Furthermore, they found that $ABCG1_{666}$ expression was two fold higher than $ABCG1_{678}$ in human monocyte-derived macrophages and liver (85). Gelissen et al., further corroborated these findings and in addition found that $ABCG1_{678}$ had a shorter half life than $ABCG1_{666}$ under basal conditions (86).

Multiple response elements and promoters at various positions have been identified for *ABCG1. ABCG1* contains a TATA promoter and two functional LXR

response elements upstream of exon 8. Conversely, a TATA-less promoter is found upstream of exons 1, 4, 5, and 6. In addition, a putative PPAR/RXR binding motif (upstream of exon 1), a putative sterol response element (upstream of exon 5), and a two putative RXR binding motifs (upstream of exon 5) have also been identified (73).

ABCG1 Tissue and Cellular Distribution

The subcellular localization of ABCG1 remains controversial, as it seems to vary by cell type, culturing conditions, and detection techniques. Intracellular, perinuclear, and cell surface localization of ABCG1 have all been reported in a variety of cells including macrophages, baby hamster kidney cells, and mouse pancreatic beta cells (87-89). Further imbuing the controversy was conflicting data from Xie et al and Wang et al, regarding whether LXR activation induced ABCG1 relocation from intracellular compartments to the plasma membrane (90,91). To date there is no consensus regarding ABCG1's intracellular localization. It is clear that further studies are necessary to elucidate ABCG1's intracellular trafficking and subsequent localization (33).

*Abcg1* is expressed in various murine and human tissues, however it is most highly expressed in the adrenal glands, lungs, heart, brain, and spleen (87). *Abcg1* is also expressed in a myriad of cell types including macrophages, lymphocytes, epithelial cells, and neurons (87).

Biological activity and regulation of ABCG

Initial functional characterization of ABCG1 demonstrated that it mediates the efflux of intracellular cholesterol and choline-phospholipids to an $HDL_3$ particle (87). Subsequently, overexpression studies have provided further insight as to the molecular role of ABCG1 by identifying protein partners, additional substrates, and novel acceptor molecules. Cross-linking experiments performed in both HEK293 cells and baby hamster kidney cells (BHK) illustrated that

ABCG1 functions as a homodimer. In addition, Western blot analysis detected several bands (120–150 kDa) after cross-linking suggesting that ABCG1 may interact with other unidentified proteins (88,92).

ABCG1 acts as a functional dimer to promote cholesterol efflux to an array of acceptors including LDL, small phospholipid vesicles, and cyclodextrin. Kobayashi et al. revealed that ABCG1 is also able to mediate cholesterol and phospholipid efflux to BSA in a concentration-dependent manner, suggesting that secreted proteins may also function as an acceptor (92). Despite its promiscuity towards acceptor molecules, ABCG1 doesn't promote efflux to an Apo-A1 particle, the predominant lipid acceptor of ABCA1 (93). This may in part be explained by the observation that ABCG1 requires cholesterol acceptors that contain phospholipids, whereas ABCA1 prefers phospholipid-free or phospholipid poor apolioproteins (93). Furthermore, unlike ABCA1, acceptor binding to the donor cell is not a requisite for ABCG1 mediated efflux. These data thereby posits that ABCG1 and ABCA1 work in distinct lipid efflux pathways (93).

Overexpression of ABCG1 in BHK cells not only promoted efflux to an exogenous acceptor molecule, but also increased the flux of cholesterol to both a cholesterol oxidase accessible pool and an ACAT substrate pool (88). This observed increase was reduced in the presence of HDL suggesting that a fraction of the ABCG1-transported cholesterol not removed by HDL translocates from the cell surface to intracellular sites where it is esterified (88). Based on these data, Vaughan and Oram propose that ABCG1 redistributes cholesterol to cell-surface domains where it becomes accessible for removal by HDL or is esterified by the ACATs (88).

In addition to promoting the transport of cholesterol and phosphotidylcholine, Sano et al showed that ABCG1 also mediates the efflux of sphingomyelin (92). In HEK293 cells expressing either ABCA1 or ABCG1, they found that the ratio of SM to PC effluxed by ABCG1 was eight times higher than

that transported by ABCA1. Therefore suggesting that ABCG1 preferentially secretes sphingomylein whereas ABCA1 prefers phosphtaydilycholine (94).

Since the homeostasis of cholesterol and sphingolipids is so tightly coordinated (28), it was not surprising that intracellular levels of sphingomyelin affected ABCG1 mediated cholesterol transport. Efflux of cholesterol and sphingomyelin by ABCG1 was reduced in LY-A cells, in which a mutation of the ceramide transfer protein CERT results in reduced intracellular sphingomyelin levels (94). Corollary experiments with CHO-K1 cells overexpressing CERT displayed an increase in ABCG1 mediated efflux of cholesterol and sphingomyelin (54). The exact mechanism by which intracellular sphingomyelin levels affect ABCG1 mediated efflux remains elusive. However, Sano et al propose that ABCG1 may preferentially function in raft domains and therefore decreasing sphingomyelin levels results in a diminishing number of ABCG1 containing raft domains (94). Furthermore, it has been reported that HDL promoted the efflux of cholesterol from raft domains of human fibroblasts and macrophages (41).

Although changes in intracellular sphingomyelin levels, have been shown to affect ABCG1 mediated transport, primary regulation of ABCG1 occurs at the transcriptional level. Initial studies showed that ABCG1 mRNA levels were highly induced when macrophages were converted to lipid-loaded “foam” cells following incubation with modified low-density lipoproteins, specific oxysterols, or following the induction of the nuclear receptor liver-X-receptor (LXR) (95). Consistent with these observations, multiple functional LXR response elements (LXREs) have been identified in both the murine and human genes (95). In addition, agonist activation of peroxisome proliferator-activated receptor, PPARγ results in increased expression of LXR and consequently LXR target genes that include ABCG1 and ABCA1 (71). Corroborating this data, Akiyama et al showed that hepatic expression of ABCG1 and ABCA1 was reduced in mice with a conditional disruption of hepatic PPARγ (96).

In vivo function of ABCG1

In order to assess the precise physiological role of ABCG1, *Abcg1*$^{-/-}$*LacZ* knock-in mice were generated. Surprisingly, unlike other LXR regulated ABC transporters (i.e ABCA1, ABCG5, and ABCG8), *Abcg1*$^{-/-}$ pups on a chow diet were healthy and did not exhibit any significant changes in weight, fertility, blood lipids, blood chemistry, or tissue pathology (43). However, when challenged with a high fat/high cholesterol diet, there was a significant accumulation of phospholipids, triglycerides, and cholesterol in the pulmonary macrophages, hepatocytes, and Kupffer cells (43). In addition, the subpleural region of the lungs of *Abcg1*$^{-/-}$ mice showed a significant increase in cholesterol clefts, lymphocytes, and the presence of classic macrophage foam cells. These phenotypes were rescued when hABCG1 was expressed in *Abcg1*$^{-/-}$ mice. Interestingly, plasma lipids in *Abcg1*$^{-/-}$ remain unchanged even when on a high fat/high cholesterol diet (97). This suggests that unlike ABCA1, ABCG1 is not a major determinant of plasma HDL levels.

Although neutral lipid and cholesterol deposition occurred in both the lung and liver of *Abcg1*$^{-/-}$ pups fed a high fat/high cholesterol diet, the pulmonary lipidosis was most striking and continued to worsen with age (regardless of diet provided) (98). The lungs of 8 month old *Abcg1*$^{-/-}$ chow fed mice exhibited significant deposition of free and esterified cholesterol in alveolar macrophages, increased surfactant levels, and enlarged pneumocyte type 2 cells containing abnormal lamellar bodies. Furthermore, this lipidosis was accelerated when *Abcg1*$^{-/-}$ mice were fed a high-fat, high-cholesterol diet, suggesting that dietary lipids contribute to the sterol imbalance in the lungs (98). In addition, *Abcg1*$^{-/}$ macrophages accumulated cholesteryl ester droplets when incubated with surfactant. Baldan et al., suggested that such a phenotype may be attributed to the continual cellular uptake of cholesterol-containing surfactant coupled with a defect in ABCG1-dependent sterol efflux (despite increased expression of ABCA1) (98).

The accumulation of cholesteryl ester droplets in pulmonary *Abcg1*$^{-/-}$ macrophages, coupled with the pivotal role that ABCG1 plays in reverse cholesterol transport in vitro, suggests that a loss of ABCG1 may contribute to the onset and progression of atherosclerosis. In order to evaluate the role of ABCG1 in atherosclerosis, three laboratories independently performed bone-marrow-transplant studies using donor cells from *Abcg1*$^{-/-}$ or wild-type mice and recipient hyperlipidemic *Ldlr*$^{-/-}$ mice (98-100). Surprisingly, both Baldan et al. and Ranalletta et al. reported a significant decrease in atherosclerotic lesion size even when the mice were challenged with a high fat/high cholesterol diet (100,101). Baldan et al. attributed the reduction in lesion size to an increase in apoptosis of the *Abcg1*$^{-/-}$ macrophages, whereas Ranalletta et al. proposed that upregulation of *Abca1* and an associated increase in apoE secretion contributed to the reduction in lesion size (100,101). Conversely, Out et al. reported a moderately significant increase in lesion size in the *Ldlr*$^{-/-}$ mice receiving bone marrow from *Abcg1*$^{-/-}$ mice (102). Furthermore, a subsequent study showed that overexpression of ABCG1 in *Ldlr*$^{-/-}$ resulted in a moderate increase in lesion size (103).

To further clarify the role of ABCG1 in atherosclerosis, cholesterol efflux and its relationship to ABCA1, *Abca1*$^{-/-}$*Abcg1*$^{-/-}$ mice were created and bone marrow from these mice was transplanted into hyperlipidemic *Ldlr*$^{-/-}$ mice (99,104) Similar to the studies described above, conflicting results from these experiments were also obtained. Out et al. reported that atherosclerotic lesions in these mice were smaller than those mice receiving *Abca1*$^{-/-}$ donor cells, whereas Yvan-Charvet et al. reported increased lesion size in mice receiving double knockout donor cells as compared to controls (99,104).

The characterization of the precise physiological role of ABCG1 is still in its infancy. Localization studies, mouse models, and overexpression studies have begun to outline a molecular mechanism for ABCG1. Discerning the role that ABCG1 plays in the intracellular distribution of sterols will be vital in seeking new

target molecules and functional pathways in the prevention and treatment of cardiovascular disease.

**Yeast as a model system to study sterol homeostasis**

The maintenance of sterol homeostasis is paramount to all eukaryotes. Sterol homeostasis is achieved by striking a precise balance between sterol synthesis and its uptake, efflux, and catabolism. Despite the importance of these homeostatic events, many aspects of these processes and their regulation remain elusive. The model eukaryote *Saccharomyces cerevisiae,* shares many aspects of sterol homeostasis with higher eukaryotes (Table 2). The application of classical and molecular genetics (including genomics) to *Saccharomyces cerevisiae* has allowed it to serve as a valuable tool in deciphering the mechanisms underlying sterol homeostasis (6). In particular I utilized this model system to further our understanding of sterol esterification and ABC transporter mediated movement of sterol across membranes. As such, the fundamentals of these particular processes in yeast are highlighted in the following section.

Ergosterol structure and synthesis

Ergosterol is the predominant sterol in budding yeast and an essential structural component of yeast membranes (105). Although it differs structurally (double bonds at $C_7$ and $C_{22}$ and a methyl group at $C_{29}$) from cholesterol, ergosterol is synthesized, regulated, and metabolized in a similar fashion (Figure 1) (106,107). Like in higher eukaryotes, budding yeast can obtain ergosterol either via its biosynthesis or its uptake from the environment. Sterol biosynthesis, which only occurs in the presence of oxygen, is comprised of over twenty distinct reactions that take place primarily in the ER (Figure 2) (105,108). The biosynthetic pathway is extensively regulated and responds to both environmental (changes in intracellular sterol levels) and transcriptional cues. A majority of the transcriptional regulation is imparted by the transcription factors, Upc2p and Ecm22p, which activate transcription by binding to common conserved sterol-regulatory elements of ergosterol biosynthetic genes (108,109).

**Sterol Esterification**

In *Saccharomyces cerevisiae,* two ACAT related enzymes, Are1p and Are2p, catalyze the esterificiation of sterols (110,111). Like in mammalian cells, steryl esters are stored in cytosolic lipid droplets as a means to protect the cell from cholesterol toxicity (111). Are1p and are2p are 49% identical and are most similar to ACAT1 at the carboxy terminus, exhibiting a 23% identity overall (https://portal.biobase-international.com/cgi bin/build_ghpywl/idb/1.0/searchengine/start.cgi).

Are1p and Are2p protein structure

The *ARE1* and *ARE2* genes produce a predicted 71 kDa and a 74 kDa protein respectively (105). In general, sequence conservation of this gene family is most pronounced toward the carboxy terminus. Are1p and Are2p both possess the conserved motifs, FYxDWWN and (H/Y)SF, of which the former most likely mediates acyl-CoA binding and the latter is required for catalytic activity. Similar to human ACAT1, deletion of a region in the N-terminus of Are2p results in a truncated isoform with increased enzymatic activity (112). Furthermore, Are2p is predicted to have multiple transmembrane domains as well as phosphorylation and N-linked glycosylation sites (112).

Are1p and Are2p biological activity and regulation

Are1p and Are2p are homotetrameric enzymes that reside in the ER. Deletion of both genes results in a viable cell that is completely void of any steryl esters. The yeast double mutant can be complemented by the heterologous expression of human ACAT1 or ACAT2 cDNAs indicating both functional and structural conservation. *ARE1* and *ARE2* genes differentially determine the sterol ester pools of the cell. The deletion of *ARE2* results in a 75% decrease in ergosteryl esters, whereas the loss of *ARE1* has no detectable impact on the production of ergosteryl esters *in vivo (112)*. These discordant phenotypes can be explained by the varying substrate specificity of the esterifying enzymes (113). Are1p primarily esterifies intermediates in the sterol biosynthetic pathway,

whereas are2p is esterifies the end product ergosterol (113). Based on their distinct substrate specificity it is not surprising that these two genes are differentially regulated in response to alterations in sterol metabolism. The *ARE1* gene is up-regulated by the accumulation of pathway intermediates, anaerobiosis, and heme deficiency (the production of which requires oxygen). Conversely, *ARE2* expression is repressed both under anaerobic and heme deficient conditions (112,113).

**Sterol Uptake**

Under aerobic conditions yeast fulfill their sterol requirement solely via its biosynthesis and therefore do not take up free sterols from the environment (114). The molecular mechanism underlying this aerobic sterol-exclusion has not yet been defined, however it is though that properties of the cell wall may prevent exogenous sterol uptake (115). Conversely, during anaerobiosis, sterol biosynthesis is inhibited and therefore yeast cells are forced to uptake sterol from the environment (116). Aerobic sterol uptake and sterol biosynthesis can occur concurrently as a result of a mutation that prevents the synthesis of heme, overexpression of the transcriptional regulator SUT1, and a gain of function mutation in the transcription factor *UPC2* (this mutant strain will be referred to as upc2-1 from herein) (117-119). *UPC2* encodes for a member of a fungal regulatory family containing the Zn $(II)_2Cys_6$ binuclear cluster DNA binding domain. Upc2p promotes sterol uptake by binding to the sterol regulatory elements in *AUS1* and *PDR11 (120)*. Aus1p and Pdr11p are members of the ABC transporter superfamily that mediate the retrograde transport of sterols (120).

Aus1p and Pdr11p protein structure

*AUS1* and *PDR11* both encode for proteins that are predicted 160 kDa and share a 65% identity. Aus1p and Pdr11p are members of the ABCG subfamily and are 25% and 28% identical to ABCG1, respectively (https://portal.biobase-

international.com/cgi-bin/build_ghpywl/idb/1.0/searchengine/start.cgi). They are full ABC transporters that are comprised of two nucleotide binding domains and two transmembrane domains. Like all members of the ABCG subfamily, the nucleotide binding domain is N-terminal to the transmembrane domains. In addition, Aus1p and Pdr11p possess a degenerate Walker A motif in the first nucleotide binding domain, a common feature of all yeast members of the ABCG subfamily (121). Specifically, the conserved lysine residue in this motif, which is thought to essential for ATP binding is substituted with a cysteine residue. The Walker A motif of Aus1p and Pdr11p contains a three amino acid deletion that encompasses the critical lysine residue (Figure 2) (121). The biochemical or functional significance of a degenerate Walker A motif in this subfamily remains unknown (121).

Aus1p and Pdr11p biological activity and regulation

In order to establish the components of non-lipoprotein-mediated sterol uptake in budding yeast, a genome wide transcriptional analysis of the upc2-1 mutant strains was utilized (120). This transcriptional profiling study identified the plasma membrane ABC transporters, Aus1p and Pdr11p, as key mediators of sterol influx. Initial functional studies of these transporters revealed that they differentially contributed to sterol uptake. An *AUS1* deletion under anaerobic conditions resulted in a significant decrease in sterol uptake. In contrast, a *PDR11* deletion under the same conditions had no discernible effect on sterol uptake (120). However, the combined loss of both ABC transporters during anaerobiosis abolished sterol uptake and severely compromised viability. The redundancy in these transporters was further demonstrated by the finding that either transporter alone can supply sufficient sterol to support anaerobic growth (120).

Based on the observation that sterol uptake is significantly decreased in *are1Δ are2Δ upc2-1* mutant, Prinz et al. examined whether Aus1p and Pdr11p play a role in the subsequent intracellular distribution of exogenous sterols (122).

Specifically, they investigated whether these two transporters mediate the non-vesicular transport of sterols to the ER. Prinz et al found that an *AUS1* or *PDR11* deletion resulted in a significant decrease in sterol esterification (used as marker for sterol movement to the ER), respectively (122). Thereby suggesting that Aus1p and Pdr11p may mediate the movement of sterols to the ER. Furthermore, they observed that exogenous cholesterol is more rapidly esterified than endogenous ergosterol. Prinz et al posit that these different rates in esterification reflect the distinct yeast raft affinities of these two sterols. Based on these data, Prinz et al propose that Aus1p and Pdr11p increase the availability of plasma membrane sterol for esterification in the ER, which in turn contributes to the net uptake of exogenous sterol by cells. In addition, they also suggest that the propensity of a sterol to be moved between the plasma membrane and ER is largely determined by its raft affinity, suggesting that raft association is a primary determinant of sterol accumulation in the PM. However, they do not provide a transport mechanism by which sterols transported by Aus1p and Pdr11p are shuttled from the plasma membrane to the ER (122).

*AUS1* and *PDR11* are primarily regulated by the transcription factors Upc2p and Ecm22p. In addition, *AUS1* and *PDR11,* like Are2p are regulated by oxygen status via the transcription factor Hap1 (120). The *PDR11* promoter contains an additional response element, a pleitropic drug resistance element, which is bound by the transcription factor Pdr1p. Although, *PDR11* expression is upregulated in response to Pdr1p binding, the functional relevance of this change in expression remains to be elucidated. Perhaps Pdr11p mediates cross-talk between the drug resistance and lipid metabolism pathway (https://portal.biobase-international.com/cgi-bin/build_ghpywl/idb/1.0/searchengine/start.cgi).

**Sterol Efflux**

In mammals, an integral component of cholesterol homeostasis is its efflux to the environment (18). Until recently, there was no evidence of sterol efflux in yeast and therefore it was thought that sterol homeostasis was maintained by the

reciprocal interconversion of free sterols and steryl esters (105). However, recent studies by Tiwari et al., identified a novel sterol acetylation/deacetylation cycle, which plays a pivotal role in controlling export of sterols from the cell. This sterol export cycle is mediated by two proteins, a sterol acetylase Atf2p and a sterol deacetylase, Say1p (123).

Atf2p and Say1p protein structure

Say1p is an ER protein that is both sequentially and functionally homologous to the human arylacetamide deacetylase, AADAC. It is an integral membrane protein that contains a putative esterase/lipase domain and three potential N-linked glycosylation sites. In addition, Say1p possesses a lipase consensus motif GXSXG and a HGGG oxyanion hole motif, which are the hallmark sequences of the prokaryotic family IV lipolytic enzymes (which display a high similarity to mammalian hormone-sensitive lipases). Atf2p is an alcohol O-acetyltransferase that is found in the ER. It is an integral membrane protein with at least two transmembrane domains. Atf2p has no know mammalian homologues however it is 35% identical to Atf1p. Atf2p has a conserved heptapeptide WRLICLP, which is proposed to be part of the active site of alcohol O-acetyltransferases (56).

Atf2p and Say1p biological activity and regulation

Biochemical analysis of a *say1Δ* strain revealed an accumulation of a sterol derivative, steryl acetate (123). Conversely, deletion of *ATF2* resulted in the absence of intracellular sterol acetate (123). Since it was already established that Atf2p possessed acetylase activity and produces sterol acetate, it was surmised that *SAY1* encoded for a deacytelase (124). Functional and biochemical characterization of a *say1Δ* strain showed that acetylated cholesterol not only accumulated intracellularly, but was also present in the culture supernatant. These data suggested that Say1p's deacteylation of sterols promotes their retention within the cell, whereas, acetylation by Atf2p marks the

sterols for export (123). Tiwari et al, showed that similar to sterol efflux in mammals, the presence of an exogenous lipid acceptor was necessary for efflux to occur (123). Furthermore, export of steryl acetate is an ATP dependent process that requires an intact secretory pathway. In order to assess if cholesteryl ester formation influences the acetylation/deactylation cycle, Tiwari et al generated a *say1Δ are1Δ are2Δ* mutant strain and assessed the presence and export of cholesteryl acetate. They found that export of cholesterol acetate occurred less efficiently in this background (123). Although Tiwari et al, described the presence of sterol efflux in yeast, they failed to show which proteins mediate the efflux of sterols (123).

Regulation of At2p and Say1p remains elusive. Tiwari et al, showed that oxygen status did not effect expression of either of these proteins. However, data presented by Wilcox et al., showed that the Atf2p promoter contains Upc2p binding sterol regulatory element and is upregulated in an upc2-1 mutant strain (120).

**Purpose of this study**

ABC transporters constitute an extensive evolutionarily conserved superfamily of integral membrane proteins have recently been implicated in intracellular lipid trafficking (70). The first example of this arose when mutations in the ABC transporter ABCA1, were identified as the molecular defect in Tangier disease, a disease typified as a defect in HDL cholesterol metabolism (125). These proteins exclusively force anterograde movement of cholesterol across the plasma membrane. In contrast, we have demonstrated that the opposite (i.e inward) transport of sterol in yeast is also dependent on two ABC transporters (Aus1p and Pdr11p). The main focus of this study is to define the parameters that influence ABC transporter mediated sterol movement across membranes. The comparison between these contrasting states (opposing directionality of the same substrate) will allow us to dissect whether sterol transport across the plasma membrane is defined by the molecule (i.e. the ABC transporter) or by

microenvironment (i.e. the status of intracellular proteins and lipids) in which it resides. In order to address this question in Chapter 2, I will express murine ABCG1 (mABCG1) in budding yeast and assess how changes in the intracellular sterol environment affect direction of transport. In the subsequent chapters (Chapter 3 and 4) we will explore how interactions with proteins in the microenvironment influence sterol transport by members of the ABCG subfamily. These studies may deepen our understanding of how members of the ABCG subfamily transport sterols and how dysregulation of this transport may contribute to the onset of atherosclerosis.

**Table 1**

| Transporter gene | Function | Lipids transported | Disease state/mutant phenotype |
|---|---|---|---|
| ABCA1 | Apo-A1 dependent formation of nascent HDL | C, PL | Tangiers Disease<br><br>Familial HDL Deficiency |
| ABCA2 | Unknown, correlated with C concentration in brain | SM, myelin | Alzheimer's Disease (putative) |
| ABCA3 | Secerete pulmonary surfactant | C, SM, PC | Neonatal surfactant deficiency, Pediatric interstitial lung disease |
| ABCA4 (ABCR) | Retinal integrity | Ret, PE | Age-related macular degeneration, Stargardt disease 1, Retinitis pigmentosa 19, |
| ABCA6 | Unknown, sterol regulated | | ? |
| ABCA7 | Unknown | C, PL | ? |
| ABCA9 | Unknown, sterol regulated | | ? |
| ABCA10 | Unknown, sterol regulated | | ? |
| ABCA12 | Maintains the integrity of lamellar granules | C, Cer, FA | Lamellar ichthyosis type 2<br><br>Harlequin ichthyosis |
| ABCB1 (MDR1) | | PL, SM, & GSL | Parkinsons |
| ABCB4 &<br><br>ABCB11 | Phosphatidlycholine Translocator | PC | Progressive Familial Intrahepatic Cholestasis |
| ABCG1 | Promote cholesterol efflux to HDL-2 & HDL-3 particles | C, SM | Athereosclerosis |
| ABCG4 | Promote cholesterol efflux to HDL-2 & HDL-3 particles | C | Athereosclerosis |
| ABCG5 & ABCG8 | Secretion of plant sterols and cholesterol into bile | C, sitosterol | Sitosterolemia |
| *AUS1, PDR11* | Influx of sterol during anaerobiosis in yeast | Ergosterol? | Anaerobic inviability |

**Table 1:** Members of the ATP binding cassette super-family of membrane associated transporters involved in lipid movement. Abbreviations; C, cholesterol; Cer, ceramide; PL, phospholipids; PC, phosphatidylcholine; SM, sphingomyelin; GSL, glycosphingolipid. FA, fatty acid.

**Table 2**

| Protein Family | Yeast Protein | Mouse Protein | % Identity (Yeast to Mouse) | Function |
|---|---|---|---|---|
| ABC Transporter | Aus1p | ABCG1 | 26% | Sterol Transport |
| ABC Transporter | Pdr11 | ABCG1 | 29% | Sterol Transport |
| ACAT | Are1p | ACAT1<br>ACAT2 | 26%<br>31% | Sterol Esterification |
| ACAT | Are2p | ACAT1<br>ACAT2 | 27%<br>31% | Sterol Esterification |

**Table 2. Conservation of key proteins involved in sterol homoeostasis.**

**Figure 1.**

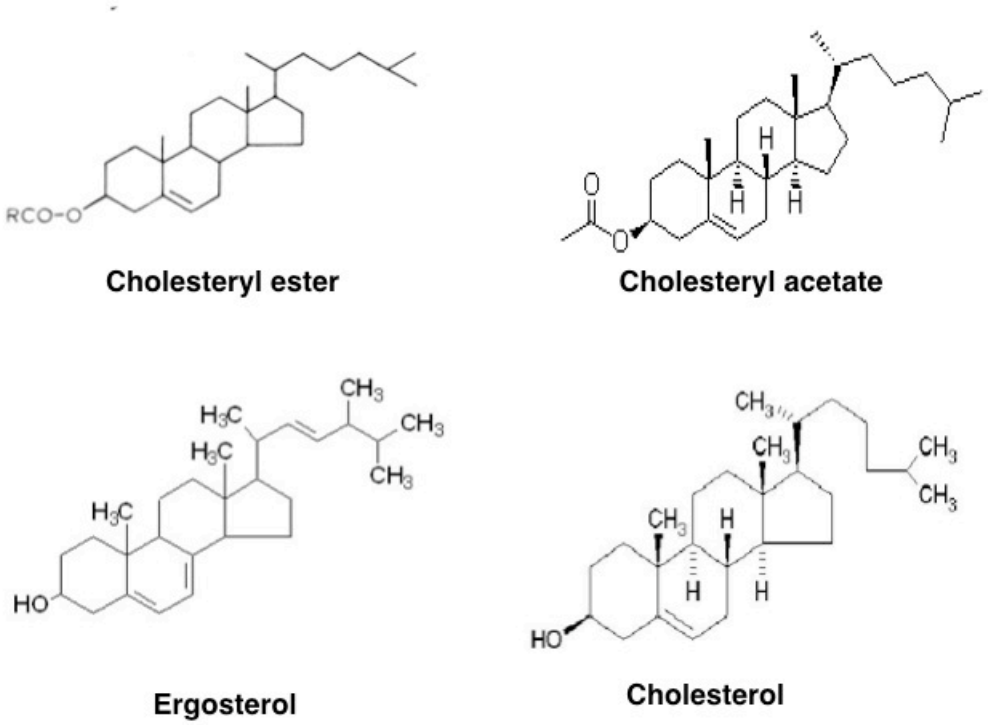


**Figure 1: Chemical structure of mammalian and plant sterols and their derivatives.** Ergosterol is structurally similar to cholesterol. Both are metabolized in a similar fashion in budding yeast (28).

**Figure 2.**

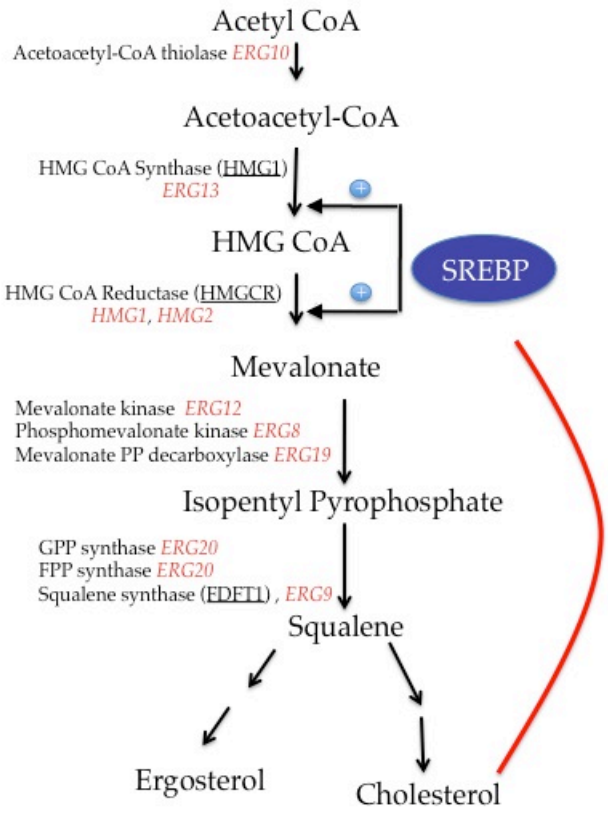


**Figure 2. A summary of the key steps in cholesterol and ergosterol biosynthesis.** Cholesterol is synthesized in almost all cell types from acetyl-CoA. Ergosterol and cholesterol synthesis is a complex process (simplified here), which involves over twenty reactions (28).

**Figure 3.**

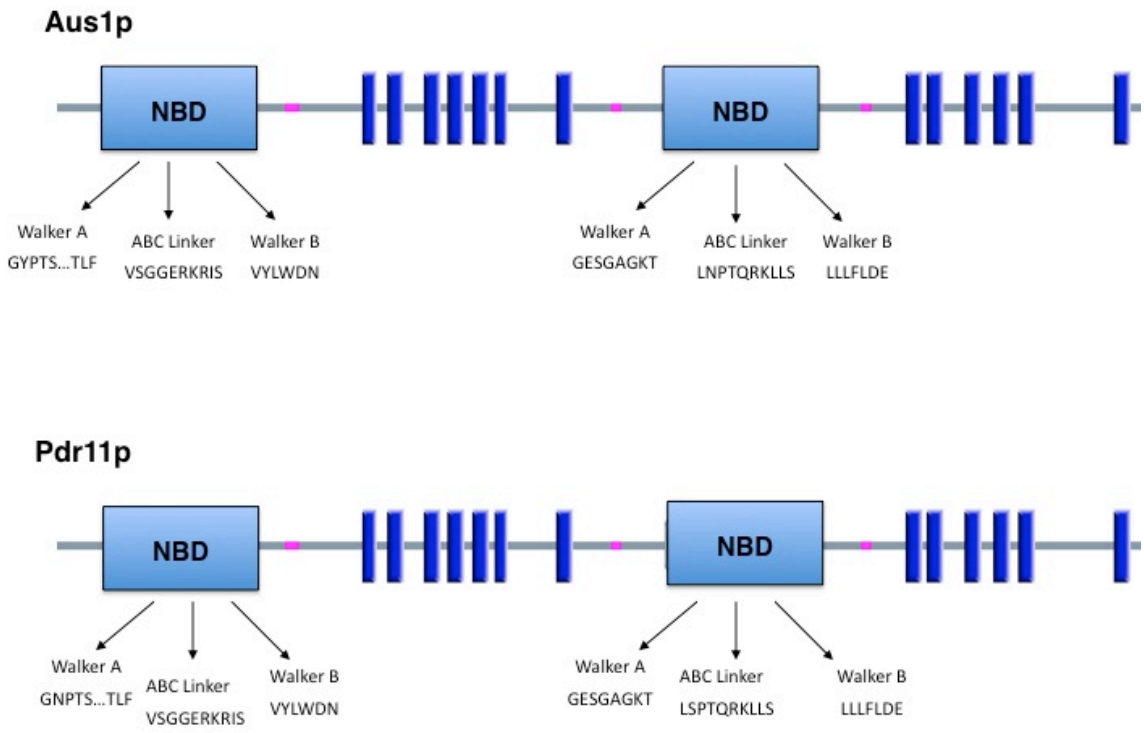


**Figure 3 Protein topology of Aus1p and Pdr11p.** Aus1p and Pdr11p are full ABC transporters that are members of the ABCG subfamily. Like all members of this subfamily, the nucleotide binding domain (NBD) is N-terminal to the transmembrane domain. Both Pdr11p and Aus1p contain a degenerate Walker A motif in NBD1.

**Figure 4**

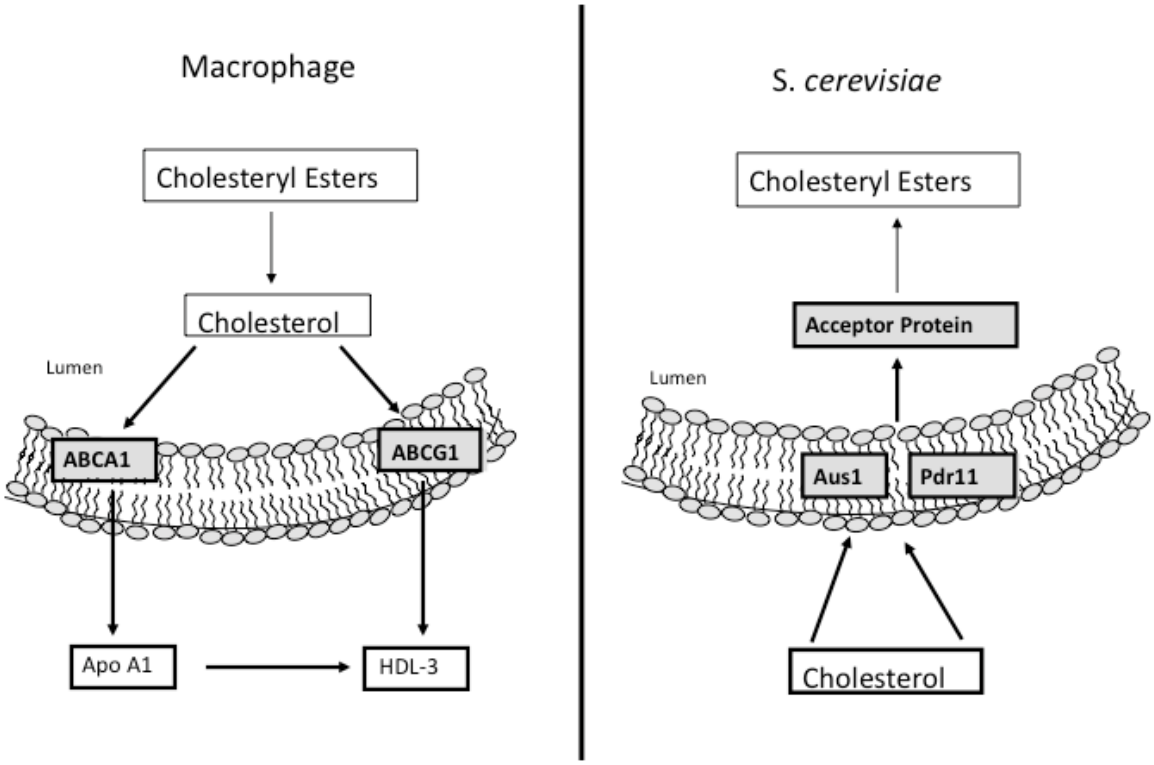


**Figure 4. A comparison of ABC transporter mediated cholesterol transport in a macrophage and budding yeast.** Cholesterol transport in both model systems is mediated by two ABC transporters that translocate a common substrate in opposite directions.

## References


1. Gibbons, G. F. (2002) *Lipids* **37**, 1153-1162
2. Ikonen, E. (2006) *Physiol Rev* **86**, 1237-1261
3. Quinn, P. J. (2010) *Prog Lipid Res* **49**, 390-406
4. Maxfield, F. R., and Tabas, I. (2005) *Nature* **438**, 612-621
5. Lange, Y., and Steck, T. L. (1996) *Trends Cell Biol* **6**, 205-208
6. Lingwood, D., and Simons, K. (2010) *Science* **327**, 46-50
7. Brown, D. A. (2006) *Physiology (Bethesda)* **21**, 430-439
8. Sengupta, P., Baird, B., and Holowka, D. (2007) *Semin Cell Dev Biol* **18**, 583-590
9. Simons, K., and Gerl, M. J. (2010) *Nat Rev Mol Cell Biol* **11**, 688-699
10. Mukherjee, S., and Maxfield, F. R. (2004) *Annu Rev Cell Dev Biol* **20**, 839-866
11. Brown, D. A., and Rose, J. K. (1992) *Cell* **68**, 533-544
12. Lingwood, D., and Simons, K. (2007) *Nat Protoc* **2**, 2159-2165
13. Montixi, C., Langlet, C., Bernard, A. M., Thimonier, J., Dubois, C., Wurbel, M. A., Chauvin, J. P., Pierres, M., and He, H. T. (1998) *EMBO J* **17**, 5334-5348
14. Roper, K., Corbeil, D., and Huttner, W. B. (2000) *Nat Cell Biol* **2**, 582-592
15. Radeva, G., and Sharom, F. J. (2004) *Biochem J* **380**, 219-230
16. Hell, S. W. (2007) *Science* **316**, 1153-1158
17. Sharma, P., Varma, R., Sarasij, R. C., Ira, Gousset, K., Krishnamoorthy, G., Rao, M., and Mayor, S. (2004) *Cell* **116**, 577-589
18. Ikonen, E., and Jansen, M. (2008) *Curr Opin Cell Biol* **20**, 371-377
19. Goldstein, J. L., DeBose-Boyd, R. A., and Brown, M. S. (2006) *Cell* **124**, 35-46
20. Brown, M. S., and Goldstein, J. L. (1999) *Proc Natl Acad Sci U S A* **96**, 11041-11048
21. Radhakrishnan, A., Goldstein, J. L., McDonald, J. G., and Brown, M. S. (2008) *Cell Metab* **8**, 512-521
22. Goldstein, J. L., and Brown, M. S. (1990) *Nature* **343**, 425-430
23. Feramisco, J. D., Goldstein, J. L., and Brown, M. S. (2004) *J Biol Chem* **279**, 8487-8496
24. Grundy, S. M. (1983) *Annu Rev Nutr* **3**, 71-96
25. Hussain, M. M., Maxfield, F. R., Mas-Oliva, J., Tabas, I., Ji, Z. S., Innerarity, T. L., and Mahley, R. W. (1991) *J Biol Chem* **266**, 13936-13940
26. Rigotti, A., Trigatti, B. L., Penman, M., Rayburn, H., Herz, J., and Krieger, M. (1997) *Proc Natl Acad Sci U S A* **94**, 12610-12615
27. Monte, M. J., Marin, J. J., Antelo, A., and Vazquez-Tato, J. (2009) *World J Gastroenterol* **15**, 804-816
28. Gulati, S., Liu, Y., Munkacsi, A. B., Wilcox, L., and Sturley, S. L. (2010) *Prog Lipid Res* **49**, 353-365
29. Chang, T. Y., Li, B. L., Chang, C. C., and Urano, Y. (2009) *Am J Physiol Endocrinol Metab* **297**, E1-9
30. Chang, C. C., Huh, H. Y., Cadigan, K. M., and Chang, T. Y. (1993) *J Biol Chem* **268**, 20747-20755

31. Oelkers, P., Behari, A., Cromley, D., Billheimer, J. T., and Sturley, S. L. (1998) *J Biol Chem* **273**, 26765-26771
32. Turkish, A., and Sturley, S. L. (2007) *Am J Physiol Gastrointest Liver Physiol* **292**, G953-957
33. Tarr, P. T., Tarling, E. J., Bojanic, D. D., Edwards, P. A., and Baldan, A. (2009) *Biochim Biophys Acta* **1791**, 584-593
34. Zhao, X., Chen, J., Lei, L., Hu, G., Xiong, Y., Xu, J., Li, Q., Yang, X., Chang, C. C., Song, B., Chang, T., and Li, B. (2009) *Acta Biochim Biophys Sin (Shanghai)* **41**, 30-41
35. Guo, Z. Y., Chang, C. C., Lu, X., Chen, J., Li, B. L., and Chang, T. Y. (2005) *Biochemistry* **44**, 6537-6546
36. Lin, S., Cheng, D., Liu, M. S., Chen, J., and Chang, T. Y. (1999) *J Biol Chem* **274**, 23276-23285
37. Cao, G., Goldstein, J. L., and Brown, M. S. (1996) *J Biol Chem* **271**, 14642-14648
38. Buhman, K. F., Accad, M., and Farese, R. V. (2000) *Biochim Biophys Acta* **1529**, 142-154
39. Khelef, N., Buton, X., Beatini, N., Wang, H., Meiner, V., Chang, T. Y., Farese, R. V., Jr., Maxfield, F. R., and Tabas, I. (1998) *J Biol Chem* **273**, 11218-11224
40. Meiner, V., Tam, C., Gunn, M. D., Dong, L. M., Weisgraber, K. H., Novak, S., Myers, H. M., Erickson, S. K., and Farese, R. V., Jr. (1997) *J Lipid Res* **38**, 1928-1933
41. Sakashita, N., Miyazaki, A., Takeya, M., Horiuchi, S., Chang, C. C., Chang, T. Y., and Takahashi, K. (2000) *Am J Pathol* **156**, 227-236
42. Uelmen, P. J., Oka, K., Sullivan, M., Chang, C. C., Chang, T. Y., and Chan, L. (1995) *J Biol Chem* **270**, 26192-26201
43. Lee, O., Chang, C. C., Lee, W., and Chang, T. Y. (1998) *J Lipid Res* **39**, 1722-1727
44. Wang, H., Germain, S. J., Benfield, P. P., and Gillies, P. J. (1996) *Arterioscler Thromb Vasc Biol* **16**, 809-814
45. Cheng, W., Kvilekval, K. V., and Abumrad, N. A. (1995) *Am J Physiol* **269**, E642-648
46. Pape, M. E., Schultz, P. A., Rea, T. J., DeMattos, R. B., Kieft, K., Bisgaier, C. L., Newton, R. S., and Krause, B. R. (1995) *J Lipid Res* **36**, 823-838
47. Yagyu, H., Kitamine, T., Osuga, J., Tozawa, R., Chen, Z., Kaji, Y., Oka, T., Perrey, S., Tamura, Y., Ohashi, K., Okazaki, H., Yahagi, N., Shionoiri, F., Iizuka, Y., Harada, K., Shimano, H., Yamashita, H., Gotoda, T., Yamada, N., and Ishibashi, S. (2000) *J Biol Chem* **275**, 21324-21330
48. Chiwata, T., Aragane, K., Fujinami, K., Kojima, K., Ishibashi, S., Yamada, N., and Kusunoki, J. (2001) *Br J Pharmacol* **133**, 1005-1012
49. Fazio, S., Major, A. S., Swift, L. L., Gleaves, L. A., Accad, M., Linton, M. F., and Farese, R. V., Jr. (2001) *J Clin Invest* **107**, 163-171
50. Anderson, R. A., Joyce, C., Davis, M., Reagan, J. W., Clark, M., Shelness, G. S., and Rudel, L. L. (1998) *J Biol Chem* **273**, 26747-26754
51. Cases, S., Novak, S., Zheng, Y. W., Myers, H. M., Lear, S. R., Sande, E., Welch, C. B., Lusis, A. J., Spencer, T. A., Krause, B. R., Erickson, S. K., and Farese, R. V., Jr. (1998) *J Biol Chem* **273**, 26755-26764

52. Yao, X. M., Wang, C. H., Song, B. L., Yang, X. Y., Wang, Z. Z., Qi, W., Lin, Z. X., Chang, C. C., Chang, T. Y., and Li, B. L. (2005) *Acta Biochim Biophys Sin (Shanghai)* **37**, 797-806
53. Parini, P., Davis, M., Lada, A. T., Erickson, S. K., Wright, T. L., Gustafsson, U., Sahlin, S., Einarsson, C., Eriksson, M., Angelin, B., Tomoda, H., Omura, S., Willingham, M. C., and Rudel, L. L. (2004) *Circulation* **110**, 2017-2023
54. Smith, J. L., Rangaraj, K., Simpson, R., Maclean, D. J., Nathanson, L. K., Stuart, K. A., Scott, S. P., Ramm, G. A., and de Jersey, J. (2004) *J Lipid Res* **45**, 686-696
55. Pramfalk, C., Davis, M. A., Eriksson, M., Rudel, L. L., and Parini, P. (2005) *J Lipid Res* **46**, 1868-1876
56. Repa, J. J., Buhman, K. K., Farese, R. V., Jr., Dietschy, J. M., and Turley, S. D. (2004) *Hepatology* **40**, 1088-1097
57. Willner, E. L., Tow, B., Buhman, K. K., Wilson, M., Sanan, D. A., Rudel, L. L., and Farese, R. V., Jr. (2003) *Proc Natl Acad Sci U S A* **100**, 1262-1267
58. Buhman, K. K., Chen, H. C., and Farese, R. V., Jr. (2001) *J Biol Chem* **276**, 40369-40372
59. Bell, T. A., 3rd, Brown, J. M., Graham, M. J., Lemonidis, K. M., Crooke, R. M., and Rudel, L. L. (2006) *Arterioscler Thromb Vasc Biol* **26**, 1814-1820
60. Farese, R. V., Jr. (2006) *Arterioscler Thromb Vasc Biol* **26**, 1684-1686
61. Moitra, K., and Dean, M. (2011) *Biol Chem* **392**, 29-37
62. Jones, P. M., O'Mara, M. L., and George, A. M. (2009) *Trends Biochem Sci* **34**, 520-531
63. Rees, D. C., Johnson, E., and Lewinson, O. (2009) *Nat Rev Mol Cell Biol* **10**, 218-227
64. Mizutani, T., Masuda, M., Nakai, E., Furumiya, K., Togawa, H., Nakamura, Y., Kawai, Y., Nakahira, K., Shinkai, S., and Takahashi, K. (2008) *Curr Drug Metab* **9**, 167-174
65. Frikke-Schmidt, R. (2010) *Atherosclerosis* **208**, 305-316
66. Brooks-Wilson, A., Marcil, M., Clee, S. M., Zhang, L. H., Roomp, K., van Dam, M., Yu, L., Brewer, C., Collins, J. A., Molhuizen, H. O., Loubser, O., Ouelette, B. F., Fichter, K., Ashbourne-Excoffon, K. J., Sensen, C. W., Scherer, S., Mott, S., Denis, M., Martindale, D., Frohlich, J., Morgan, K., Koop, B., Pimstone, S., Kastelein, J. J., Genest, J., Jr., and Hayden, M. R. (1999) *Nat Genet* **22**, 336-345
67. Bodzioch, M., Orso, E., Klucken, J., Langmann, T., Bottcher, A., Diederich, W., Drobnik, W., Barlage, S., Buchler, C., Porsch-Ozcurumez, M., Kaminski, W. E., Hahmann, H. W., Oette, K., Rothe, G., Aslanidis, C., Lackner, K. J., and Schmitz, G. (1999) *Nat Genet* **22**, 347-351
68. Rust, S., Rosier, M., Funke, H., Real, J., Amoura, Z., Piette, J. C., Deleuze, J. F., Brewer, H. B., Duverger, N., Denefle, P., and Assmann, G. (1999) *Nat Genet* **22**, 352-355
69. Vaughan, A. M., and Oram, J. F. (2006) *J Lipid Res* **47**, 2433-2443
70. Aye, I. L., Singh, A. T., and Keelan, J. A. (2009) *Chem Biol Interact* **180**, 327-339
71. Baldan, A., Bojanic, D. D., and Edwards, P. A. (2009) *J Lipid Res* **50 Suppl**, S80-85

72. Xu, J., Liu, Y., Yang, Y., Bates, S., and Zhang, J. T. (2004) *J Biol Chem* **279**, 19781-19789
73. Baldan, A., Tarr, P., Lee, R., and Edwards, P. A. (2006) *Curr Opin Lipidol* **17**, 227-232
74. Zhou, S., Morris, J. J., Barnes, Y., Lan, L., Schuetz, J. D., and Sorrentino, B. P. (2002) *Proc Natl Acad Sci U S A* **99**, 12339-12344
75. Jonker, J. W., Buitelaar, M., Wagenaar, E., Van Der Valk, M. A., Scheffer, G. L., Scheper, R. J., Plosch, T., Kuipers, F., Elferink, R. P., Rosing, H., Beijnen, J. H., and Schinkel, A. H. (2002) *Proc Natl Acad Sci U S A* **99**, 15649-15654
76. Mickley, L., Jain, P., Miyake, K., Schriml, L. M., Rao, K., Fojo, T., Bates, S., and Dean, M. (2001) *Mamm Genome* **12**, 86-88
77. Wang, N., Lan, D., Chen, W., Matsuura, F., and Tall, A. R. (2004) *Proc Natl Acad Sci U S A* **101**, 9774-9779
78. Tarr, P. T., and Edwards, P. A. (2008) *J Lipid Res* **49**, 169-182
79. Wang, N., Yvan-Charvet, L., Lutjohann, D., Mulder, M., Vanmierlo, T., Kim, T. W., and Tall, A. R. (2008) *FASEB J* **22**, 1073-1082
80. Graf, G. A., Yu, L., Li, W. P., Gerard, R., Tuma, P. L., Cohen, J. C., and Hobbs, H. H. (2003) *J Biol Chem* **278**, 48275-48282
81. Yu, L., Hammer, R. E., Li-Hawkins, J., Von Bergmann, K., Lutjohann, D., Cohen, J. C., and Hobbs, H. H. (2002) *Proc Natl Acad Sci U S A* **99**, 16237-16242
82. Yu, L., von Bergmann, K., Lutjohann, D., Hobbs, H. H., and Cohen, J. C. (2004) *J Lipid Res* **45**, 301-307
83. Wilund, K. R., Yu, L., Xu, F., Hobbs, H. H., and Cohen, J. C. (2004) *J Lipid Res* **45**, 1429-1436
84. Croop, J. M., Tiller, G. E., Fletcher, J. A., Lux, M. L., Raab, E., Goldenson, D., Son, D., Arciniegas, S., and Wu, R. L. (1997) *Gene* **185**, 77-85
85. Engel, T., Bode, G., Lueken, A., Knop, M., Kannenberg, F., Nofer, J. R., Assmann, G., and Seedorf, U. (2006) *FEBS Lett* **580**, 4551-4559
86. Gelissen, I. C., Cartland, S., Brown, A. J., Sandoval, C., Kim, M., Dinnes, D. L., Lee, Y., Hsieh, V., Gaus, K., Kritharides, L., and Jessup, W. (2010) *Atherosclerosis* **208**, 75-82
87. Klucken, J., Buchler, C., Orso, E., Kaminski, W. E., Porsch-Ozcurumez, M., Liebisch, G., Kapinsky, M., Diederich, W., Drobnik, W., Dean, M., Allikmets, R., and Schmitz, G. (2000) *Proc Natl Acad Sci U S A* **97**, 817-822
88. Vaughan, A. M., and Oram, J. F. (2005) *J Biol Chem* **280**, 30150-30157
89. Sturek, J. M., Castle, J. D., Trace, A. P., Page, L. C., Castle, A. M., Evans-Molina, C., Parks, J. S., Mirmira, R. G., and Hedrick, C. C. (2010) *J Clin Invest* **120**, 2575-2589
90. Xie, Q., Engel, T., Schnoor, M., Niehaus, J., Hofnagel, O., Buers, I., Cullen, P., Seedorf, U., Assmann, G., and Lorkowski, S. (2006) *Arterioscler Thromb Vasc Biol* **26**, e143-144; author reply e145
91. Wang, N., Ranalletta, M., Matsuura, F., Peng, F., and Tall, A. R. (2006) *Arterioscler Thromb Vasc Biol* **26**, 1310-1316
92. Kobayashi, A., Takanezawa, Y., Hirata, T., Shimizu, Y., Misasa, K., Kioka, N., Arai, H., Ueda, K., and Matsuo, M. (2006) *J Lipid Res* **47**, 1791-1802

93. Sankaranarayanan, S., Oram, J. F., Asztalos, B. F., Vaughan, A. M., Lund-Katz, S., Adorni, M. P., Phillips, M. C., and Rothblat, G. H. (2009) *J Lipid Res* **50**, 275-284
94. Sano, O., Kobayashi, A., Nagao, K., Kumagai, K., Kioka, N., Hanada, K., Ueda, K., and Matsuo, M. (2007) *J Lipid Res* **48**, 2377-2384
95. Venkateswaran, A., Laffitte, B. A., Joseph, S. B., Mak, P. A., Wilpitz, D. C., Edwards, P. A., and Tontonoz, P. (2000) *Proc Natl Acad Sci U S A* **97**, 12097-12102
96. Akiyama, T. E., Sakai, S., Lambert, G., Nicol, C. J., Matsusue, K., Pimprale, S., Lee, Y. H., Ricote, M., Glass, C. K., Brewer, H. B., Jr., and Gonzalez, F. J. (2002) *Mol Cell Biol* **22**, 2607-2619
97. Kennedy, M. A., Barrera, G. C., Nakamura, K., Baldan, A., Tarr, P., Fishbein, M. C., Frank, J., Francone, O. L., and Edwards, P. A. (2005) *Cell Metab* **1**, 121-131
98. Baldan, A., Tarr, P., Vales, C. S., Frank, J., Shimotake, T. K., Hawgood, S., and Edwards, P. A. (2006) *J Biol Chem* **281**, 29401-29410
99. Out, R., Hoekstra, M., Meurs, I., de Vos, P., Kuiper, J., Van Eck, M., and Van Berkel, T. J. (2007) *Arterioscler Thromb Vasc Biol* **27**, 594-599
100. Ranalletta, M., Wang, N., Han, S., Yvan-Charvet, L., Welch, C., and Tall, A. R. (2006) *Arterioscler Thromb Vasc Biol* **26**, 2308-2315
101. Baldan, A., Pei, L., Lee, R., Tarr, P., Tangirala, R. K., Weinstein, M. M., Frank, J., Li, A. C., Tontonoz, P., and Edwards, P. A. (2006) *Arterioscler Thromb Vasc Biol* **26**, 2301-2307
102. Out, R., Hoekstra, M., Hildebrand, R. B., Kruit, J. K., Meurs, I., Li, Z., Kuipers, F., Van Berkel, T. J., and Van Eck, M. (2006) *Arterioscler Thromb Vasc Biol* **26**, 2295-2300
103. Basso, F., Amar, M. J., Wagner, E. M., Vaisman, B., Paigen, B., Santamarina-Fojo, S., and Remaley, A. T. (2006) *Biochem Biophys Res Commun* **351**, 398-404
104. Yvan-Charvet, L., Ranalletta, M., Wang, N., Han, S., Terasaka, N., Li, R., Welch, C., and Tall, A. R. (2007) *J Clin Invest* **117**, 3900-3908
105. Sturley, S. L. (2000) *Biochim Biophys Acta* **1529**, 155-163
106. Basson, M. E., Thorsness, M., and Rine, J. (1986) *Proc Natl Acad Sci U S A* **83**, 5563-5567
107. Hampton, R. Y., and Rine, J. (1994) *J Cell Biol* **125**, 299-312
108. Sturley, S. L., Culbertson, M. R., and Attie, A. D. (1991) *J Biol Chem* **266**, 16273-16276
109. Lewis, T. L., Keesler, G. A., Fenner, G. P., and Parks, L. W. (1988) *Yeast* **4**, 93-106
110. Yang, H., Bard, M., Bruner, D. A., Gleeson, A., Deckelbaum, R. J., Aljinovic, G., Pohl, T. M., Rothstein, R., and Sturley, S. L. (1996) *Science* **272**, 1353-1356
111. Leber, R., Zinser, E., Zellnig, G., Paltauf, F., and Daum, G. (1994) *Yeast* **10**, 1421-1428
112. Guo, Z., Cromley, D., Billheimer, J. T., and Sturley, S. L. (2001) *J Lipid Res* **42**, 1282-1291
113. Jensen-Pergakes, K., Guo, Z., Giattina, M., Sturley, S. L., and Bard, M. (2001) *J Bacteriol* **183**, 4950-4957
114. Lorenz, R. T., Rodriguez, R. J., Lewis, T. A., and Parks, L. W. (1986) *J Bacteriol* **167**, 981-985

115. Raychaudhuri, S., and Prinz, W. A. (2006) *Biochem Soc Trans* **34**, 359-362
116. Gollub, E. G., Trocha, P., Liu, P. K., and Sprinson, D. B. (1974) *Biochem Biophys Res Commun* **56**, 471-477
117. Bourot, S., and Karst, F. (1995) *Gene* **165**, 97-102
118. Shianna, K. V., Dotson, W. D., Tove, S., and Parks, L. W. (2001) *J Bacteriol* **183**, 830-834
119. Vik, A., and Rine, J. (2001) *Mol Cell Biol* **21**, 6395-6405
120. Wilcox, L. J., Balderes, D. A., Wharton, B., Tinkelenberg, A. H., Rao, G., and Sturley, S. L. (2002) *J Biol Chem* **277**, 32466-32472
121. Gottesman, M. M., and Ambudkar, S. V. (2001) *J Bioenerg Biomembr* **33**, 451-451
122. Li, Y., and Prinz, W. A. (2004) *J Biol Chem* **279**, 45226-45234
123. Tiwari, R., Koffel, R., and Schneiter, R. (2007) *EMBO J* **26**, 5109-5119
124. Mason, A. B., and Dufour, J. P. (2000) *Yeast* **16**, 1287-1298
125. Kang, M. H., Singaraja, R., and Hayden, M. R. (2010) *Trends Cardiovasc Med* **20**, 41-49

# Chapter 2: Changes in the Intracellular Sterol Environment Influence Transport Activity of Members of the ABCG Subfamily

## Abstract

ATP-binding cassette (ABC) transporters represent a group of evolutionarily conserved transmembrane proteins that have recently been implicated in intracellular lipid trafficking. Most significantly, mutations in the ABC transporter ABCA1, were found to be the underlying molecular defect in Tangier disease, highlighting its role as a key regulator of HDL metabolism. ABCA1 along with ABCG1/G4 (members of the ABCG subfamily) are recognized as key components of the reverse cholesterol transport pathway. To date, the ABC superfamily in higher eukaryotes has been associated with anterograde movement of sterol across the plasma membrane. However, we have demonstrated that the opposite (i.e inward) transport of sterol in yeast is also dependent on two members of the ABCG subfamily (Aus1p and Pdr11p), raising the question whether direction of transport is an inherent property of the transporter or is dictated by the lipid and protein microenvironment in which the transporter resides. To answer this question we expressed mABCG1 in budding yeast and assessed intracellular cholesterol levels in various genetic backgrounds. We found that expression of mABCG1 in budding yeast can increase or decrease the concentration of exogenous sterols found inside the cell in response to an altered intracellular sterol microenvironment. Moreover, we found that Aus1p and Pdr11p contribute to the efflux of a sterol derivative, steryl acetate. A deletion of either *AUS1* or *PDR11* results both in a significant intracellular accumulation and a decrease in the extracellular concentration of cholesteryl acetate. Our findings suggest that ABC transporter activity for this subfamily is influenced by the intracellular sterol environment.

## Introduction

The fundamental role of the plasma membrane is to provide a barrier to the extracellular environment, while precisely regulating the transit of molecules in and out of cell. ATP-binding cassette (ABC) transporters are essential constituents of the membrane transport machinery (1). These transporters utilize energy derived from ATP binding and/or hydrolysis to transport a vast array of substrates across membranes, usually against a concentration gradient (1). This protein superfamily represents one of the largest classes of transport proteins and is conserved throughout evolution (2). *Human ABC transporters are classified into seven families (six of which are found in Saccharomyces cerevisiae) (3), based on* similarity in protein topology, number of domains, and on sequence identity in the nucleotide binding and transmembrane domains. Members of the seven families of human ABC transporters mediate various biological processes such as cholesterol and lipid transport, multidrug resistance, and the ATP-dependent regulation of ion channels. Mutations in these proteins have been associated with a myriad of diseases, including cystic fibrosis, Tangier disease, and diabetes (2).

As many as one third of human ABC transporters facilitate lipid or cholesterol movement across membranes (4). ABC transporters were first implicated in intracellular cholesterol trafficking when mutations in ABCA1, were identified as the molecular defect in Tangier disease, highlighting its role as a key regulator of HDL metabolism (5). Today, ABCA1 along with ABCG1/G4 are recognized as key components of the reverse cholesterol transport pathway (6). ABCG1 and ABCG4 act in concert with ABCA1 to maximize the removal of excess cholesterol from cells by promoting cholesterol efflux onto mature and nascent HDL particles, respectively (7). To date, mammalian ABC transporters are exclusively associated with efflux of cholesterol (4).

In budding yeast, as in mammalian cells, members of the ABCG subfamily facilitate sterol transport from membranes (8). Aus1p and Pdr11p are full ABC

transporters, which are 26% and 27% identical to ABCG1, respectively (https://portal.biobase-international.com/cgi bin/build_ghpywl/idb/1.0/searchengine/start.cgi). In contrast to their mammalian counterparts, Aus1p and Pdr11p mediate sterol influx from the environment when sterol biosynthesis is compromised such as during anaerobiosis (8). The deletion of either *AUS1* or *PDR11* results in a significant decrease in sterol uptake and esterification. The loss of both ABC transporters during anaerobiosis results in a complete abatement of sterol import and a loss of viability, which can be complemented by the expression of either transporter (8). In addition to Aus1p and Pdr11p, the ACAT related sterol esterifying enzymes (Are1p and Are2p) and Dan1p, a cell wall mannoprotein, also play an instrumental role in mediating sterol influx (8,9). Deletion of these genes produces a significant decrease in sterol uptake (8). However, the precise mechanism by which these proteins mediate sterol influx has not been elucidated.

Once imported into the cell via the sterol influx pathway, it was previously thought that sterols in budding yeast undergo one of two possible fates. Incoming sterols can either be incorporated into membranes or esterified and stored in cytosolic lipid droplets (10,11). Recent data has shown that sterols can also be acetylated and effluxed from the cell (12). Steryl acetate export is mediated by a sterol acetylation/deacetylation cycle, in which acetylation by Atf2p marks the sterol for export, whereas deactelyation by Say1p targets it for retention in the cell. Moreover, steryl acetate efflux requires ATP, the presence of an exogenous acceptor molecule, and an intact secretory pathway (12). Characterization of the efflux pathway is incomplete, as the mechanisms that mediate the actual efflux of steryl acetate have not been identified.

Cholesterol movement across membranes in budding yeast and mammalian cells requires members of the ABCG subfamily (4,8). In either model system, these transporters localize to the plasma membrane where they promote the flux of cholesterol across a membrane (8,13). However, the net transport of cholesterol occurs in opposite directions. The transport of the same sterol

substrate in opposite directions in these two model systems, highlights an important question about the mechanism by which ABC transporters mediate the transport of sterols. In particular what determines directionality of transport? The comparison between these contrasting states (opposite transport of the same substrate) will allow us to dissect whether sterol transport is an inherent property of the transporter or dictated by the microenvironment (defined as the surrounding proteins and lipids that the transporter resides in) (Chapter 1, Figure 4). We hypothesize that directionality of transfer is either an inherent property of the transporter or determined by the microenvironment in which it resides.

In order to elucidate the mechanisms that dictate direction of transport we expressed murine ABCG1 (mABCG1) in budding yeast and assessed cholesterol flux. We observed that expression of mABCG1 varied the concentration of exogenous radiolabelled cholesterol found within the cell, depending on sterol status of the intracellular microenvironment. Furthermore, we found that the budding yeast orthologues of ABCG1, Aus1p and Pdr11p, contribute to the efflux of cholesteryl acetate as a function of their interactions with the cellular lipid and proteo-lipid environment. These finding suggest that mABCG1, Aus1p, and Pdr11p promote bi-directional transport in order to maintain sterol homeostasis. This is the first example of eukaryotic ABC transporters being able to mediate anterograde and retrograde transport of sterol and a sterol derivative. The manner in which this is achieved will be the focus of this chapter.

**Materials and Methods**

*General*.Yeast strains used in this study are isogenic with the strain W303-1A (*Table 1)*. These strains were transformed with pRS424-GPD/ABCG1 or pRS424-GPD using lithium acetate followed by prototrophic selection. *SAY1* deletion strains were generated using the one-step PCR mediated gene disruption (14).

*Analysis of exogenous sterol accumulation, acetylation, and esterification.* In pulse label studies cells were grown to mid-log phase in the appropriate media

and inoculated with 1% tyloxapol/ethanol (1:1) and 0.01 μCi/ml [4-$^{14}$C]cholesterol for four hours. The net accumulation of [4-$^{14}$C]cholesterol in the cells was measured by scintillation counting. For steady state studies, cells were grown for approximately 20 h in the indicated media containing 1% tyloxapol/ethanol (1:1) and 0.01 μCi/ml [4-$^{14}$C] cholesterol. The net accumulation of [4-$^{14}$C]cholesterol in the cells was measured by scintillation counting. Assays were performed on three independent isolates of each genotype. Statistical analysis was performed using Student's *t* tests.

For quantification of cholesteryl acetate, mutant strains were cultured with 1% tyloxapol/ethanol (1:1) and 0.01 μCi/ml [4-$^{14}$C]cholesterol for 20 hours. Cells were washed and grown in fresh media containing 40 μg/ml of cold cholesterol for 20 hours. Lipid were extracted from the media and the dried cell pellet by organic extraction by established methods and resolved by TLC in petroleum ether/diethyl ether/acetic acid (84:15:1). Lipids were detected using iodine staining and quantified via scintillation counting. Assays were performed on three independent isolates of each genotype. Statistical analysis was performed using Student's *t* tests.

*Northern Blotting*. RNA was isolated as previously described and resolved on a 1.2% agarose, formaldehyde gel. The membrane was hybridized with a random oligonucleotide-primed (Stratagene) [$^{32}$P dCTP-labeled probe, made from PCR-generated inserts of each gene examined. The hybridization was carried out in QuikHyb buffer (Stratagene) for 1 h at 65 °C. The membrane was washed twice with 2× saline-sodium citrate (SSC) buffer, 0.1% sodium lauryl sulfate (SDS) at room temperature and once with 0.1× SSC, 0.1% SDS at 65 °C.

*Growth Curves*. Growth curves were obtained using a Microbiology Workstation Bioscreen C (Thermo Electron Corp.) and Research Express Bioscreen C software (Transgalactic Ltd.). Cultures (three isolates per genotype) were normalized to an $A_{600}$ of 0.1, and 10 μl of each strain was added to 290 μl of the appropriate media per well.

*Lipid Droplet Isolation and Quantification*. The indicated strains were grown in 500 ml YPD overnight at 30 °C for 20 hours. Cells were washed and lysed, and microsomes were prepared from a 100,000 × *g* spin, as previously described. The lipid rich fraction at top of the centrifuge tube was collected. Lipids were extracted as described above. Protein concentrations were determined utilizing the Lowry method.

**Results**

Expression of *mABCG1 mediates sterol transport in budding yeast.* ABCG1 plays a pivotal role in promoting cholesterol efflux and is the most similar mammalian transporter to Aus1p and Pdr11p (45% and 44% sequence similarity, respectively). All three proteins are members of the ABCG subfamily and therefore possess the characteristic topology of having their nucleotide binding domain N-terminal to the transmembrane domain (Chapter 1, Figure 3) (15,16). To determine if mABCG1 can modulate sterol transport in budding yeast, we expressed mABCG1 in strains deleted for key mediators of sterol influx. These null mutants were generated in a *upc2-1* background, which consists of a gain of function mutation in the transcription factor *UPC2* that allows for aerobic sterol uptake (17). Expression of mABCG1 mRNA was confirmed by northern blot analysis (Figure 1A & 1B). Additionally, to ensure that expression of mABCG1 does not hinder the enhanced transcriptional regulation conferred by *upc2-1*, we assessed the expression of a known Upc2p target, *DAN1* in the presence of mABCG1. We found that expression of *DAN1* was unaffected by mABCG1 (Figure 1C). This indicates that transcriptional regulation by Upc2-1p is unaltered in strains expressing vector control or mABCG1.

To ascertain the ability of mABCG1 to compensate for the loss of either Aus1p or Pdr11p, we expressed mABCG1 in strains deleted for either endogenous ABC transporter (Figure 2A). These strains were grown to mid-log and then pulse labeled with [$^{14}$C] cholesterol. Due to the limited availability of radiolabled ergosterol, [$^{14}$C] cholesterol is used as a marker for sterol metabolism

in budding yeast. Previous studies have shown that cholesterol is taken up, metabolized, and trafficked in a manner similar to ergosterol (9)(4). Expression of mABCG1 in *pdr11Δ* and *aus1Δ* strains resulted in approximately 100% and 200% increases respectively, in intracellular cholesterol as compared to vector control (Figure 2A). This suggests that mABCG1 is able to mediate the influx of cholesterol in the absence of the endogenous sterol-importing ABC transporters and is therefore a functional homologue of Aus1p and Pdr11p. Furthermore, expression of mABCG1 in an *AUS1* deletion strain produced a significant increase in steryl esters, indicating that mABCG1 mediated influx reflects metabolism of sterol and not just binding to the cell (Figure 2B). Additionally, it also suggests that cholesterol imported by mABCG1 is trafficked and metabolized in a similar manner to sterols influxed by Aus1p and Pdr11p. Expression of mABCG1 had the most striking effect in an *are1Δ are2Δ* double deletion, where it increased sterol influx five times more than vector control (Figure 2A). Expression of mABCG1 had no effect on intracellular cholesterol levels in an *aus1Δ pdr11Δ* strain (Figure 2A). Conversely, the presence of mABCG1 in a *upc2-1* strain resulted in a decrease in intracellular cholesterol levels as compared to vector control (in a *upc2-1* strain) (Figure 2A). This data suggests that mABCG1 may be promoting cholesterol efflux in this context.

In order to further demonstrate the manner in which ABCG1 mediated activity responds to the cells needs, we labeled cells expressing mABCG1 to steady state with [$^{14}$C] cholesterol (Figure 3). We found that expression of mABCG1 produces a 75% increase in intracellular cholesterol in a *upc2-1* strain, whereas it decreases cholesterol levels in an *are1Δ are2Δ* strain by 50%. In an *aus1Δ* strain, expression of mABCG1 had no effect on intracellular sterol levels as compared to vector control. These data suggest that mABCG1 is able to modulate intracellular cholesterol levels presumably by mediating both influx and efflux of cholesterol. Furthermore, it appears that the cellular microenvironment influences how mABCG1 modulates intracellular cholesterol levels.

*Cholesteryl Acetate efflux is affected by the deletions of Aus1p, Pdr11p, and the esterifying enzymes*. To assess if yeast members of the ABCG subfamily are capable of promoting bi-directional transport, we measured the acetylation of [$C^{14}$] cholesterol in the absence of Aus1p or Pdr11p (Figure 4A & 4B). We found that deletion of either *AUS1* or *PDR11* in a *SAY1* mutant strain results in a significant intracellular accumulation of cholesteryl acetate and a significant decrease in extracellular cholesteryl acetate. Additionally, there was no significant difference in the percent of free cholesterol or cholesteryl ester between the double and single mutants. These data represent the first example of a eukaryotic ABC transporter mediating influx and efflux in the same organism.

In addition to Aus1p and Pdr11p, it has been shown that a deletion of the cell wall protein *DAN1* and the esterifying enzymes, *ARE1* and *ARE2* significantly decrease sterol uptake (8,9). In order to ascertain if these proteins also play a significant role in the export of cholesteryl acetate, we measured the percent of [$^{14}$C] cholesterol that is acetylated in a *dan1Δ say1* and an *are1Δ are2Δ say1Δ* strain (Figure 4). We found that efflux of cholesteryl acetate is independent of Dan1p. In contrast, the *are1Δ are2Δ say1Δ* strain exhibited an estimated four-fold increase in intracellular cholesteryl acetate levels as compared to *say1Δ*. This data suggests that excess free cholesterol is acetylated and primed for export, in the absence of the esterification reaction.

*Ergosteryl acetate accumulation doesn't affect viability.* To discern if the cholesteryl acetate accumulation seen in the *aus1Δ say1Δ, pdr11Δ say1Δ,* and *are1Δ are2Δ say1Δ* strains is toxic, we performed a viability assay in the presence of 160μg/ml of cholesterol (Figure 5). This concentration of cholesterol is eight times higher than what is utilized to support anaerobic growth. We found that the double and triple deletion strains grew at a similar rate as a *say1Δ* single deletion in the presence of excess exogenous cholesterol. This therefore suggests that this cholesterol derivative is stored in such a manner that it is not toxic to the cell.

*Ergosteryl acetate is found in lipid droplets.* Lipid droplets protect the cell from sterol toxicity by providing an inert respository for excess free cholesterol. To determine if lipid droplets play a similar role for cholesteryl acetate, we isolated lipid droplets and looked for the presence of cholesteryl acetate (Figure 6). Lipid droplets from an *aus1Δ say1Δ* and *say1Δ* strain contained cholesteryl acetate. This data demonstrates that cholesteryl acetate can be stored in a lipid droplet.

*mABCG1 promotes free cholesterol and cholesteryl acetate efflux in a say1Δ*. The established role of mammalian ABC transporters is to promote sterol efflux, as such we wanted to assay if mABCG1 can also efflux cholesteryl acetate (Figure 7). We found that mACBG1 was unable to rescue the cholesteryl acetate accumulation observed in an *aus1Δ say1Δ* and in an *are1Δ are2Δ say1Δ* strain. However when expressed in a *say1Δ* strain, mABCG1 significantly increased the efflux of both cholesteryl acetate and free cholesterol.

**Discussion**

Cholesterol homeostasis is essential to the cell and therefore is precisely regulated by multiple proteins and pathways working in concert (18). ABC transporter mediated movement of cholesterol is an integral component of cholesterol homeostasis; the loss of which in some conditions can result in significantly decreased viability in both macrophages and budding yeast (8,18). However, despite the pivotal role that ABC transporters play in preserving cholesterol homeostasis, very little is known about the mechanism that facilitates transport of sterols by these proteins (4). The data presented here demonstrate that alterations in the sterol microenvironment of the cell influence the transport properties of these proteins. We found that expression of mABCG1 in budding yeast is capable of altering intracellular cholesterol levels.

Expression of mABCG1 in a *upc2-1* strain produced a significant decrease in intracellular sterols as compared to vector control in the same background.

This observation may be attributed to the fact that in a *upc2-1* strain, sterol biosynthesis and sterol uptake occur concurrently (4), therefore mABCG1 mediated efflux may provide the cell with a rapid and alternate sterol detoxification pathway. Conversely, when mABCG1 was expressed in strains with diminished sterol uptake (*aus1Δ, pdr11Δ, are1Δ are2Δ)* it produced a significant increase in sterol influx as compared to vector control. This increase in uptake may reflect the cell's metabolic need for sterols. Moreover, the partial rescue of the sterol uptake phenotype of *are1Δ are2Δ* by the expression of an ABC transporter, suggests that the decrease in uptake seen in an *are1Δ are2Δ* strain (9) may be due to a negative feedback inhibition of Aus1p and Pdr11p. Surprisingly, mABCG1 was unable to mediate sterol influx in an *aus1Δ pdr11Δ* strain. This observation may demonstrate an inability of mABCG1 to interact with cell wall proteins that have been shown to mediate sterol influx (8). Alternatively, mABCG1 mediated sterol transport may require that sterol first bind to to Aus1p or Pdr11p and as a result requires their expression to mediate sterol influx.

When we performed a steady state label of the various deletion strains we found conflicting results from our pulse label studies. Expression of mABCG1 in *upc2-1*, *are1Δ are2Δ,* and *aus1Δ* strains produces a significant increase, a significant decrease, and no change in intracellular sterol levels respectively.

We hypothesize that the opposing effects exerted by mABCG1 are due to the varying intracellular cholesterol kinetics seen in a transient state (pulse label) versus a steady state. The opposing effects exerted by mABCG1 in these two contrasting states in the same strain highlights that the metabolic needs and environment of the cell modulate cholesterol transport by mABCG1. The data presented here exhibits the first occurrence of a mammalian ABC transporter mediating retrograde transport of cholesterol depending on the cellular context. Moreover, we have shown that expression of mABCG1 in budding yeast can also decrease intracellular levels and promote cholesterol efflux. Similar to mammalian cells, efflux of cholesterol by ABCG1 in budding yeast was accompanied by a corresponding decrease in intracellular cholesterol levels. As

such we propose that mABCG1 mediated decrease in intracellular levels reflects efflux of sterols.

Similarly, we have also shown that Aus1p and Pdr11p may mediate bi-directional transport. In addition to their established role of promoting sterol influx (8), we have shown that Aus1p and Pdr11p contribute to the efflux of cholesteryl acetate. However, surprisingly deletion of either transporter did not abolish cholesteryl acetate completely. This data suggests that either transporter can partially compensate for the loss of the other. The observation that Atf2p, Aus1p and Pdr11p function in the same pathway is corroborated by Wilcox et al., who reported that these genes are all upregulated by a common transcription factor, Upc2p (8). The production and export of cholesteryl acetate contributes to the maintenance of sterol homeostasis (12). Therefore, like mABCG1, Aus1p and Pdr11p, can alter direction of transport of direction to preserve sterol homeostasis. Surprisingly, expression of mABCG1 was not able to rescue the intracellular cholesteryl acetate accumulation associated with an *are1Δ are2Δ say1Δ* or *aus1Δ say1Δ* mutants. In both strains, sterol uptake and esterification is significantly decreased (4). As such these strains may be compensating for the loss of a sterol resevoir by storing steryl acetate, as seen in an *aus1Δ say1Δ* mutant. Conversely, when the ability to store sterols is intact such as in a *say1Δ* strain, then the homeostatic reaction is pushed towards efflux. This data further indicates that the sterol microenvironment of the cell, in this case steryl ester stores, may influence ABCG1 mediated transport activity.

We have utilized *a model system to explore the factors that* influence direction of transport by members of the ABCG subfamily. Our data collectively shows that changes in the surrounding sterol environment of the transporter can elicit a change in direction of substrate transport. Moreover, this data suggests that direction of transport is not a static property of the transporter but rather can adapt in response to environmental cues. Similarly, expression of mABCG1 in baby hamster kidney cells redistributed membrane cholesterol to cholesterol oxidase-accessible surface domains, which could then either be effluxed to $HDL_3$

or influxed to the esterifying enzymes (19). As such we posit that cholesterol transporting ABC transporters do not possess directionality *per se*, but utilize energy from ATP hydrolysis to redistribute membrane cholesterol in order to enhance its rate of projection from the membrane. Biophyscial studies have demonstrated that sterols not in lipid ordered domains are more susceptible to cholesterol oxidase and possess enhanced collisional interactions with water-soluble reactants (20). However, the observation that ABC transporter mediated cholesterol movement does indeed modulate direction in response to the cellular environment can't be ignored. We propose that direction of transport is dictated by cellular cues, specifically, by the balance of extracellular and intracellular protein/lipid acceptors. Interestingly, in baby hamster kidney cells the proportion of free cholesterol imported to the ACATs decreased in the presence of $HDL_3$ (19). This suggests that the presence of $HDL_3$ tipped the direction of transport towards efflux (19). Identifying the intracellular and extracellular acceptor molecules will be paramount in understanding how these ABC transporters maintain cholesterol homeostasis. The data presented here highlights the constant need of the cell to strike a precise balance between sterol esterification and efflux. In the next two chapters we further expound on the proteins that help mediate and regulate this balance.

**Table 1. Strains utilized in this study**

| Strain | Relevant Genotype | Reference |
|---|---|---|
| SCY955 | *MAT**a upc2-1 hi**, ade2-1, can1-1, trp1-1, ura3-1, his3-11, 15, leu2-3, 112* | (4) |
| SCY1837 | *MAT**a upc2-hi,** ade2-1, can1-1, trp1-1, ura3-1, his3-11, 15, leu2-3, 112, pdr11::URA3, GFP-AUS1* | (4) |
| SCY2916 | *MAT**a upc2-1 hi,** ade2-1, can1-1, trp1-1, ura3-1, his3-11, 15, leu2-3, 112, aus1::URA3, GFP-PDR11* | (4) |
| SCY267 | *MAT**a upc2-1 hi,** ade2-1, can1-1, trp1-1, ura3-1, his3-11, 15, leu2-3, 112, are1::HIS2, are2::URA3* | (4) |
| SCY1296 | *MAT**a upc2-1 hi,** ade2-1, can1-1, trp1-1, ura3-1, his3-11, 15, leu2-3, 112, dan1::URA3* | (4) |
| SCY2120 | *MAT**a upc2-1 hi,** ade2-1, can1-1, trp1-1, ura3-1, his3-11, 15, leu2-3, 112, aus1::URA3, pdr11::LEU2* | (4) |
| SCY1837a | *MAT**a upc2-hi,** ade2-1, can1-1, trp1-1, ura3-1, his3-11, 15, leu2-3, 112, pdr11::URA3, GFP-AUS1, say1::Nat* | This study |
| SCY2196a | *MAT**a upc2-1 hi,** ade2-1, can1-1, trp1-1, ura3-1, his3-11, 15, leu2-3, 112, aus1::URA3, GFP-PDR11, say1::Nat* | This study |
| SCY1296a | *MAT**a upc2-1 hi,** ade2-1, can1-1, trp1-1, ura3-1, his3-11, 15, leu2-3, 112, dan1::URA3, say1::Nat* | This study |
| SC207a | *MAT**a upc2-1 hi,** ade2-1, can1-1, trp1-1, ura3-1, his3-11, 15, leu2-3, 112, are1::HIS2, are2::URA3, say1::NAT* | This study |

**Table 2. Primers utilized in this study**

| Primer | Sequence |
|---|---|
| 5' *SAY1* KO | ATGGCAGCCAACTCTGGTCTCGACTCAAAAGTTGAATATTAT CGGCTTCAAcatggaggcccagaataccc |
| 3' *SAY1* KO | TCAGGATTGCATAAACTCAAGAATGCGAGCGATAGATGGTA TGTTGGTCCgcagtatagcgaccagcattcac |

**Figure 1**

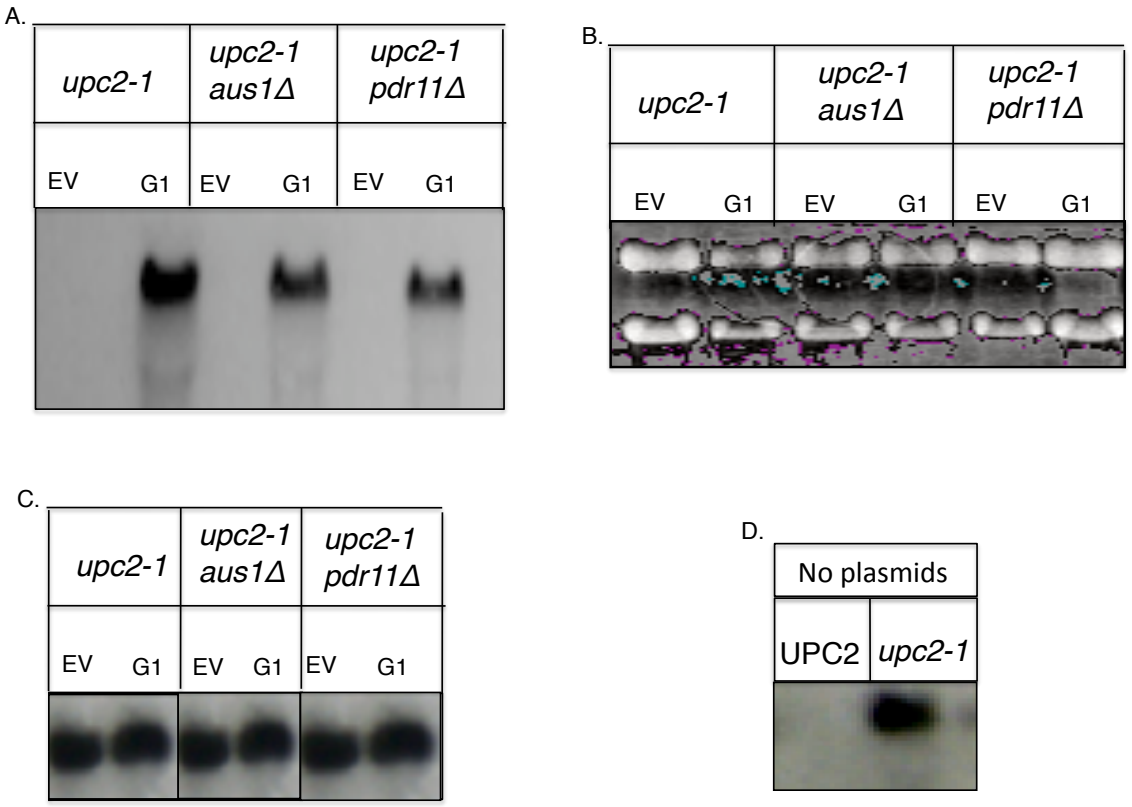


**Figure 1**. **Northern blot analysis of mabcg1 and *DAN1* expression in strains expressing mABCG1.**

**A.** The indicated strains were transformed with PRS424-GPD and PRS424-GPD/mABCG1. RNA was isolated from these strains and subjected to northern blot analysis utilizing a [$^{32}$P]dCTP-labeled probe made from PCR-generated inserts of mABCG1. We found mABCG1 expression in various genetic backgrounds. **B.** Ethidium bromide staining exhibits equal loading of RNA.

**C.** RNA was isolated from the indicated strains and subjected to northern blot analysis utilizing a [$^{32}$P]dCTP-labeled probe made from PCR-generated inserts of *DAN1*. *DAN1* expression was unaffected by the presence of a mABCG1. **D.** RNA was isolated from UPC2 and *upc2-1* strains and subjected to northern blot analysis utilizing a [$^{32}$P]dCTP-labeled probe made from PCR-generated inserts of *DAN1*.

**Figure 2**

**A**

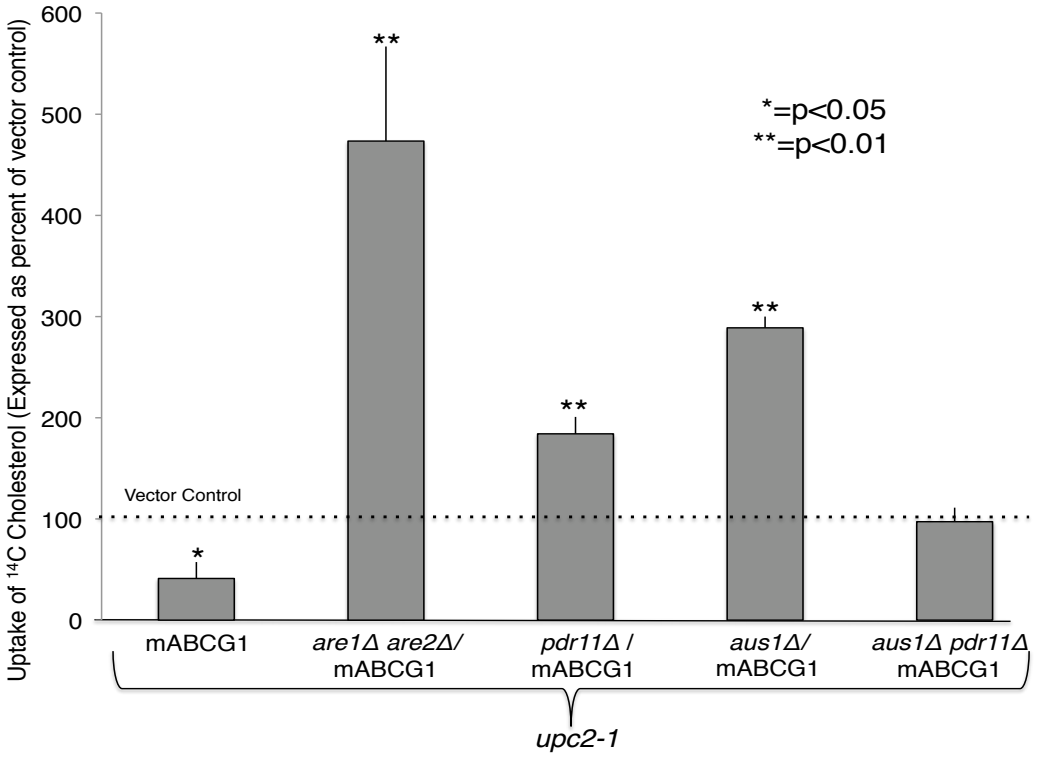


**Figure 2A. Expression of mABCG1 alters intracellular cholesterol concentration and distribution.** The indicated strains were transformed with pRS424-GPD (empty vector or vector control) or pRS424-GPD/mABCG1. Cells were grown to mid-log phase and labeled with media containing 0.01 µCi/ml [4-$^{14}$C]cholesterol for four hours. Net accumulation $^{14}$C]cholesterol in the cells was measured as described under "Experimental Procedures". Experiments were performed in triplicate and the data above reflects the mean % of ± S.E intracellular [4-$^{14}$C]cholesterol of vector control in the same background. Asterisks denote statistically significant difference from vector control for strains of the same background expressing pRS424-GPD/mABCG1 with $p<0.05$ (*) and $p<0.001$ (**) by unpaired t-test.

**B.**

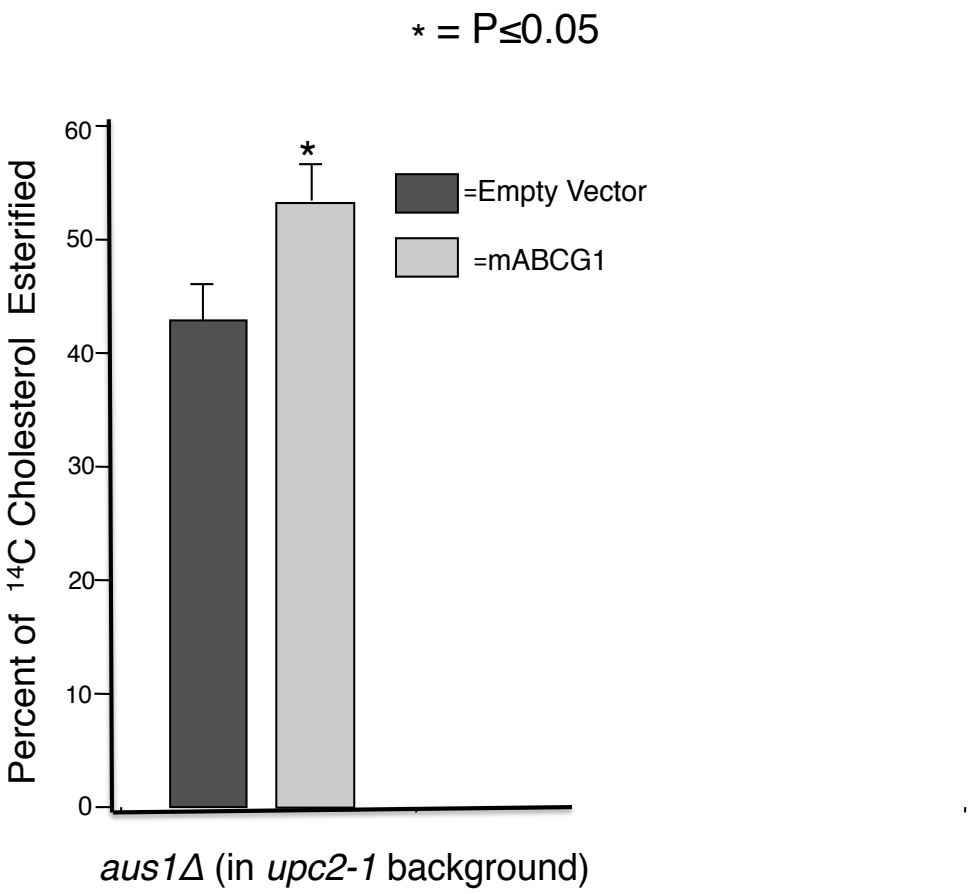


**Figure 2B. Expression of mABCG1 alters intracellular cholesterol concentration and distribution** Cells were grown to mid-log phase and labeled with media containing 0.01 µCi/ml [4-$^{14}$C]cholesterol for four hours. Lipids were extracted from the dried pellet by organic extraction and resolved by TLC in petroleum ether/diethyl ether/acetic acid (84:15:1). Experiments were performed in triplicate and the data above reflects the mean % of ± S.E intracellular [4-$^{14}$C]cholesterol of vector control in the same background. Asterisks denote statistically significant difference from vector control for strains of the same background expressing pRS424-GPD/mABCG1 with $p<0.05$ (*) by unpaired t-test.

**Figure 3**

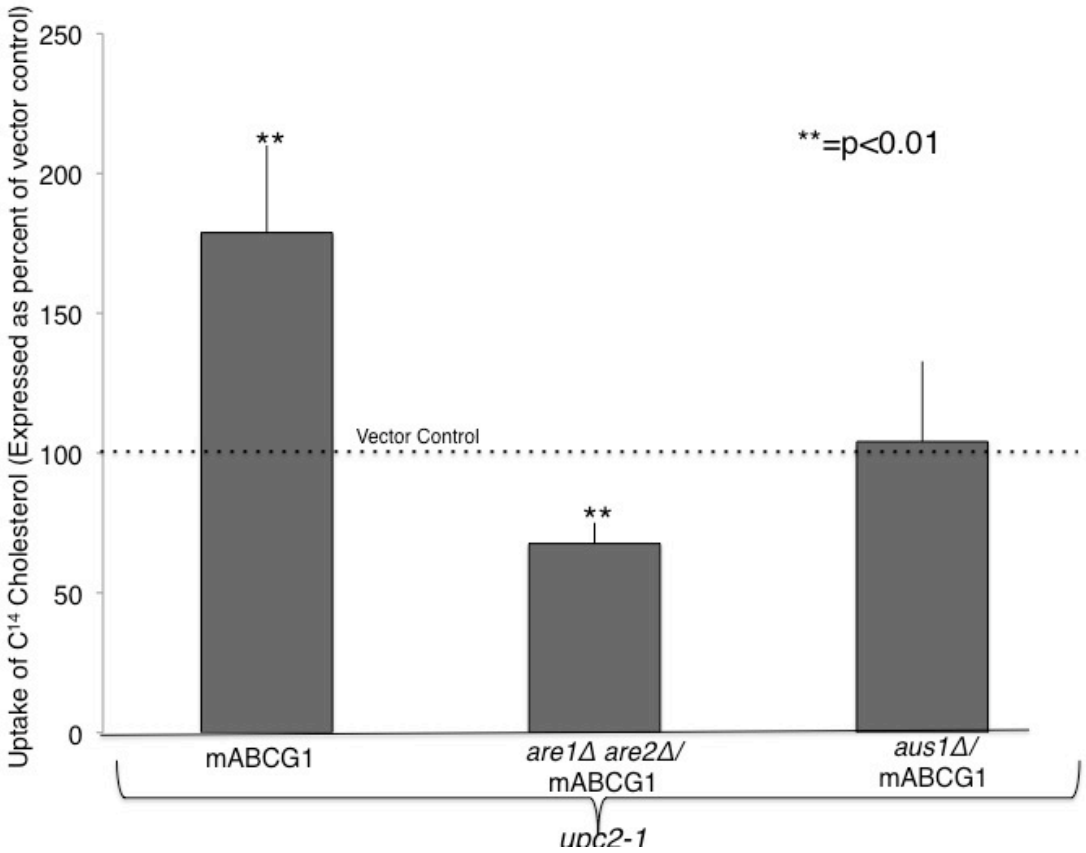


**Figure 3. Expression of mABCG1 alters intracellular cholesterol levels in cells labeled to steady state with [4-$^{14}$C]cholesterol.** Cells were grown for approximately 20 hours in the appropriate media containing 1% tyloxapol/ethanol (1:1) and 0.01 µCi/ml [4-$^{14}$C]cholesterol. Net accumulation of [4-$^{14}$C]cholesterol in the cells was measured as described under "Experimental Procedures" and reflects the mean % of cholesteryl ester of the *upc2-1* hi strain. Experiments were performed in triplicate and and the data above reflects the mean % of ± S.E intracellular [4-$^{14}$C]cholesterol of vector control in the same background. Asterisks denote statistically significant difference from vector control for strains of the same background expressing pRS424-GPD/mABCG1 with $p<0.01$ (**) by unpaired t-test.

**Figure 4.**

**A**

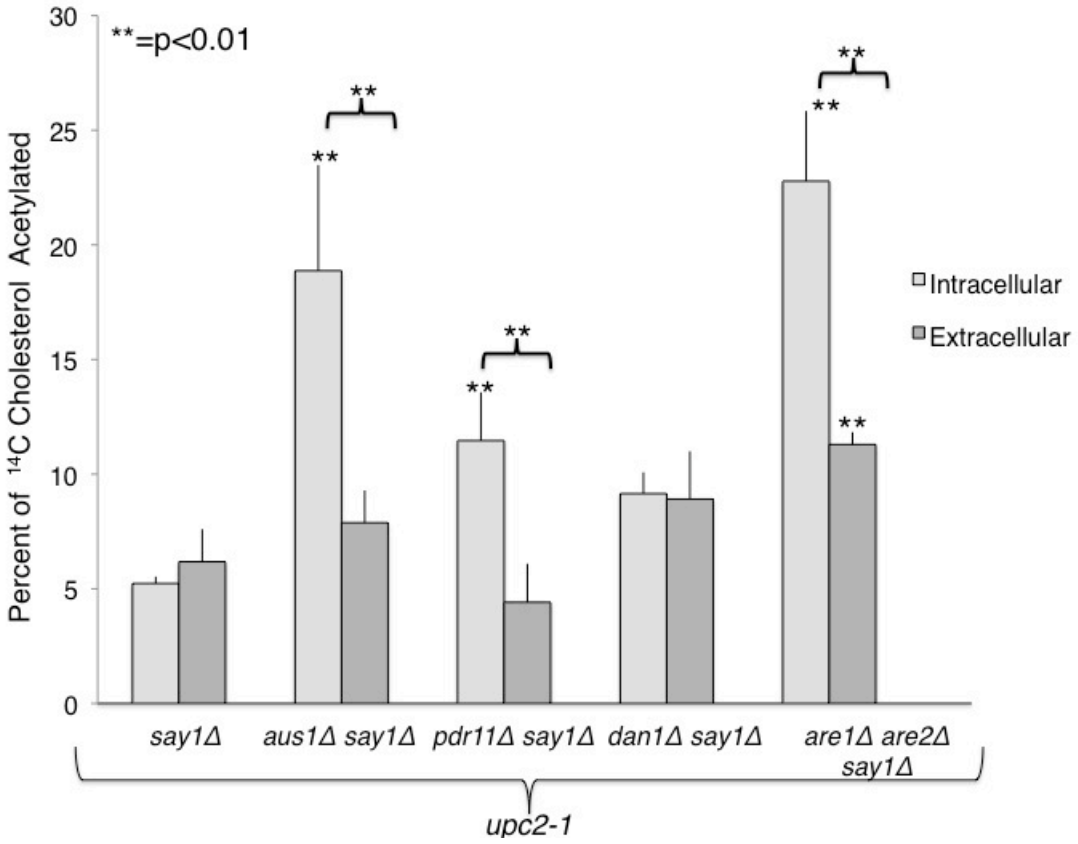


**Figure 4A. Aus1p, Pdr11p, and the esterifying enzymes affect cholesteryl acetate metabolism. A.** The indicated strains were cultured with 1% tyloxapol/ethanol (1:1) and 0.01 µCi/ml [4-$^{14}$C]cholesterol for 20 hours. Cells were washed and grown in fresh media containing 40 ug/ml of cold cholesterol for 20 hours. Lipid were extracted, resolved, and quantified as described in "Materials and Methods". Experiments were performed in triplicate and the data above reflects the mean % of ± S.E exogenous [4-$^{14}$C]cholesterol acetylated intracellularly and in the culture media. Asterisks denote statistically significant difference from the control strain with $p<0.01$ (**) by unpaired t-test.

**B.**

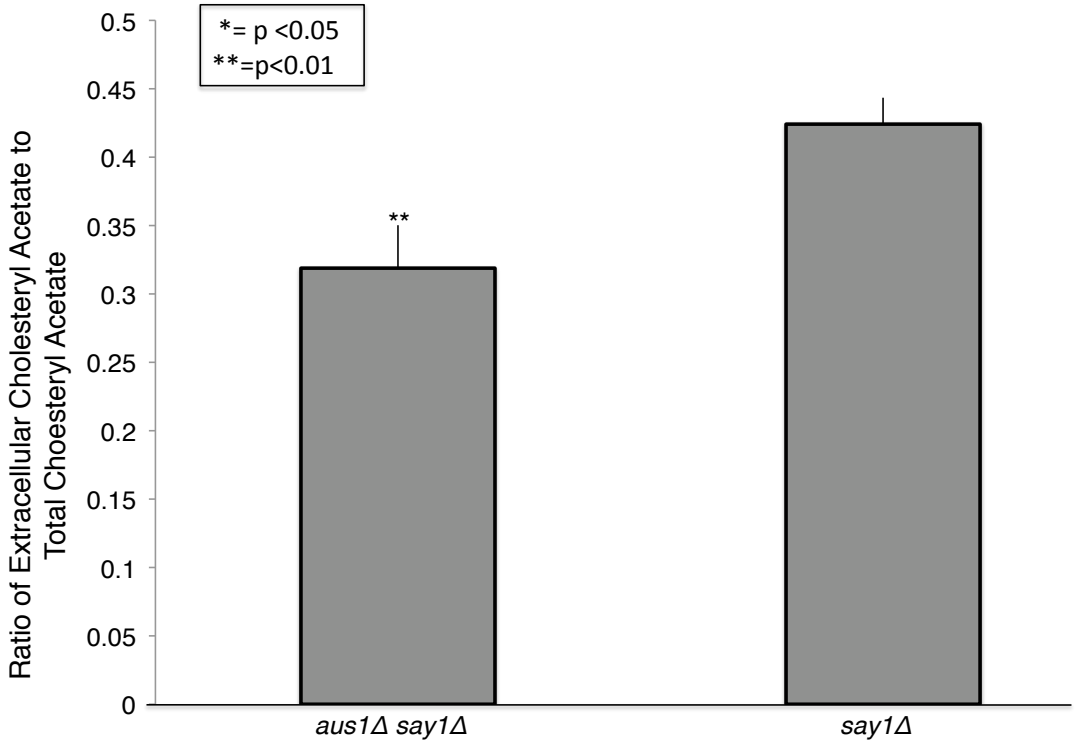


**Figure 4B. Aus1p, Pdr11p, and the esterifying enzymes affect cholesteryl acetate metabolism. A.** The indicated strains were cultured with 1% tyloxapol/ethanol (1:1) and 0.01 µCi/ml [4-$^{14}$C]cholesterol for 20 hours. Cells were washed and grown in fresh media containing 40 ug/ml of cold cholesterol for 20 hours. Lipid were extracted, resolved, and quantified as described in "Materials and Methods". Experiments were performed in triplicate and the data above reflects the ratio of % of exogenous [4-$^{14}$C]cholesterol acetylated over total % of ± S.E exogenous [4-$^{14}$C]cholesterol acetylated . Asterisks denote statistically significant difference from the control strain with $p<0.05$ (*) and $p<0.01$ (**) by unpaired t-test.

**C.**

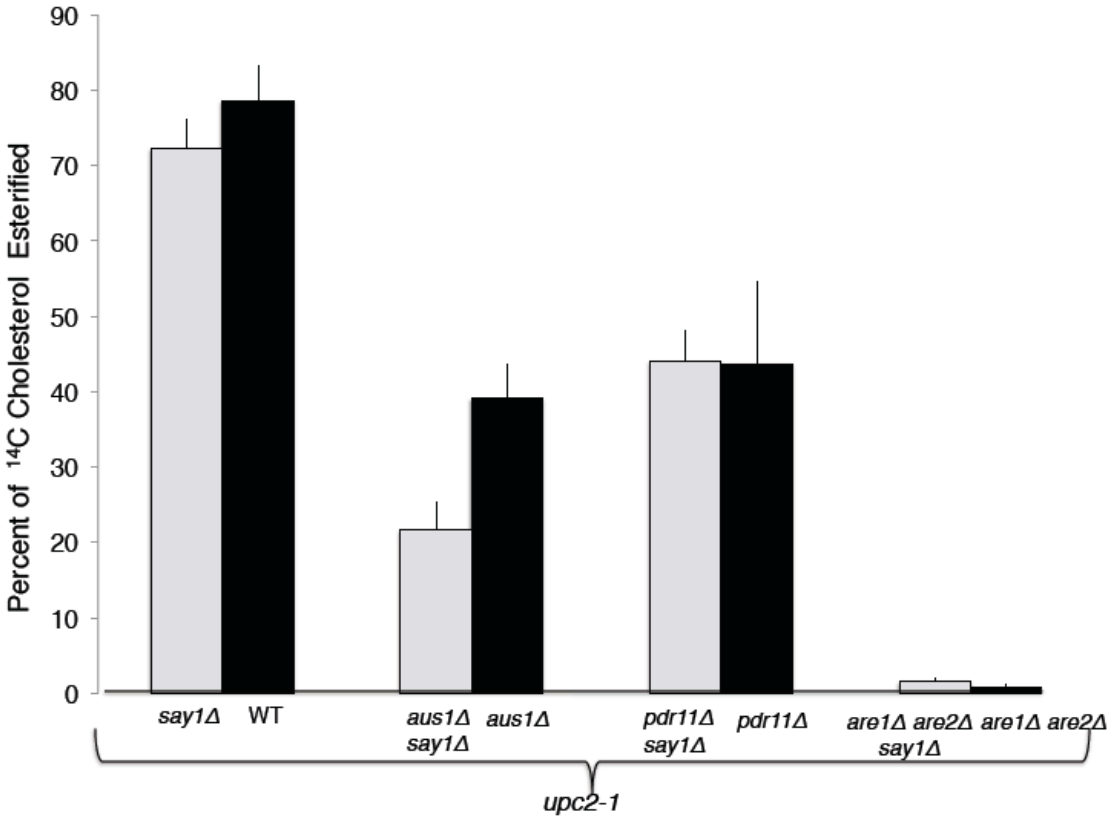


**Figure 4C. Aus1p, Pdr11p, and the esterifying enzymes affect cholesteryl acetate metabolism. C**. The indicated strains were cultured with 1% tyloxapol/ethanol (1:1) and 0.01 µCi/ml [4-$^{14}$C]cholesterol for 20 hours. Lipid were extracted, resolved, and quantified as described in "Materials and Methods". Experiments were performed in triplicate and the data above reflects the mean % of ± S.E [4-$^{14}$C]cholesterol esterified. There was no statistically significant difference from the control strain as assessed by unpaired t-test.

**D.**

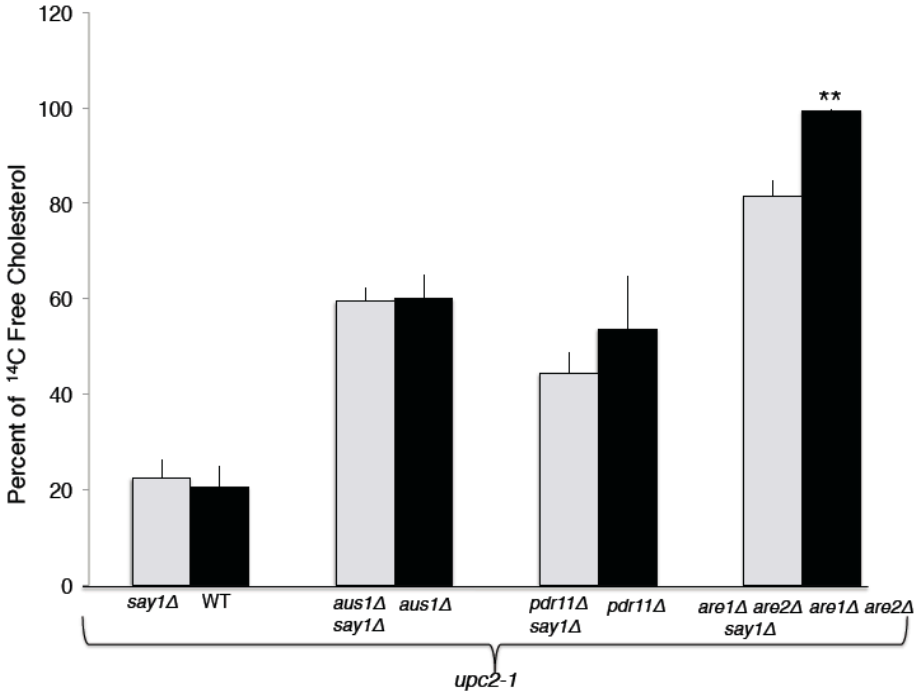


**Figure 4D. Aus1p, Pdr11p, and the esterifying enzymes affect cholesteryl acetate metabolism.** The indicated strains were cultured with 1% tyloxapol/ethanol (1:1) and 0.01 µCi/ml [4-$^{14}$C]cholesterol for 20 hours. Lipid were extracted, resolved, and quantified as described in "Materials and Methods". Experiments were performed in triplicate and the data above reflects the mean % of ± S.E free [4-$^{14}$C]cholesterol. Asterisks denote statistically significant difference from the control strain with $p<0.01$ (**) by unpaired t-test.

**Figure 5**

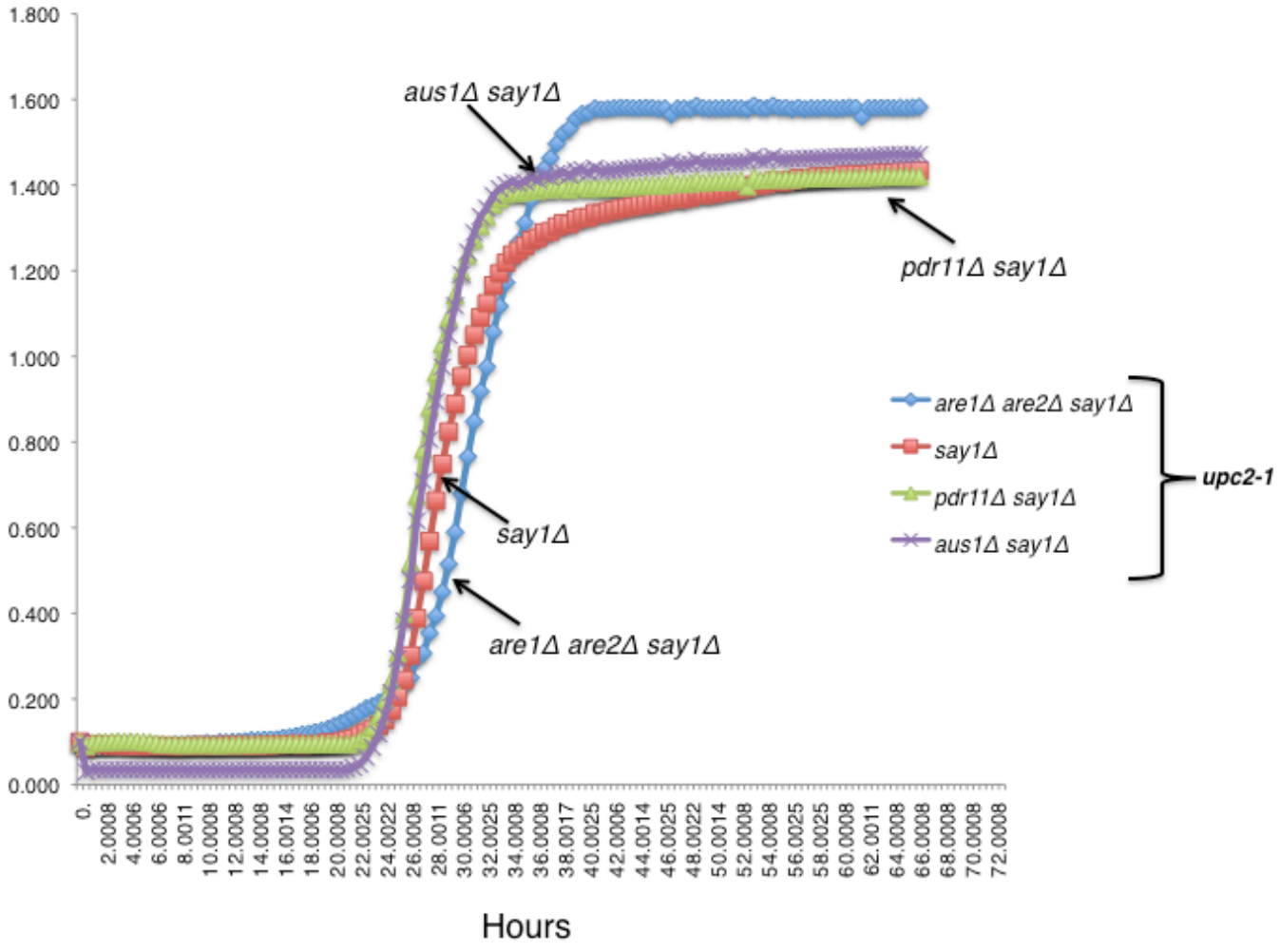


**Figure 5. Ergosteryl Acetate accumulation does not affect viability.**

Growth curves were obtained using a Microbiology Workstation Bioscreen C (Thermo Electron Corp.) and Research Express Bioscreen C software (Transgalactic Ltd.). Cultures (three isolates per genotype) were normalized to an $A_{600}$ of 0.1, and 10 µl of each strain was added to 290 µl of the appropriate media per well.

**Figure 6**

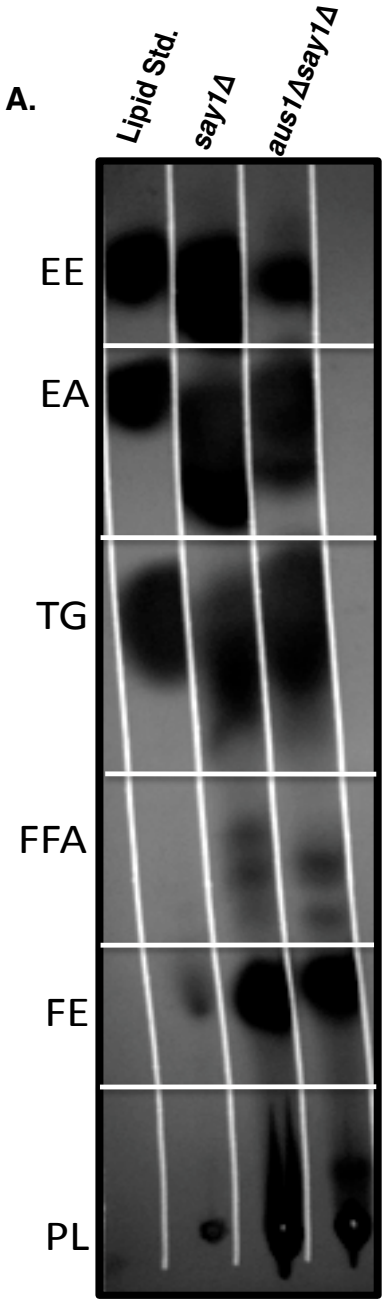


**Figure 6A. Ergosteryl Acetate is found in lipid droplets. A.** Dilute inoculation of each strain into 500 ml of YPD were grown overnight at 30 °C into log phase Lipid droplets were isolated as described in "Materials and Methods". Lipids were extracted as described in "Materials and Methods". Abbreviations: EE-Ergosteryl Ester, EA-Ergosteryl Acetate, TG-triglycerides, FFA-free fatty acids, FE-Free ergosterol, PL-Phospholipids.

**B.**

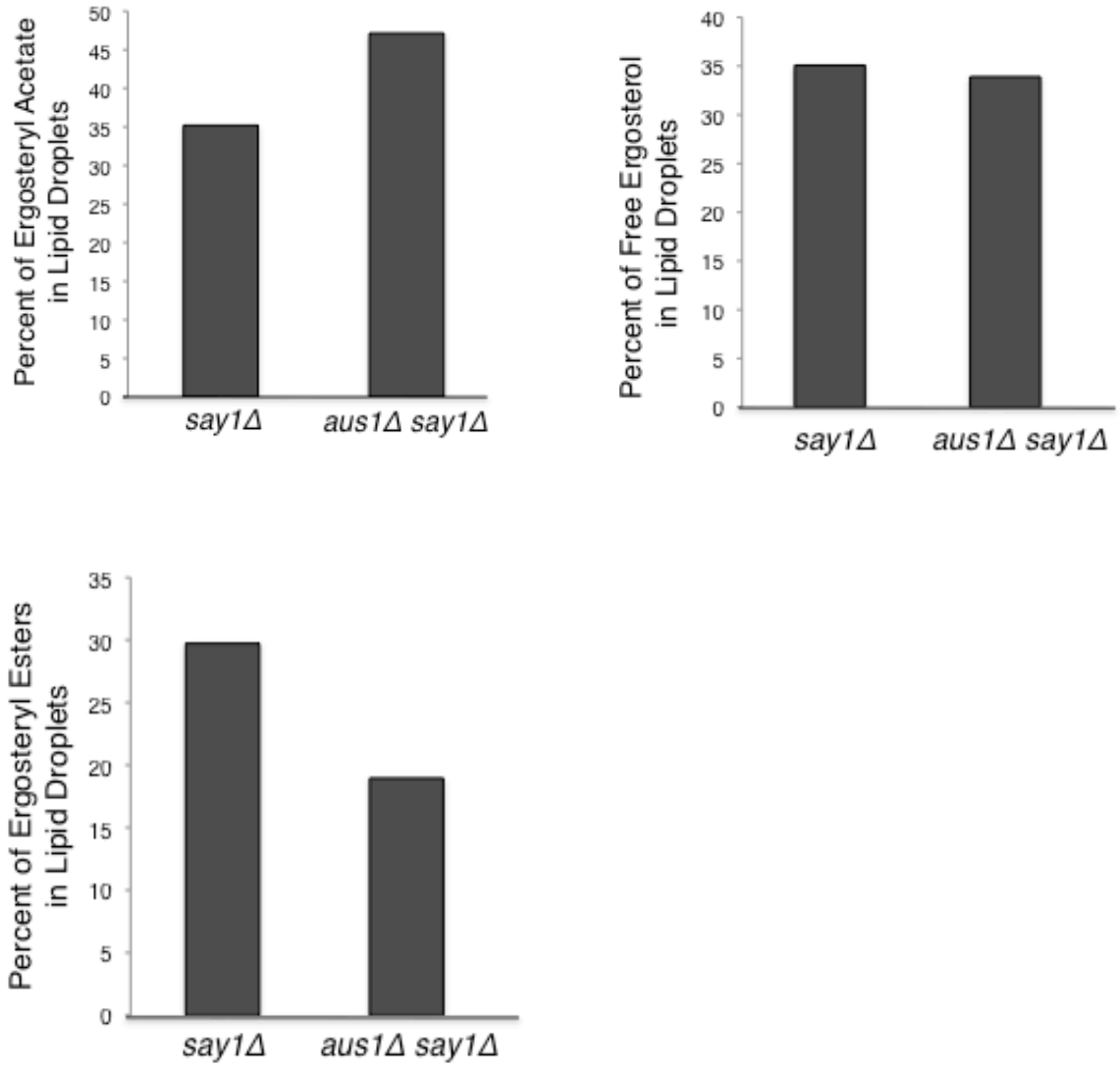


**Figure 6B. Ergosteryl Acetate is found in lipid droplets.** Extracted lipids were quantified via image J analysis.

**Figure 7.**

**A.**

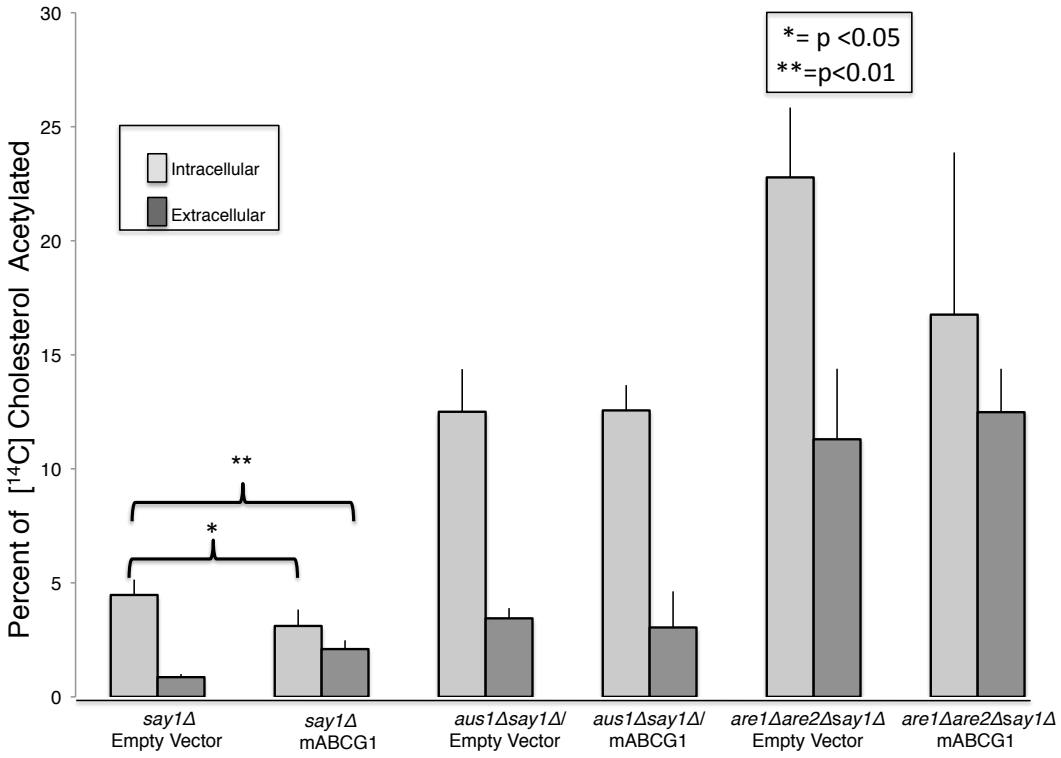


**Figure 7A. mABCG1 promotes cholesteryl acetate and free cholesterol efflux in a *say1Δ* mutant only.** The indicated strains were transformed with pRS424-GPD (empty vector) or pRS424/mABCG1. These strains were cultured with 1% tyloxapol/ethanol (1:1) and 0.01 µCi/ml [4-$^{14}$C]cholesterol for 20 hours. Cells were washed and grown in fresh media containing 40 ug/ml of cold cholesterol for 20 hours. . Lipid were extracted, resolved, and quantified as described in "Materials and Methods". Experiments were performed in triplicate and the data above reflects the mean of % of ± S.E exogenous [4-$^{14}$C]cholesterol acetylated. Asterisks denote statistically significant difference from empty vector in the same strain background with $p<0.05$ (*) and $p<0.01$ (**) by unpaired t-test.

**B.**

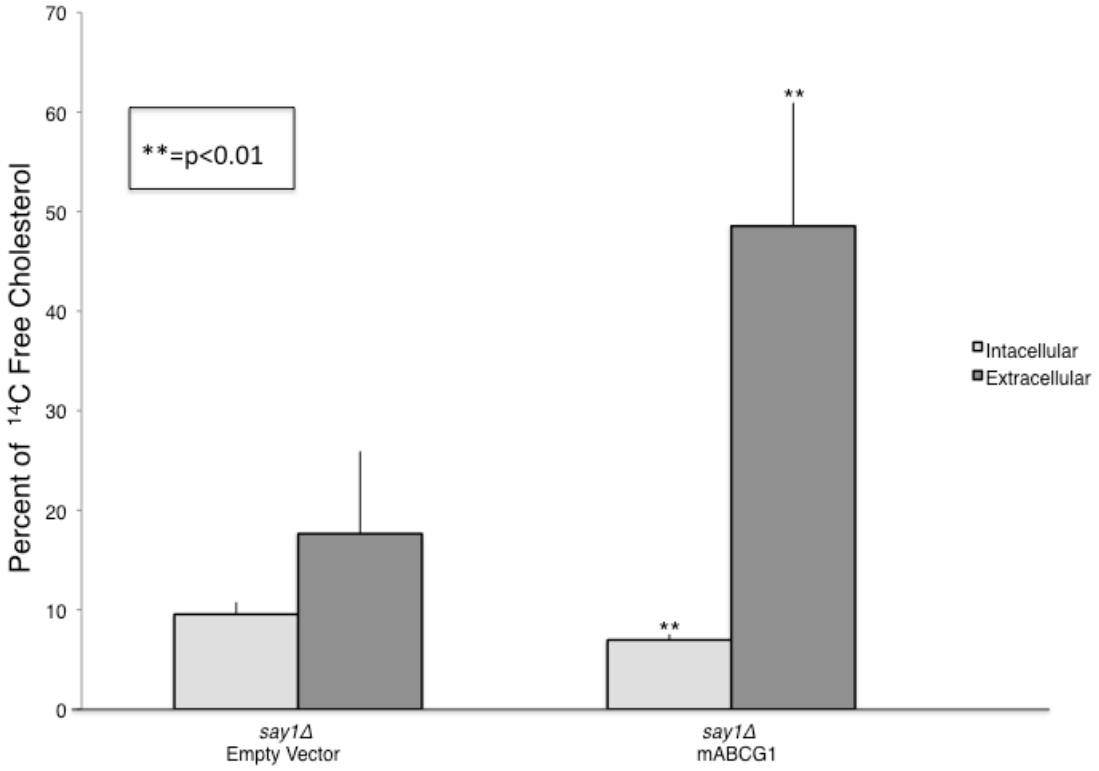


**Figure 7B. mABCG1 promotes cholesteryl acetate and free cholesterol efflux in a *say1Δ* mutant only.** The indicated strains were transformed with pRS424-GPD (empty vector) or pRS424/mABCG1. These strains were cultured with 1% tyloxapol/ethanol (1:1) and 0.01 µCi/ml [4-$^{14}$C]cholesterol for 20 hours. Cells were washed and grown in fresh media containing 40 ug/ml of cold cholesterol for 20 hours. . Lipid were extracted, resolved, and quantified as described in "Materials and Methods". Experiments were performed in triplicate and the data above reflects the mean of % of ± S.E free [4-$^{14}$C]cholesterol. Asterisks denote statistically significant difference from empty vector in the same strain background with $p<0.01$ (**) by unpaired t-test.

## References


1. Dean, M., and Allikmets, R. (2001) *J Bioenerg Biomembr* **33**, 475-479
2. Rees, D. C., Johnson, E., and Lewinson, O. (2009) *Nat Rev Mol Cell Biol* **10**, 218-227
3. Kovalchuk, A., and Driessen, A. J. (2010) *BMC Genomics* **11**, 177
4. Aye, I. L., Singh, A. T., and Keelan, J. A. (2009) *Chem Biol Interact* **180**, 327-339
5. Bodzioch, M., Orso, E., Klucken, J., Langmann, T., Bottcher, A., Diederich, W., Drobnik, W., Barlage, S., Buchler, C., Porsch-Ozcurumez, M., Kaminski, W. E., Hahmann, H. W., Oette, K., Rothe, G., Aslanidis, C., Lackner, K. J., and Schmitz, G. (1999) *Nat Genet* **22**, 347-351
6. van der Velde, A. E. (2010) *World J Gastroenterol* **16**, 5908-5915
7. Vaughan, A. M., and Oram, J. F. (2006) *J Lipid Res* **47**, 2433-2443
8. Wilcox, L. J., Balderes, D. A., Wharton, B., Tinkelenberg, A. H., Rao, G., and Sturley, S. L. (2002) *J Biol Chem* **277**, 32466-32472
9. Li, Y., and Prinz, W. A. (2004) *J Biol Chem* **279**, 45226-45234
10. Yang, H., Bard, M., Bruner, D. A., Gleeson, A., Deckelbaum, R. J., Aljinovic, G., Pohl, T. M., Rothstein, R., and Sturley, S. L. (1996) *Science* **272**, 1353-1356
11. Leber, R., Zinser, E., Zellnig, G., Paltauf, F., and Daum, G. (1994) *Yeast* **10**, 1421-1428
12. Tiwari, R., Koffel, R., and Schneiter, R. (2007) *EMBO J* **26**, 5109-5119
13. Wang, N., Lan, D., Chen, W., Matsuura, F., and Tall, A. R. (2004) *Proc Natl Acad Sci U S A* **101**, 9774-9779
14. Erdeniz, N., Mortensen, U. H., and Rothstein, R. (1997) *Genome Res* **7**, 1174-1183
15. Croop, J. M., Tiller, G. E., Fletcher, J. A., Lux, M. L., Raab, E., Goldenson, D., Son, D., Arciniegas, S., and Wu, R. L. (1997) *Gene* **185**, 77-85
16. Gottesman, M. M., and Ambudkar, S. V. (2001) *J Bioenerg Biomembr* **33**, 453-458
17. Jensen-Pergakes, K., Guo, Z., Giattina, M., Sturley, S. L., and Bard, M. (2001) *J Bacteriol* **183**, 4950-4957
18. Maxfield, F. R., and Tabas, I. (2005) *Nature* **438**, 612-621
19. Vaughan, A. M., and Oram, J. F. (2005) *J Biol Chem* **280**, 30150-30157
20. Steck, T. L., and Lange, Y. (2010) *Trends Cell Biol* **20**, 680-687

# Chapter 3: Characterizing Protein-Protein Interactions for the Yeast Acyl-Coenzyme A:sterol Acyltransferase, Are2p by Integrated Split-Ubiquitin Membrane Yeast Two-Hybrid Analysis

## Abstract

The esterification of sterols by the acyl-coenzyme A:cholesterol acyltransferases (ACATs) represents a critical component of intracellular cholesterol homeostasis. However, the mechanism by which sterol substrates are transported to the ACATs remains poorly defined. In order to elucidate this transport pathway, we performed a split-ubiquitin membrane yeast two-hybrid, utilizing the budding yeast orthologue of the ACATs, ACAT-related enzyme 2 (Are2p). As a result of our screen we identified nine potential interacting partners of Are2p. Strains deleted for these genes all exhibit sensitivity to exogenous cholesterol and five of these display decreased esterification activity. We also demonstrated that two of the hits, *mfb1Δ* and *cos8Δ* are synthetically lethal with *are1Δ are2Δ* in the presence of tunicamycin and myriocin respectively. Additionally, we found that Are2p physically interacts with Pdr11p, a member of the G sub-family of ATP binding cassette (ABC) membrane transporters.

## Introduction

Eukaryotic membranes are comprised of a precise lipid organization that is acclimatized for optimal cellular function (1). Cholesterol is a cardinal determinant of this membrane lipid organization and therefore is subject to scrupulous regulation. The cell possesses an armamentarium of mechanisms and metabolic pathways that work in concert to achieve cholesterol homeostasis (1). The esterification of cholesterol by the ACATs is a first line defense mechanism employed by the cell against increasing cholesterol levels. A 10% increase in cell surface cholesterol results in a 3- fold increase in esterification activity within an hour (2). Similarly, in budding yeast the ACATs also play an essential role in maintaining sterol homeostasis. The absence of the sterol esterifying enzymes produces a decrease in sterol biosynthesis or sterol uptake (3). Despite the paramount role the ACATs play in maintaining intracellular cholesterol equilibrium, the mechanisms by which sterols are shuttled to the ACATs are unknown (4). Abrogation of classical sterol transport mechanisms such as membrane vesicle trafficking or the endosomal-lysosomal pathway in model systems does not effect esterification of sterols originating from the cell surface (3,5). These data suggest that transport of the sterol substrate to the ACATs may be facilitated by soluble sterol binding proteins or a previously uncharacterized vesicular system.

To date, little progress has been made towards identifying molecular components of this transit despite its major contribution to sterol homeostasis within the cell. This may in part be due to the inability of prevailing methodologies to identify protein partners for membrane proteins (6). Yeast two-hybrid systems are the most frequently used method to detect protein-protein interactions (7). However, intrinsic to this system is it's bias towards detecting interactions between soluble proteins and their binding partners. Transmembrane proteins are significantly underrepresented in these studies due to their hydrophobic nature and their inability to successfully translocate to the nucleus, a requirement

of yeast two hybrid systems (7). Recently a modified yeast two hybrid has been devised to allow for the identification of integral membrane interacting proteins. In the split ubiquitin membrane yeast two hybrid, a membrane protein of interest or the "bait," is fused to the C-terminal half of ubiquitin (Cub), along with an artificial transcription factor that consists of the bacterial LexA-DNA binding domain and the *Herpes simplex* VP16 transactivator protein (8). This strain is then transformed with the “prey”, a yeast DNA library comprised of DNA fragments that are fused to the N-terminal half of ubiquitin (Nub). Upon interaction of two proteins, the ubiquitin moiety is reconstituted (Cub + Nub) and is subsequently recognized by cellular ubiquitin proteases resulting in the cleavage of the transcription factor. The released transcription then enters the nucleus and activates transcription of the reporter genes (8).

In order to elucidate the mechanisms of sterol transport from the cell surface to the ACATs, we performed an integrated membrane split ubiquitin yeast two hybrid utilizing the yeast ACAT related esterifying enzyme, Are2p as bait. As a result we identified nine putative Are2p interacting proteins. In order to explore the role of these interactors in sterol metabolism, we performed a series of viability assays in the presence of exogenous cholesterol and drugs that perturb sterol homeostasis. As a result we found that *MFB1* and *COS8* are synthetically lethal with *are1Δ are2Δ* in the presence of tunicamycin and myriocin respectively. Analysis of the viability assays demonstrated that the interactors assayed, play a previously uncharacterized role in sterol homeostasis.

**Materials and Methods**

*General*. Yeast strains used in this study are isogenic with the strain W303-1A (*Table 1)*. Deletion strains were generated using the one-step PCR mediated gene disruption (9) . We were unable to create a deletion of *COS12* in the W303 background.

*Growth Curves*. Growth curves were obtained using a Microbiology Workstation Bioscreen C (Thermo Electron Corp.) and Research Express Bioscreen C

software (Transgalactic Ltd.). Cultures (three isolates per genotype) were normalized to an $A_{600}$ of 0.1, and 10 µl of each strain was added to 290 µl of the appropriate media per well.

*Analysis of exogenous sterol accumulation and esterification.* Cells were grown for approximately 20 h in the indicated media containing 1% tyloxapol/ethanol (1:1) and 0.01 µCi/ml [4-$^{14}$C]cholesterol. Sterols were extracted and analyzed via thin layer chromatography (8).

*Matlab Analysis: Maximum Rate and Time at Maximum Rate quantification*- The MATLAB program was programmed by Kelly Ruggles in order to find the slope of the growth curve at each time point, and then identifying the maximum slope (or rate) for each triplicate in each strain. The time (in hours) at which this slope was reached was also stored in a new matrix table. Values of these variables were calculated for each individual growth curve. Statistical significance was obtained by performing an unpaired t-test for each growth parameter. The values were calculated as follows:

$$WT_{norm} = \frac{WT_{YPD}}{WT_{YPD+Drug}} \qquad xxx\Delta_{norm} = \frac{xxx\Delta_{YPD}}{xxx\Delta_{YPD+drug}} \qquad RateRatio = \frac{xxx\Delta_{norm}}{avg(WT_{norm})}$$

$$t_{norm} = t_{YPD} - t_{YPD+drug}$$
$$TimeRatio = t_{norm(xxx\Delta)} - t_{norm(WT)}$$

$$OD_{norm} = \frac{OD_{SCD}}{OD_{SCD+PO}} \qquad ODRatio = \frac{OD_{norm(xxx\Delta)}}{OD_{norm(WT)}}$$

*Pronger assay and anaerobic growth.* Aliquots from 2 ml media were plated as serial dilutions and grown anaerobically for 3 days on YEPD plates supplemented with 20 µg/ml ergosterol and 0.5% Tween 80 as an oleate source. Anaerobic growth was achieved using BD PharMingen, $CO_2$-generating gas packs and jars

as described previously. Attainment of anaerobiosis was monitored by the inability of normal strains to grow in the absence of exogenous sterol.

**Results**

*Characterization of Are2p integrated split-ubiquitin membrane yeast two-hybrid.* In order to execute this screen the C-terminus of Are2p was fused in frame with the Cub construct via homologous recombination in the yeast reporter strain THY AP4 (8). To assess if the Cub-tagged bait protein was properly inserted into the membrane and not self-activating, we transformed these strains with control prey plasmids containing an ER protein, Ost1p that is fused to either NubI (a hyperactive positive control) or NubG (comprised of a point mutation that inhibits interaction). The Are2p-Cub construct was able to interact with the positive control Ost1-Nub1 and did not exhibit any growth in the presence of Ost1-NubG. Furthermore, metabolic incorporation studies demonstrated that this construct exhibits esterification activity (Figure 1). These experiments demonstrate that Are2p-Cub is expressed, correctly inserted into the membrane, and possesses esterfication activity. The Are2p-Cub containing strain was subsequently transformed with a yeast genomic “prey” library. Two hundred colonies were scored as positives for activation of the reporter system, which is measured by growth on media lacking histidine and adenine or blue colony color in the presence of X-gal. Genomic DNA was extracted from these colonies, transformed back into the bait strain, and growth on the appropriate media was assessed. Eighty-five of these colonies activated the indicated reporter genes in the presence of the Are2p bait. Eighty percent of the plasmid DNA retrieved from these colonies represented background noise such as stretches of the mitochondrial genome, autonomously replicating sequences, or non-coding regions. Seventeen sequences encoded for open reading frames. Of these, eight proteins were eliminated based on redundancy with other split ubiquitin screens or not being in frame. As a result nine proteins remained after all of the

verification assays were completed (Table 2). Of these nine, Cos8p was the only hit identified in the screen twice, with two non-overlapping sequences. Some of the interactors identified have previously known interactions either with each other or Are2p. Pdr11p (a member of the ATP binding cassette transporter superfamily) and Are2p have both been implicated in playing an integral role in the import of sterols (10,11). Additionally, Cos12p has been reported to physically interact with Nup84p and is part of the same protein family (the DUP380 family) as Cos8p (https://portal.biobase-international.com/cgi-bin/build_ghpywl/idb/1.0/searchengine/start.cgi). Moreover, the double deletion of *GLT1* and *MFB1* has been shown to produce a synthetic sick phenotype (http://drygin.ccbr.utoronto.ca/). In order to further elucidate the functional and genetic interactions of these proteins, we performed an esterification assay and a series of viability tests.

*Five Deletion Mutants of Are2p Interactors Exhibit a Significant Decrease in Sterol Esterifcation*. The primary role of Are2p is to esterify sterols and as such its deletion results in a 75% decrease in sterol esterification (10). To assess if the interactors identified play a role in transport of sterols to Are2p or regulate the esterifying enzyme, we created a deletion mutant of each of the nine candidate genes in a *upc2-1* strain and measured the esterification of exogenous radiolabelled cholesterol. The *upc2-1* strain contains a gain of function mutation in the transcription factor encoded by *UPC2*, that facilitates aerobic sterol influx. Of the nine mutants, deletion of *COS8*, *SIP18*, *MFBI* and *YJR*096W and particularly *PDR11,* resulted in significant decreases in the percent of exogenous sterol esterified (Figure 2). Pdr11p works in concert with its closest paralog, Aus1p, to mediate the influx of sterols during anaerobiosis (11). Due to their high degree of similarity and functional redundancy in sterol uptake (11) we also assessed sterol esterification in an *aus1* deletion. We found that loss of *AUS1* results in a profound decrease in the percent of sterol esterification (Figure 2).

These data implicate that these protein either mediate sterol transport or positively regulated Are2p.

*All of the interacting proteins are sensitive to excess cholesterol in the media.* The esterification of free sterols represents a major sterol detoxification pathway in yeast (10). To delineate if Are2p interacting proteins mediate sterol detoxification, we assessed viability of the deletion mutants (in a *upc2-1* background) in the presence of 150 μg/ml of cholesterol. This concentration of cholesterol is seven and a half times greater than what is utilized to support anaerobic growth (12). Viability is defined as a composite of three parameters, which include the rate of growth, the time it takes to reach the maximum rate optical density (OD), and the OD at the peak of growth. Although all of the hits displayed a significant sensitivity to increased exogenous cholesterol, none were as striking as a *nup84Δ* strain (Figure 3). This data suggests that these interacting proteins play a role in maintaining cholesterol homeostasis although to varying degrees.

*Aus1Δ, Cos8Δ, and Glt1Δ are sick anaerobically when deleted in an are1Δ are2Δ strain.* To investigate the role of these interactors in sterol uptake under physiological conditions, deletion mutants were grown anaerobically. *Aus1Δ* was the only single mutant to show a slight decrease in growth. However, *Cos8Δ are1Δ are2Δ, aus1Δ are1Δ are2Δ, and glt1Δ are1Δ are2Δ* all grew worse when compared to their respective single deletion or an *are1Δ are2Δ* double mutant (Figure 4A & 4B). This data suggests that these three proteins may mediate alternate pathways that help maintain sterol homeostasis in the absence of the esterification reaction.

*Deletion mutants in a upc2-1 background exhibit flucanazole sensitivity. ARE1* and *ARE2* genes differentially determine the sterol ester pools of the cell due to their disparate substrate specificity (13). Are1p primarily esterifies intermediates

in the sterol biosynthetic pathway, whereas are2p is esterifies the end product ergosterol (7). To assess if the interactors demonstrate similar substrate specificity as Are2p, we assessed the viability of the deletion mutants in the presence of fluconazole. Fluconazole is a triazole antifungal drug that inhibits the fungal cytochrome P450 enzyme, 14$\alpha$-demethylase. As a result, fluconazole prevents the conversion of lanosterol to ergosterol and therefore produces an intracellular accumulation of 4α-methyl-sterols (normally substrates for Are1p) (7,10). We found that a deletion of *COS8, GLT1, MFB1, NUP84,* or *PDR11* in a *upc2-1* background all grew significantly slower than the control strain (Figure 5). Interestingly, deletions of *MFB1, PDR11*, and *COS8* displayed a significant decrease in the percent of sterol esterified (Figure 3). This data suggests that either these proteins may play a dual role in positively regulating both Are1p and Are2p or they able to transport various sterol substrates.

*A majority of the Are2p interacting proteins display a myriocin related phenotype.* The metabolism of sphingolipids and cholesterol are precisely co-regulated (14). To investigate whether the identified hits play a role in sphingolipid metabolism we measured their viability in the presence of myriocin. Myriocin is an inhibitor of serine palmyitoyltransferase, the enzyme that catalyzes the first step in sphingosine biosynthesis. Myriocin treatment results in a depletion of intracellular sphingolipids and a concurrent increase in free sterols (presumably due to loss of lipid rafts) (3). In 50 ng/ml of myriocin, only a *NUP84* deletion (in a wild type background) exhibited a significant decrease in viability, whereas *glt1Δ, mfb1Δ, pdr11Δ, cos8Δ,* and *sip18Δ* strains all grew significantly better than the control strain (Figures 6A, 6B, & 6C). The most striking myriocin phenotype was observed in a *cos8Δ are1Δ are2Δ* strain, which was synthetic lethal in 60ng/ml of myriocin (Figure 6D). This data suggests that these proteins share an essential biological function in response to myriocin treatment. In contrast *sip18Δ are1Δ are2Δ,* grew significantly better than an *are1Δ are2Δ* strain, suggesting that Sip18p may be a negative regulator of Are1p and Are2p (Figure 6D). In an *upc2-*

*1* background, only an A*US1* deletion resulted in significantly diminished growth (Figure 6E).

*A majority of the hits display a tunicamycin related phenotype*. The unfolded protein response (UPR) is an evolutionarily conserved series of reactions that mediate the folding, processing, export, and degradation of misfolded proteins. In addition to protein misfolding, lipid and structural changes in membranes may also induce the UPR (15). To investigate the relationship of the interactors and the UPR, we treated the various deletion strains with tunicamycin, an established inducer of the UPR (16). The most compelling phenotype was observed in an *mfb1 are1Δ are2Δ* strain, which exhibited a synthetic lethal phenotype, suggesting that these proteins mediate compensatory parallel pathways in response to an induction of the UPR (Figure 7A). Conversely, we found that *cos8Δ are1Δ are2Δ, sip18Δ are1Δ are2Δ, and nup84Δ are1Δ are2Δ* strains all grew significantly better than an *are1Δ are2Δ* strain (Figure 7A). In an *upc2-1* background, *cos8Δ, are2Δ,* and *sip18Δ* all displayed a significant decrease in viability (Figure 7B).

**Discussion**

The esterification of sterols represents a critical component of sterol homeostasis that is conserved throughout eukaryotic evolution (1). Despite its fundamental role in preserving dynamic sterol equilibrium, there is exiguous information regarding how sterol substrates are transported to the enzymes (2). In order to identify components of this sterol transport pathway we performed a membrane split ubiquitin yeast two hybrid utilizing Are2p as our bait. As a result of our screen and subsequent viability assays we discovered nine putative Are2p interacting proteins and established a previously uncharacterized role for them in mediating sterol homeostasis. Interestingly, we demonstrated that two of the hits, *mfb1Δ* and *cos8Δ* are synthetically lethal with *are1Δ are2Δ* in the presence of tunicamycin and myriocin respectively. This is particularly striking as true

synthetic lethal phenotypes are rare, occurring less than one percent in genome wide screens (17).

Cos8 is a member of the duplicated (DUP) gene family, one of the largest and uncharacterized gene families in budding yeast (18). Broadly, it is thought that this family of proteins may act as facilitators activating or stabilizing membrane proteins, as is the suggested role for Cos3p's interaction with Nha1p (a $Na^+/H^+$ antiporter) (18). Although there is a dearth of information regarding the specific function of Cos8p, there is some evidence that suggests Cos8p may negatively regulate the synthesis of very long chain fatty acids and consequently sphingolipid production (19). As such we hypothesize that Cos8p may co-regulate the esterification reaction (postivie regulation) and sphigolipid biosynthesis (negative regulation), providing another point of cross-talk between these two major metabolic pathways. Further characterization of this interaction is necessary to further elucidate the role of Cos8p in sterol esterification and metabolism.

Mfb1p, is a mitochondrial protein that regulates the mitochondrial tubular network and is a member of the F-box protein family (15). This protein family acts as adaptors for multiple proteins, mediating the formation of macromolecular complexes that play key roles in diverse cellular processes (20). The role for mitochondria in sterol uptake and metabolism in yeast has been established but not characterized in-depth (21). Therefore, a physical interaction between the esterifying enzyme and a mitochondrial protein is not that surprising. However, the synthethic lethality between these genes in response to tunicamycin was unexpected, as none of these proteins have been previously implicated in mediating the UPR. This data suggests that Mfb1p and the esterifying enzymes may play an overlapping essential role in inducing the UPR. Interestingly, studies from mammalian cells and *Caenorhabditis elegans* have shown the existence of a mitochondrial UPR response that activates transcription of nuclear-encoded mitochondrial chaperone genes to promote protein homeostasis within the

organelle (22). Based on these findings we propose that the loss of intracellular sterol stores during budding (period of increased membrane proliferation) may have a two-fold effect: one it may inhibit mitochondrial tubular proliferation (which may induce the mitochondrial UPR) and two induce the UPR due to defects in membrane proliferation. As a result of this hyperinduction of the UPR, this strain is inviable. However, further characterization of this interaction and the role of this complex in the induction of UPR is necessary.

Our intent when we performed this screen was to find a putative soluble protein that mediates the transport of sterols from the cell surface to the ACATs. Interestingly, we found that Pdr11p, an ABC transporter that mediates sterol uptake may physically interacts with Are2p. Therefore this data suggests that the plasma membrane ABC transporter participates in a protein complex that directly transfers sterols to the ACAT enzymes, negating the need for an intermediary sterol transport protein. In the following chapter we will further expound on this hypothesis by confirming the physical interaction and exploring its physiological implications.

**Figure 1**

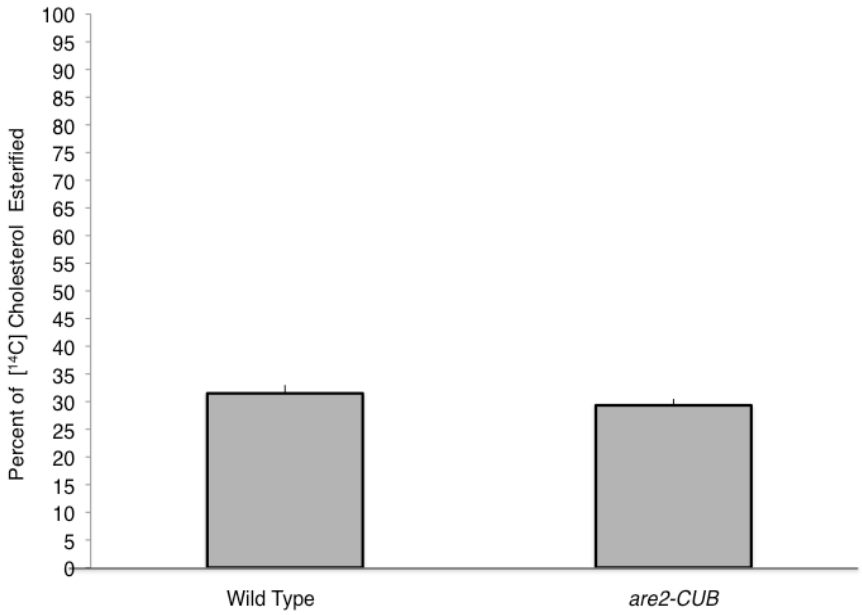


**Figure 1. The *are2*-Cub construct is able to esterify sterols comparable to wild type.** The indicated strains were grown for 18 h to mid-log phase in YEPD media containing 1% tyloxapol/ethanol (1:1), fatty acids (Tween 80), unlabeled cholesterol (20 µg/ml), and 0.01 µCi/ml [4-$^{14}$C]cholesterol. Anaerobic growth was achieved using BD PharMingen, $CO_2$-generating gas packs and jars. Lipids were extracted, resolved, and quantified as described in "Materials and Methods". Experiments were performed in triplicate and the data above reflects the mean % of ± S.E [4-$^{14}$C]cholesterol esterified. There was no statistically significant difference from the control strain as assessed by unpaired t-test.

**Figure 2**

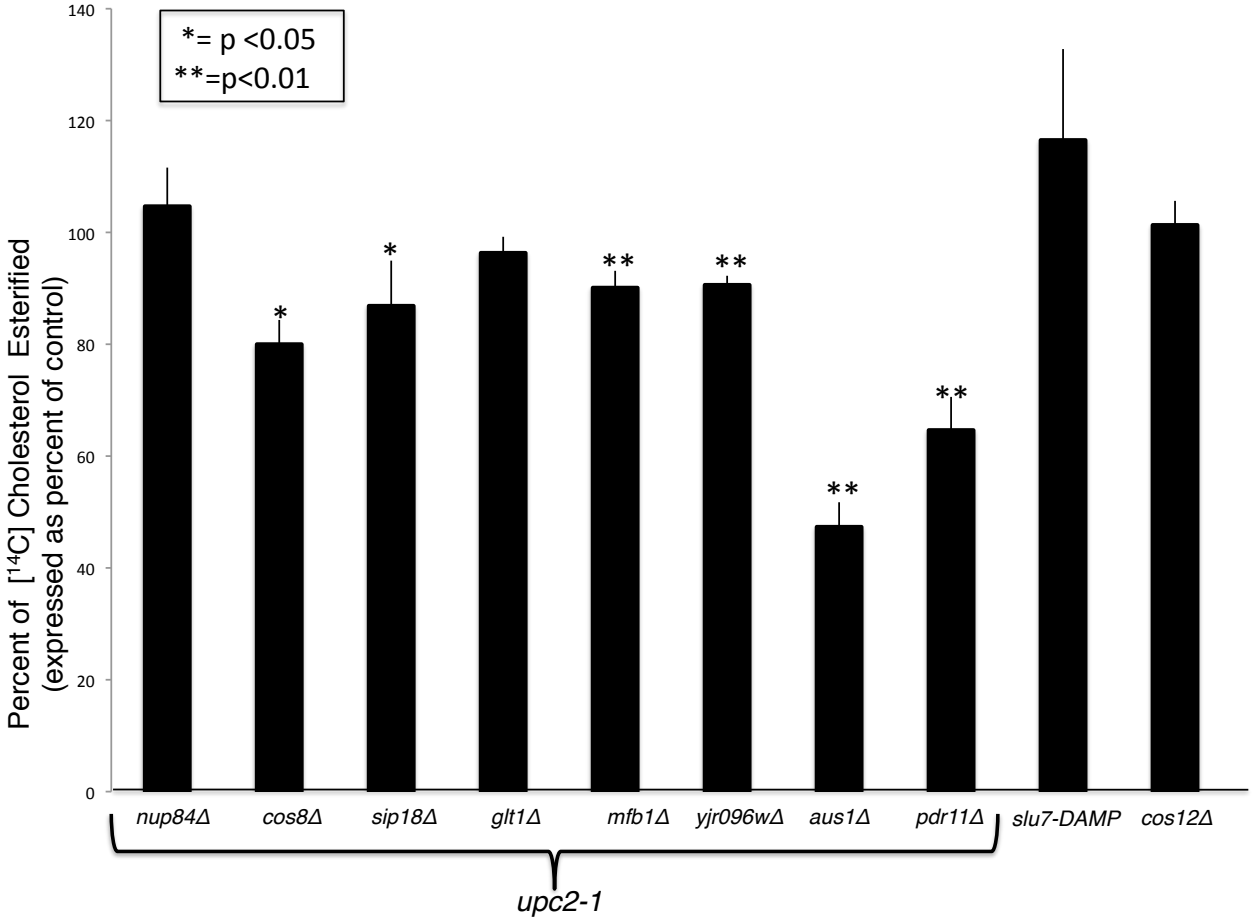


**Figure 2**. **Decreased esterification activity is associated with a majority of the interactors.** The indicated genes were deleted in a *upc2-1* strain. These strains were cultured with 1% tyloxapol/ethanol (1:1) and 0.01 µCi/ml [4-$^{14}$C]cholesterol for 20 hours. All other strains were grown for 18 h to mid-log phase in YEPD media containing 1% tyloxapol/ethanol (1:1), fatty acids (Tween 80), unlabeled cholesterol (20 µg/ml), and 0.01 µCi/ml [4-$^{14}$C]cholesterol. Anaerobic growth was achieved using BD PharMingen, $CO_2$-generating gas packs and jars (Wilcox paper). The cell pellets were washed twice with 0.5% tergitol and once with $dH_2O$, and lyophilized. Lipids were extracted, detected and quantified as described in "Materials and Methods". Experiments were performed in triplicate and the data above reflects the mean % ± S.E of [4-$^{14}$C]cholesterol esterified. Asterisks denote statistically significant difference from the control strain with $p<0.05$ (*) and $p<0.01$ (**) by unpaired t-test.

**Figure 3**

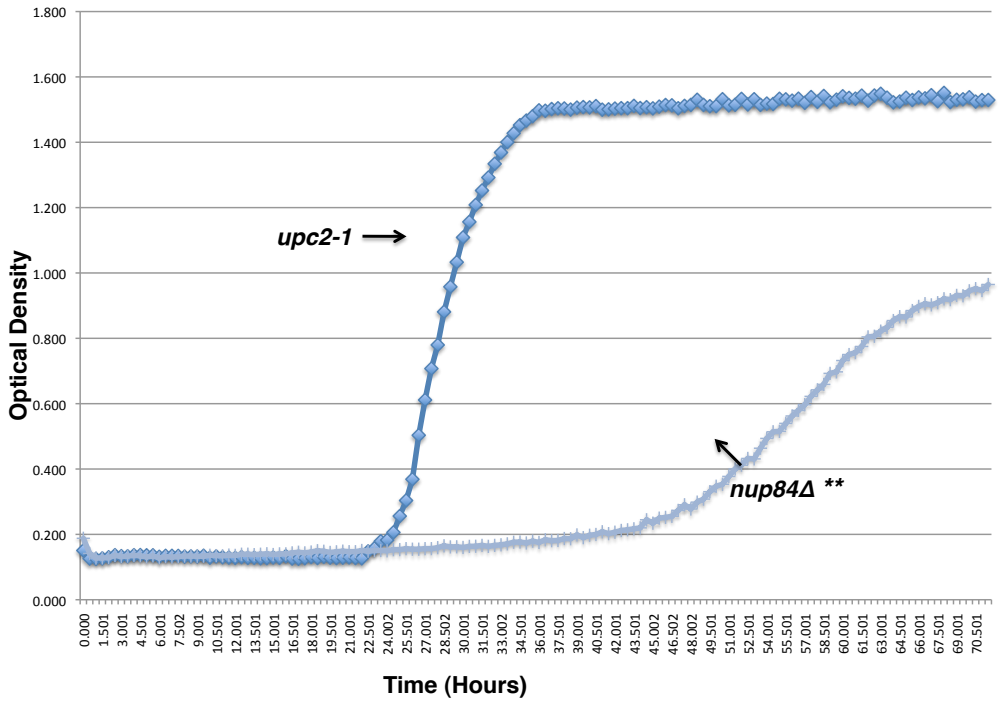


**Figure 3.** ***nup84Δ displays significant sensitivity to exogenous cholesterol.***
The indicated strains were grown in 150 µg/ml of cholesterol in 1:1 tyloxapol:ethanol for 72 hours. ODs were assessed as described in "Materials and Methods". Experiments were performed in triplicate. Asterisks denote statistically significant difference from the control strain (upc2-1) for the time it takes to reach the maximum rate OD with $p<0.01$ (**) by unpaired t-test.

**Figure 4**

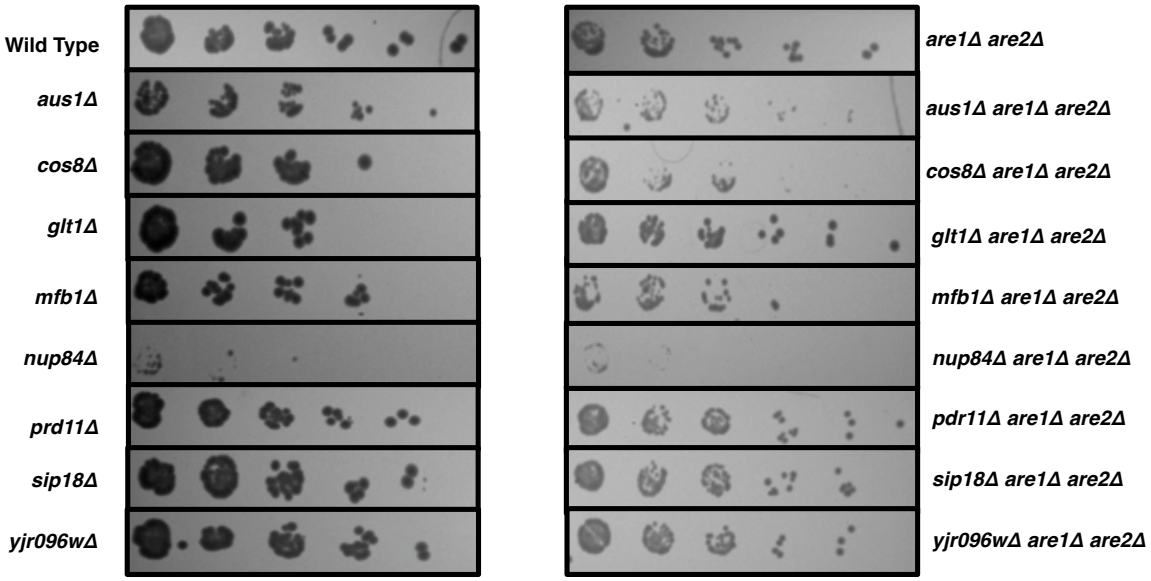


**B.**

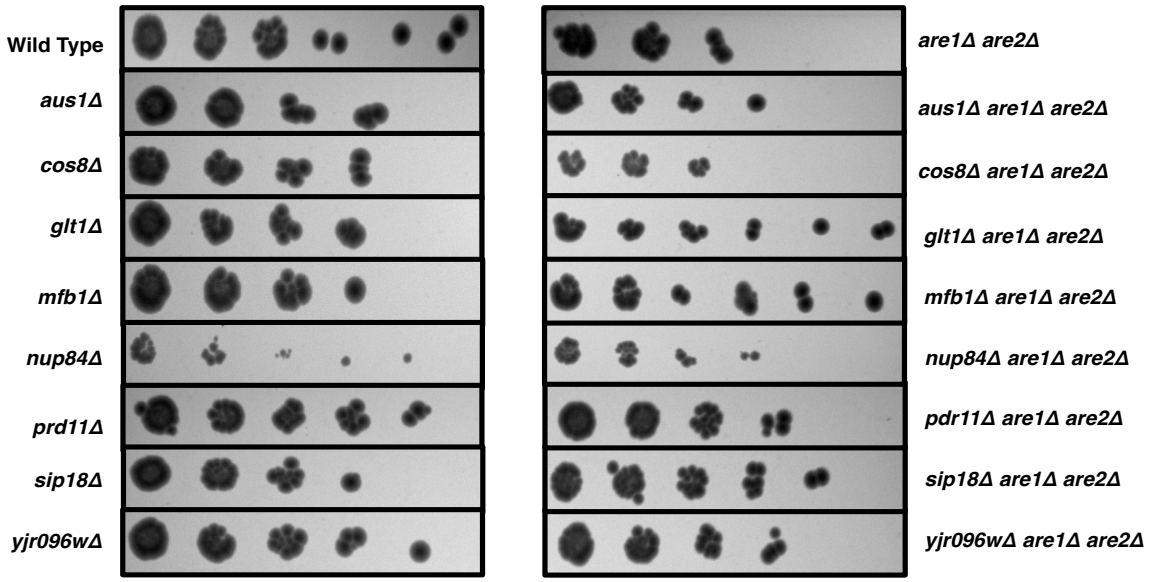


**Figure 4. Anaerobic viability of deletion mutants.** *Cos8Δ, aus1Δ, and glt1Δ* are synthetic sick with *are1Δ are2Δ* under anaerobic conditions. Serial dilutions of the indicated strains were done on plates containing cholesterol (20 µg/ml) and Tween 80. Anaerobic growth was achieved using BD PharMingen, $CO_2$-generating gas packs. **B.** The same strains were grown on YPD aerobically as a positive control.

**Figure 5**

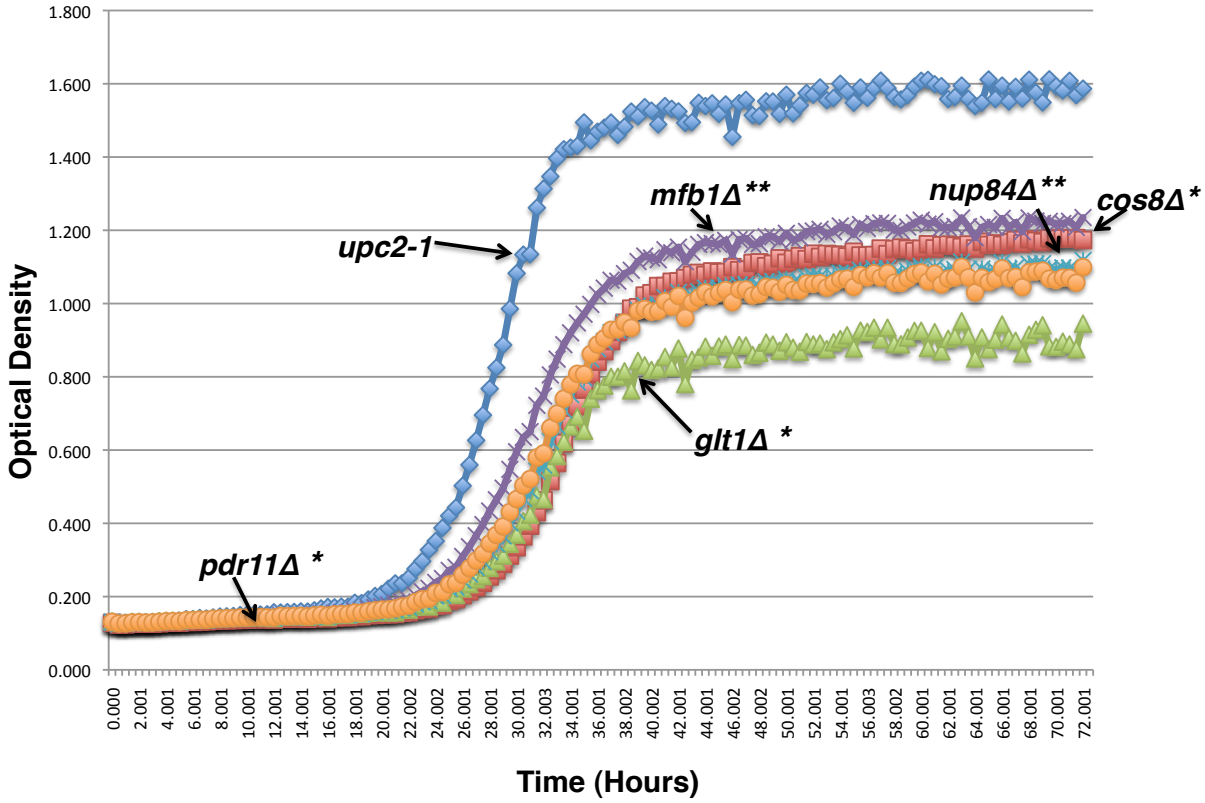


**Figure 5. A significant number of *Upc2-1* deletion mutants exhibit sensitivity to flucanazole.** The indicated strains were grown in the presence of 20 µg/ml of flucanazole. ODs were obtained as described in "Materials and Methods. Experiments were performed in triplicate. Asterisks denote statistically significant difference from the control strain (upc2-1) for the time it takes to reach the maximum rate OD (*nup84Δ*) and OD at the peak of growth (*mfb1Δ, cos8Δ, glt1Δ, pdr11Δ*.) Statistical significance with $p<0.05$ (*) with $p<0.01$ (**) was assessed by unpaired t-test.

## Figure 6

**A.**

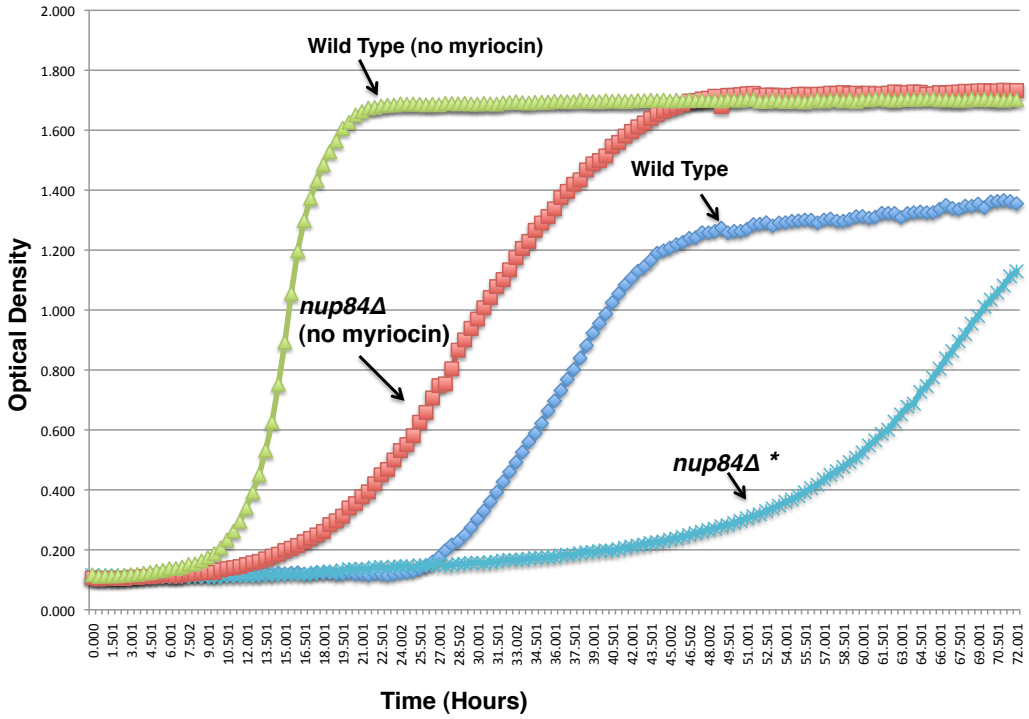


**Figure 6A. A majority of the hits display a myriocin related phenotype.** The indicated strains were grown in 50 ng/ml of myriocin for 72 hours. Experiments were performed in triplicate. Asterisks denote statistically significant difference from the control strain for the time it takes to reach the maximum rate OD (*nup84Δ*). Statistical significance with $p<0.05$ (*) with $p<0.01$ (**) was assessed by unpaired t-test.

**B.**

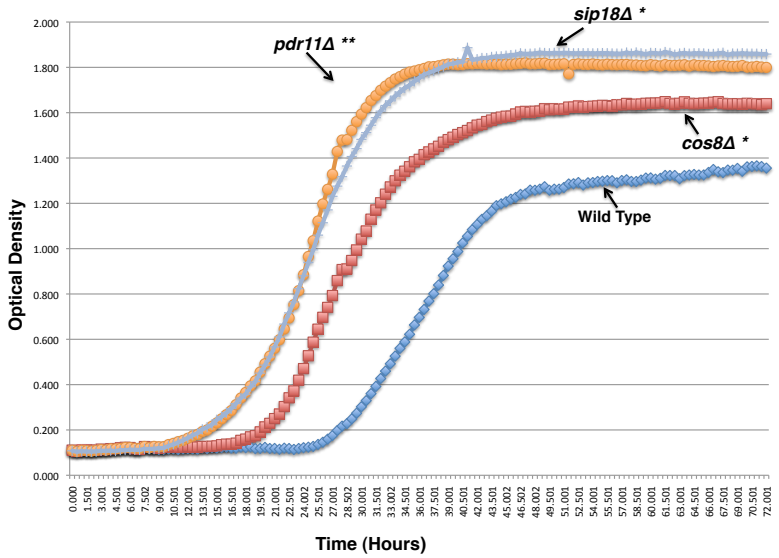


**C.**

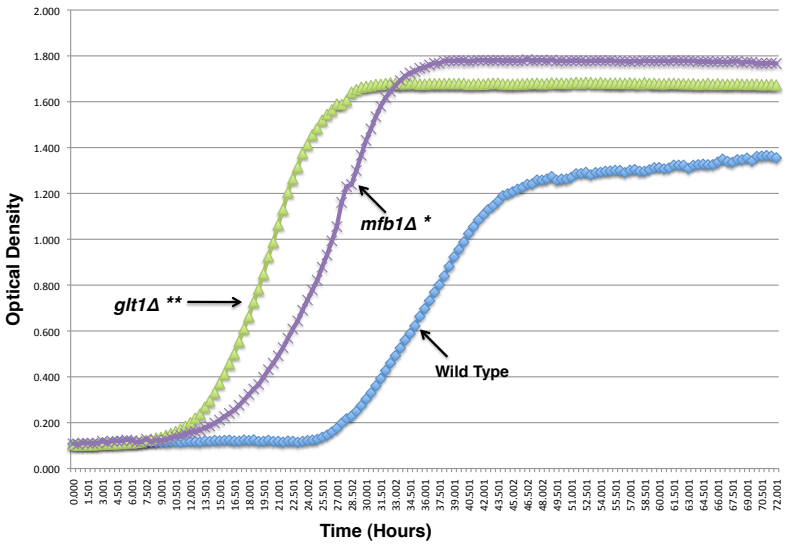


**Figure 6 B&C. A majority of the hits display a myriocin related phenotype.**

The indicated strains were grown in 50 ng/ml of myriocin for 72 hours. Experiments were performed in triplicate. Asterisks denote statistically significant difference from the control strain for the time it takes to reach the maximum rate OD (*pdr11Δ, mbb1Δ, glt1Δ*), OD at the peak of growth (*cos8Δ),* and rate of growth (*sip18Δ).* Statistical significance with $p<0.05$ (*) with $p<0.01$ (**) was assessed by unpaired t-test.

**D.**

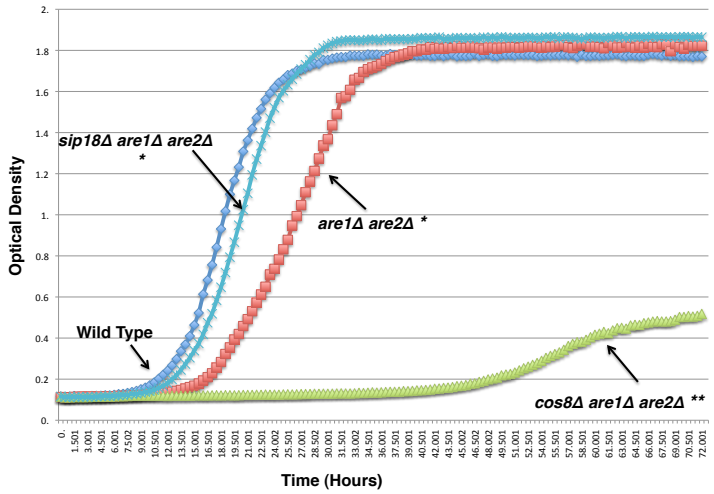


**E.**

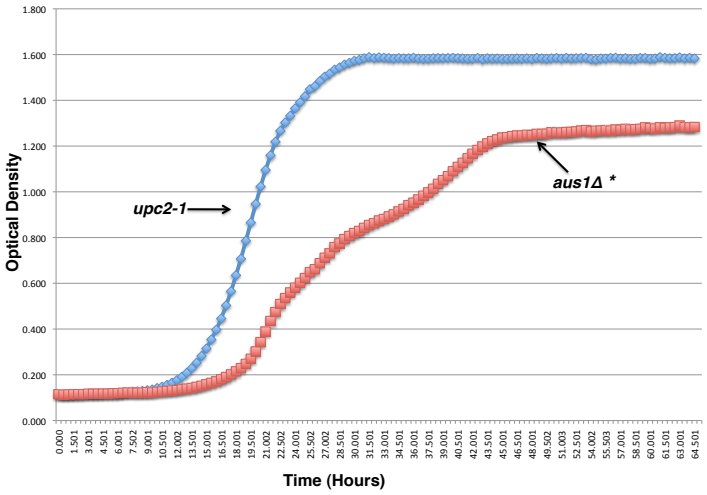


**Figure 6 D&E. A majority of the hits display a myriocin related phenotype.** significance with p<0.05 (*) with p<0.01 (**) was assessed by upaired t-test. The indicated strains were grown in 60 ng/ml of myriocin for 72 hours ODs were obtained as described in “Materials and Methods”. Experiments were performed in triplicate. Asterisks denote statistically significant difference from the control strain for OD at the peak of growth and rate of growth. Statistical significance with p<0.05 (*) with p<0.01 was assessed by unpaired t-test.

**Figure 7**

**A.**

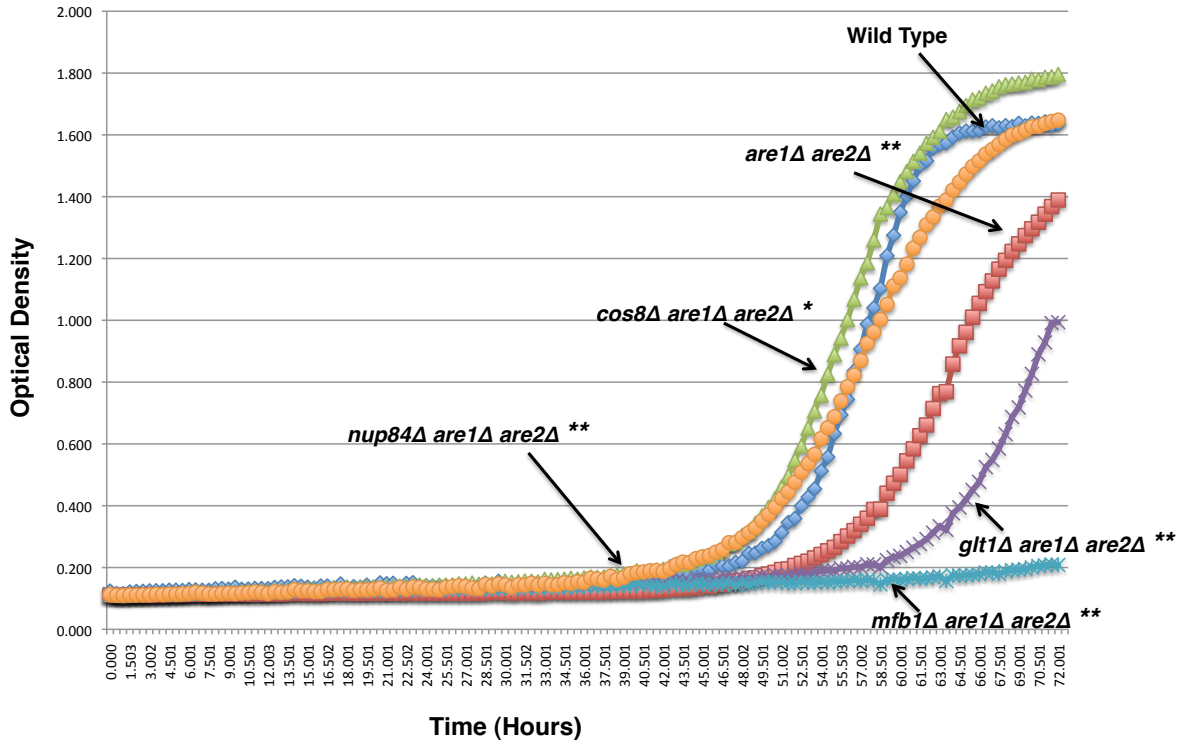


**Figure 7A. Tunicamycin Sensitivity of the Interactors.** The indicated strains were grown in 0.6 µg/ml of Tunicamycin for 72 hours. ODs were obtained as described in "Materials and Methods". Experiments were performed in triplicate. Asterisks denote statistically significant difference from the control strain for the OD at the peak of growth (*glt1Δ are1Δ are2Δ* and *mfb1Δ are1Δ are2Δ*) and for the time it takes to reach the maximum rate OD (*nup84Δ are1Δ are2Δ* and *cos8Δ are1Δ are2Δ*). Statistical significance with $p<0.05$ (*) with $p<0.01$ (**) was assessed by unpaired t-test.

**B.**

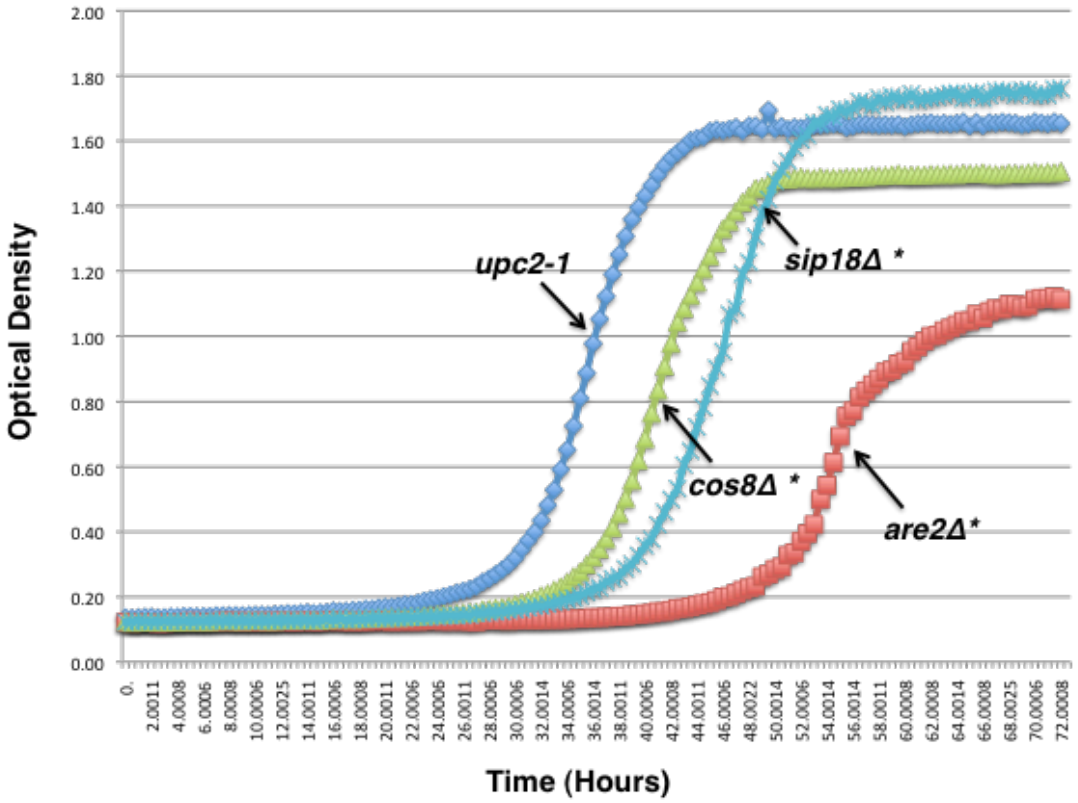


**Figure 7B. Tunicamycin Sensitivity of the Interactors.** The indicated strains were grown in 0.6 µg/ml of Tunicamycin for 72 hours. ODs were obtained as described in "Materials and Methods". Experiments were performed in triplicate. Asterisks denote statistically significant difference from the control strain (upc2-1) for the time it takes to reach the maximum rate OD (*nup84Δ are1Δ are2Δ* and *cos8Δ are1Δ are2Δ*). Statistical significance with $p<0.05$ (*) with $p<0.01$ (**) was assessed by unpaired t-test.

**Table 1: Strains utilized in this study.**

| Strain | Relevant Genotype |
|---|---|
| SCY955 | *MAT**a upc2-1 hi**, ade2-1, can1-1, trp1-1, ura3-1, his3-11, 15, leu2-3, 112* |
| SCY955a | *MAT**a upc2-1 hi**, ade2-1, can1-1, trp1-1, ura3-1, his3-11, 15, leu2-3, 112, aus1::NAT* |
| SCY955b | *MAT**a upc2-1 hi**, ade2-1, can1-1, trp1-1, ura3-1, his3-11, 15, leu2-3, 112, pdr11::NAT* |
| SCY955c | *MAT**a upc2-1 hi**, ade2-1, can1-1, trp1-1, ura3-1, his3-11, 15, leu2-3, 112, cos8::NAT* |
| SCY955d | *MAT**a upc2-1 hi**, ade2-1, can1-1, trp1-1, ura3-1, his3-11, 15, leu2-3, 112, glt1::NAT* |
| SCY955e | *MAT**a upc2-1 hi**, ade2-1, can1-1, trp1-1, ura3-1, his3-11, 15, leu2-3, 112, mfb1::NAT* |
| SCY955f | *MAT**a upc2-1 hi**, ade2-1, can1-1, trp1-1, ura3-1, his3-11, 15, leu2-3, 112, nup84::NAT* |
| SCY955g | *MAT**a upc2-1 hi**, ade2-1, can1-1, trp1-1, ura3-1, his3-11, 15, leu2-3, 112, sip18::NAT* |
| SCY955h | *MAT**a upc2-1 hi**, ade2-1, can1-1, trp1-1, ura3-1, his3-11, 15, leu2-3, 112, yjr096w::NAT* |
| SCY955i | *MAT**a upc2-1 hi**, ade2-1, can1-1, trp1-1, ura3-1, his3-11, 15, leu2-3, 112, are2::URA* |
| SCY325 | *MAT**a**, ade2-1, can1-1, trp1-1, ura3-1, his3-11, 15, leu2-3, 112* |
| SCY325a | *MAT**a**, ade2-1, can1-1, trp1-1, ura3-1, his3-11, 15, leu2-3, 112, aus1::NAT* |
| SCY325b | *MAT**a**, ade2-1, can1-1, trp1-1, ura3-1, his3-11, 15, leu2-3, 112, pdr11::NAT* |
| SCY325e | *MAT**a**, ade2-1, can1-1, trp1-1, ura3-1, his3-11, 15, leu2-3, 112, cos8::NAT* |
| SCY325f | *MAT**a**, ade2-1, can1-1, trp1-1, ura3-1, his3-11, 15, leu2-3, 112, glt1::NAT* |
| SCY325g | *MAT**a**, ade2-1, can1-1, trp1-1, ura3-1, his3-11, 15, leu2-3, 112, mfb1::NAT* |
| SCY325h | *MAT**a**, ade2-1, can1-1, trp1-1, ura3-1, his3-11, 15, leu2-3, 112, nup84::NAT* |
| SCY325i | *MAT**a**, ade2-1, can1-1, trp1-1, ura3-1, his3-11, 15, leu2-3, 112, sip18::NAT* |
| SCY325j | *MAT**a**, ade2-1, can1-1, trp1-1, ura3-1, his3-11, 15, leu2-3, 112, yjr096w::NAT* |
| SCY1090 | *MAT**a**, ade2-1, can1-1, trp1-1, ura3-1, his3-11, 15, leu2-3, 112, are1::HIS, are2::LEU* |

| Strain | Relevant Genotype |
|---|---|
| SCY1090b | *MAT**a**, ade2-1, can1-1, trp1-1, ura3-1, his3-11, 15, leu2-3, 112, are1::HIS, are2::LEU, aus1::NAT* |
| SCY1090c | *MAT**a**, ade2-1, can1-1, trp1-1, ura3-1, his3-11, 15, leu2-3, 112, are1::HIS, are2::LEU, pdr11::NAT* |
| SCY1090d | *MAT**a**, ade2-1, can1-1, trp1-1, ura3-1, his3-11, 15, leu2-3, 112, are1::HIS, are2::LEU, cos8::NAT* |
| SCY1090e | *MAT**a**, ade2-1, can1-1, trp1-1, ura3-1, his3-11, 15, leu2-3, 112, are1::HIS, are2::LEU, glt1::NAT* |
| SCY1090f | *MAT**a**, ade2-1, can1-1, trp1-1, ura3-1, his3-11, 15, leu2-3, 112, are1::HIS, are2::LEU, mfb1::NAT* |
| SCY1090g | *MAT**a**, ade2-1, can1-1, trp1-1, ura3-1, his3-11, 15, leu2-3, 112, are1::HIS, are2::LEU, nup84::NAT* |
| SCY1090h | *MAT**a**, ade2-1, can1-1, trp1-1, ura3-1, his3-11, 15, leu2-3, 112, are1::HIS, are2::LEU, sip18::NAT* |
| SCY1090i | *MAT**a**, ade2-1, can1-1, trp1-1, ura3-1, his3-11, 15, leu2-3, 112, are1::HIS, are2::LEU, yjr096w::NAT* |
| Cos12 | *MAT*a/α *his3Δ1/his3Δ1 leu2Δ0/leu2Δ0 LYS2/lys2Δ0 met15Δ0/MET15 ura3Δ0/ura3Δ0, cos12::KAN* |
| *Slu7*-DAmp | *MAT*a/α *his3Δ1/his3Δ1 leu2Δ0/leu2Δ0 LYS2/lys2Δ0 met15Δ0/MET15 ura3Δ0/ura3Δ0, slu7*-DAmp |

**Table 2. Characterization of Hits**

| Hit | Protein Family | Localization | Function | Human Orthologue | % Identity | Known Interactions |
|---|---|---|---|---|---|---|
| Cos8p | DUP380 | ER, NE | Unknown | NA | NA | NA |
| Cos12p | DUP380 | ER | Unknown | NA | NA | Nup84 (physical) Pdr11p (genetic correlation) |
| Glt1p | NA | Mitochondrion | Glutamate synthase activity | DPYD | 22% | Mfb1 (negative genetic) |
| Mfb1p | F-box | MOM | Required for normal mitochondria tubulation | NA | NA | Glt1 (negative genetic) |
| Nup84p | NA | NE | Nuclear pore organization and biogenesis | NUP107 | 20% | Cos12p (physical) |
| Pdr11p | ABC Transporter | PM, microsomes | Sterol Uptake | ABCG1 | 27% | NA |
| Sip18p | NA | Cytoplasm | Phospholipid Binding | NA | NA | NA |
| YJR096Wp | Aldo-keto reductase (AKR) | Cytoplasm, Nucleus | General pentose sugar reductase | AKR1B1 | 37% | NA |

**Table 2. Characterization of hits.** Abbreviations: NE-nuclear envelope, MOM-mitochondrial outer membrane, ER-endoplasmic reticulum, PM-plasma membrane

## References


1. Maxfield, F. R., and Tabas, I. (2005) *Nature* **438**, 612-621
2. Steck, T. L., and Lange, Y. (2010) *Trends Cell Biol* **20**, 680-687
3. Li, Y., and Prinz, W. A. (2004) *J Biol Chem* **279**, 45226-45234
4. Tabas, I., Rosoff, W. J., and Boykow, G. C. (1988) *J Biol Chem* **263**, 1266-1272
5. Skiba, P. J., Zha, X., Maxfield, F. R., Schissel, S. L., and Tabas, I. (1996) *J Biol Chem* **271**, 13392-13400
6. Paumi, C. M., Menendez, J., Arnoldo, A., Engels, K., Iyer, K. R., Thaminy, S., Georgiev, O., Barral, Y., Michaelis, S., and Stagljar, I. (2007) *Mol Cell* **26**, 15-25
7. Thaminy, S., Miller, J., and Stagljar, I. (2004) *Methods Mol Biol* **261**, 297-312
8. Iyer, K., Burkle, L., Auerbach, D., Thaminy, S., Dinkel, M., Engels, K., and Stagljar, I. (2005) *Sci STKE* **2005**, pl3
9. Erdeniz, N., Mortensen, U. H., and Rothstein, R. (1997) *Genome Res* **7**, 1174-1183
10. Yang, H., Bard, M., Bruner, D. A., Gleeson, A., Deckelbaum, R. J., Aljinovic, G., Pohl, T. M., Rothstein, R., and Sturley, S. L. (1996) *Science* **272**, 1353-1356
11. Wilcox, L. J., Balderes, D. A., Wharton, B., Tinkelenberg, A. H., Rao, G., and Sturley, S. L. (2002) *J Biol Chem* **277**, 32466-32472
12. Gollub, E. G., Trocha, P., Liu, P. K., and Sprinson, D. B. (1974) *Biochem Biophys Res Commun* **56**, 471-477
13. Jensen-Pergakes, K., Guo, Z., Giattina, M., Sturley, S. L., and Bard, M. (2001) *J Bacteriol* **183**, 4950-4957
14. Gulati, S., Liu, Y., Munkacsi, A. B., Wilcox, L., and Sturley, S. L. (2010) *Prog Lipid Res* **49**, 353-365
15. Tabas, I., and Ron, D. (2011) *Nat Cell Biol* **13**, 184-190
16. Lecca, M. R., Wagner, U., Patrignani, A., Berger, E. G., and Hennet, T. (2005) *FASEB J* **19**, 240-242
17. Dixon, S. J., Costanzo, M., Baryshnikova, A., Andrews, B., and Boone, C. (2009) *Annu Rev Genet* **43**, 601-625
18. Despons, L., Wirth, B., Louis, V. L., Potier, S., and Souciet, J. L. (2006) *Trends Genet* **22**, 10-15
19. Bailly-Bechet, M., Borgs, C., Braunstein, A., Chayes, J., Dagkessamanskaia, A., Francois, J. M., and Zecchina, R. (2011) *Proc Natl Acad Sci U S A* **108**, 882-887
20. Kondo-Okamoto, N., Ohkuni, K., Kitagawa, K., McCaffery, J. M., Shaw, J. M., and Okamoto, K. (2006) *Mol Biol Cell* **17**, 3756-3767
21. Schneiter, R. (2007) *Biochimie* **89**, 255-259
22. Haynes, C. M., and Ron, D. (2010) *J Cell Sci* **123**, 3849-3855

# Chapter 4: Physical Interactions between AcylCoA-Sterol-Acyltransferases and ATP binding cassette transporters.


## Abstract

Acyl-coenzyme A:cholesterol acyltransferases (ACATs) play a pivotal role in intracellular lipid and membrane homeostasis by catalyzing the esterification of free sterols with fatty acids. Surprisingly, the mechanism by which the substrates are delivered to the ACATs remains poorly defined. We performed a membrane-associated yeast two hybrid screen utilizing the budding yeast ortholog of the ACATs, ACAT-related enzyme 2 (Are2p) to identify protein interactions that mediate lipid transfer. We discovered that in addition to undergoing self-multimerization, Are2p physically interacts with Aus1p and Pdr11p, members of the G sub-family of ATP binding cassette (ABC) membrane transporters. Are2p, Aus1p, and Pdr11p were found to co-localize to the endoplasmic reticulum and the plasma membrane in cold detergent resistant membrane microdomains (DRMs) and to co-immunoprecipitate after covalent crosslinking. Deletion of either ABC transporter resulted in Are2p re-localization from DRMs to a detergent soluble fraction as well as a significant decrease in the percent of sterol esterified. This phenomenon is evolutionarily conserved in the murine lung where Abcg1p and Acat1p were observed to co-localize with flotillin-1, a marker of DRMs. We propose that co-localization and complex formation of sterol esterification enzymes and ABC transporters in DRMs reflects a novel mechanism that directs membrane sterols to the esterification reaction.

**Introduction**

Cholesteryl esters play an integral role in a myriad of metabolic processes including lipoprotein assembly in the liver and intestine, intestinal cholesterol absorption, as well as cholesterol and fatty acid storage in cytoplasmic lipid droplets. The latter event provides a reservoir that safely sequesters these toxic substrates until they are required for membrane assembly. The catalysis of sterol esterification is performed by the Acyl-coenzyme A:cholesterol acyltransferases (ACATs) and is conserved throughout eukaryotic evolution. In mammalian cells, the ACAT gene family is tripartite, comprising ACAT1, ACAT2 and DGAT1 (the latter enzyme esterifies diacylglycerols not sterols). In *Saccharomyces cerevisiae,* sterol esterification is mediated by two *A*CAT *r*elated *e*nzymes, Are1p and Are2p. The deletion of *ARE2* encoding the major isoform results in a 75% decrease in ergosteryl or cholesteryl esters, whereas deletion of both sterol esterifying genes results in a viable yeast cell without steryl esters but control levels of trigycerides. The yeast double mutant can be complemented by the heterologous expression of human ACAT1 or ACAT2 cDNAs indicating both functional and structural conservation of these pathways from yeast to metazoans. The ACAT reaction is regulated primarily at the posttranslational level by allosteric activation of the enzyme by sterols (1). This can be demonstrated both *in vitro* and *in vivo*, the latter observation indicating that the transport of these membrane components to the esterification enzymes is a significant regulatory component of this metabolic pathway.

The ACAT protein has been long regarded as integral to the ER membrane (2,3) with as many as seven transmembrane domains in the case of ACAT1 (4). The functional size of native ACAT in rat liver microsomes ranged from 170 to 224 kDa based on radiation inactivation experiments (5,6) while the predicted size of the monomeric ACAT1 protein is ~64.8 kDa. Moreover, cross-linking studies indicated that ACAT1 purified from rat adrenal gland microsomes exists as oligomeric complexes *in vitro*. Human ACAT1 most likely interacts with itself and this was confirmed by biochemical studies performed in intact cells and

*in vitro* (7). The ACAT catalytic complex may be solely composed of ACAT1 or other proteins including ACAT2.

Despite playing a pertinent role in both cholesterol metabolism and in the development of atherosclerosis, the mechanism by which the cholesterol substrate reaches the ACATs remains elusive. Approximately 50% of the cholesterol substrate for ACAT1 originates from a cholesterol oxidase accessible, endogenous cellular pool (8). The esterification of this endogenous pool of sterol is unaffected by energy depletion, inhibition of membrane vesicle trafficking, and defects in the endosomal-lysosomal pathway (9). These data suggest that transport of the sterol substrate to the ACATs may be facilitated by soluble sterol binding proteins or a previously uncharacterized vesicular system. To date, little progress has been made towards identifying molecular components of this transit despite its major contribution to sterol fluxes within the cell.

In order to determine if protein-protein interactions mediate sterol transport to sites of esterification from the plasma membrane, we performed a split-ubiquitin, membrane yeast two-hybrid screen utilizing the major yeast ACAT enzyme, Are2p, as bait. As a result of our screen we identified nine putative Are2p interacting proteins (Chapter 3, Figure 3). Surprisingly, among these proteins was the ABC transporter, Pdr11p, which along with Aus1p mediates sterol influx during anaerobiosis. These findings suggest that plasma membrane ABC transporters participate in a protein complex that directly transfers sterols to the ACAT enzymes and thus regulates the esterification pathway.

**EXPERIMENTAL PROCEDURES**

*General*. Yeast strains used in this study are isogenic with the strain W303-1A (*MAT*a *ade2-1, can1-1, trp1-1, ura3-1, his3-11, 15, leu2-3, 112*. The *upc2-1* high and low alleles were monitored by quantitative sterol uptake and by PCR of the *UPC2* and *HAP1* loci(10). Deletion mutant strains were generated and confirmed by established methods (Chapter 3, Table 1). Yeast transformation was

performed with lithium acetate followed by selection on YPD and 100ug/L of nourseothricin. HA tagged constructs of Are1p and Are2p were made as previously described (11)

*Analysis of exogenous sterol accumulation and esterification.* Cells were grown for approximately 20 h in the indicated media containing 1% tyloxapol/ethanol (1:1) and 0.01 μCi/ml [4-$^{14}$C]cholesterol. Sterols were extracted and analyzed via thin layer chromatography (12) .

*Isolation of lipid rafts from murine lung.* Approximately 300 mg of mouse lung was homogenized in 1 ml of lysis buffer (1% Triton X-100, 25mM HEPES, pH 6.5, 150 mM NaCl, 1 mm EDTA, 1mM PMSF, and protease cocktail (Roche Molecular Biochemicals, Indianapolis, IN, USA)) and held at 4°C for 30 minutes. The extract was mixed with 1 ml of 2.5M sucrose and overlaid with 6 ml of 30% sucrose, 25 mM Hepes 150 mM NaCl) and 4 ml of 5% sucrose and centrifuged for 18h at 4°C at 39,000 rpm. The gradient was separated into 12 fractions, collected from the top.

*Isolation of lipid rafts from budding yeast.* 10–20 $OD_{600}$ units of yeast were grown at 30°C to log phase and lysed in 750 μl of TNE buffer (50 mM Tris·HCl, pH 7.4, 150 mM NaCl, 5 mM EDTA 1 mM PMSF and 2.5 μg/ml chymostatin, leupeptin, antipain, and pepstatin) by glass bead disruption at 4°C. Cleared lysates (400 *μ*l), were pre-incubated with Triton X-100 (1% final) for 30 min on ice and mixed with 2 volumes of 60% Optiprep and overlaid with 2.7 ml of 30% Optiprep in TNE. Samples were centrifuged at 45,000 rpm for 2 h. Nine fractions of equal volume were collected from the top.

*Subcellular fractionation.* Membrane preparations from cells grown for 18 h were subjected to discontinuous gradient ultracentrifugation (12).

Cross linking and immunoprecipitation. Yeast microsomes (13,14) were resuspended in phosphate buffered saline (PBS)/1 mM phenylmethylsulphonylfluoride and incubated on ice for 0.5 h. followed by cross-linking with Dithiobis Succinimidyl Propionate (DSP). (2 mM final concentration)

for 0.5 h at room temperature. The reaction was quenched with 50 mM of Tris–HCl pH 7.4 at room temperature for 15 min and solubilized in 10 mM Hepes (pH 7.5), 150 mM NaCl, 1% Triton X-100, and protease inhibitors. YFP tagged proteins were immunoprecipitated with anti-GFP conjugated agarose beads at 4°C, washed three times and incubated at 59 °C for 15 m. in SDS sample buffer containing 50 mM DTT. Immunoprecipitation of the HA-epitope tagged enzyme (12CA5, Boehringer-Mannheim) from microsomes were performed in the presence of the RIPA buffer (9.1 mM $Na_2HPO_4$, 1.7 mM $NaH_2PO_4$, 150 mM NaCl, 1% Triton X-100, 0.5% deoxycholate, 0.1% SDS). Immunoprecipitates were collected on protein G agarose beads (Gibco BRL). Immunocomplexes were washed in the RIPA buffer, resuspended in SDS-sample buffer containing b-mercaptoethanol, and resolved by 6.5% SDS-PAGE and immunoblotting with chicken anti-Are2p (15) or rabbit anti-HA (Santa Cruz Biotech) antibodies.
*Interaction Screens.* Two versions of yeast two hybrid screens were used for these studies. The “interaction-trap” version and the membrane split ubiquitin was executed as previously described (11) (Chapter 3).

β-Galactosidase assays. Quantitative β-galactosidase activity assays of cell lysates were performed as previously described (11).

**RESULTS**

*Sterol esterification in yeast acts independently of endosomal- vacuolar protein sorting.* The transport of sterols to the ER from the periphery of the cell is integral to cellular sterol homeostasis. This is achieved by a myriad of mechanisms, both spontaneous and protein mediated, vesicular and non-vesicular. Sterol esterification at the ER accomplishes a key change in both physico-chemical and biological properties of this lipid (polar to non-polar, membrane participating to storage form) that essentially terminates the transport reaction and removes the sterol from a regulatory pool. In yeast, sterol transport and subsequent esterification is unaffected by the inhibition of vesicular trafficking and

independent of the coat forming protein complexes COPI and COPII (16). In metazoans, the endocytic pathway is a key component of sterol transport from the plasma membrane to intracellular organelles. In *S. cerevisiae*, a number of genes have been identified in screens for mutants defective in the internalization of pheromone receptor or the fluid-phase endocytic marker, lucifer yellow (17). One of these mutants, *end3*, a member of the evolutionarily conserved EH (Eps15 homology) domain family in yeast, exhibits a clear defect in internalization, temperature-sensitive growth, and defects in organization of the actin cytoskeleton (17). In order to assess the role of the endocytic pathway in transporting sterol to the esterifying enzyme, we measured the percent of radiolabeled exogenous cholesterol that is esterified in an *END3* null mutant. We found that abrogation of this pathway had no significant impact on sterol esterification (Figure 1). Similarly we assessed the VPS (vacuolar protein sorting) pathway that mediates protein transport from the late Golgi to the lysosome-like vacuole and thus its integrity. The analogous endosomal/lysosomal pathway of multicellular organisms recycles cholesterol between the plasma membrane and lysosomes and ultimately the ER. In yeast, more than 50 vps mutants, disrupt transport to the vacuole. These mutants have been categorized based on their morphology as well as their vacuolar protein sorting and acidification defects. In order to ascertain the contribution of this pathway in transporting sterols to the ACATs, we measured the percent of sterol esterified in 3 distinct *vps* mutants (vps18, 21, and 28). We found that disrupting the activity of the vacuole in this fashion did not decrease sterol esterification. These data suggest that sterol delivery to the site of esterification is independent of the retrograde vesicular transport system and the endocytic pathway leading us to pursue the role of lipid transporters and protein-protein interactions in this process.

*Multimerization of sterol esterification enzymes.* Numerous precedents suggest that the sterol esterification reaction is performed by a multimeric complex (5-7). To investigate the self-association of these enzymes, we utilized a variant of the

yeast two-hybrid (Y2H) system that primarily detects the interaction of soluble domains of partner proteins (18,19). The full-length open reading frames of *ARE1* and *ARE2* were fused to the operator binding domain of LexA (pLexA-*ARE1,* pLexA-*ARE2*) or to a transcription activation domain (pAD-*ARE1,* pAD-*ARE2*). Expression and esterification activity of the LexA or AD fusion proteins were confirmed by immunoblotting and metabolic incorporation studies. These constructs were co-transformed with a *LacZ* reporter plasmid and assessed by quantitative liquid β-galactosidase assays. The yeast ACATs homomultimerize in this context (Table 1); β-galactosidase activity was significantly elevated when pLexA-*ARE2* was cotransformed with pAD-*ARE2*. Similarly, the Are1p fusion proteins encoded by pAD-*ARE1* and pLexA-*ARE1* formed an active complex and activated transcription of the reporter gene (Table 1). Interestingly, despite extensive sequence conservation between these enzyme isoforms (20), we saw no evidence for heteromeric interactions; the combination of pLexA-*ARE1* and pAD-*ARE2* or pAD-*ARE1* and pLexA-*ARE2* did not significantly activate reporter expression (Table 1).

The physical associations between the ACAT isoforms were further assessed and confirmed by co-immunoprecipitation experiments with epitope tagged active forms of the Are proteins. An *are1Δ are2Δ* strain was co-transformed with control or HA-*ARE* expression plasmids. Microsomes from these strains were immunoprecipitated with anti-HA antibody and the eluted proteins were blotted using the chicken anti-Are2p antibody or the anti-HA antibody (Figure 2). We observed that Are2p but not Are1p could be co-immunoprecipitated with HA-Are2p corroborating the two hybrid interactions,

*Are2p interacting proteins.* The aforementioned Y2H interaction assay was used to screen a yeast genomic library, but to no avail (11). Several putative interacting proteins were identified (*HKR1*, *ECM27*, YOR223w, *FET3* and *BUD4*), however the deletion of any of these genes had no detectable impact on several parameters of sterol homeostasis, including sterol esterification. To identify more

meaningful ACAT binding proteins, we performed an integrated split- ubiquitin membrane yeast two hybrid screen utilizing Are2p as bait. This particular Y2H system permits the *in vivo* detection of membrane associated protein-protein interactions (21). Since the sterol esterification reaction and the ACAT molecules are membrane associated, we reasoned that this form of the two-hybrid system, had greater potential to reveal meaningful *trans*-acting interactions. To accomplish this screen, the C-terminus of Are2p was fused in frame with a Cub-YFP-TF moiety via homologous recombination in the yeast reporter strain THY AP4. The activity of this construct was also confirmed by metabolic incorporation studies (Chapter 3, Figure 1). We then transformed this strain with a yeast genomic "prey" library. As a result of our screen we found nine putative in-frame, interacting proteins (Table 2). Of these interactors, Cos12p has been reported to physically interact with Nup84p and is part of the same protein family (the DUP380 family) as Cos8p. To assess the individual role of each protein in sterol esterification, we created a deletion mutant of each of the nine candidate genes in a *upc2-1* strain and measured the esterification of radiolabelled cholesterol. The *upc2-1* strain contains a gain of function mutation in the transcription factor encoded by *UPC2*, that facilitates aerobic sterol influx (22). Of the nine mutants, deletion of *COS8*, *SIP18*, *MFBI* and *YJR*096W and particularly *PDR11,* resulted in significant decreases in exogenous sterol esterification (Chapter 3, Figure 2). Pdr11p and its closest paralog, Aus1p, mediate the influx of sterols during anaerobiosis (10). Corroborating our previous work we found that an *aus1* deletion also results in a profound decrease in sterol esterification, even after compensation for the reduction in sterol uptake associated with this mutant (Chapter 3, Figure 2). We propose that Pdr11p (and likely Aus1p) act with Are2p to modulate the sterol esterification pathway.

*Aus1p and Pdr11p localize to plasma membrane and microsomal fractions.* Aus1p and Pdr11p are full ABC transporters that mediate the retrograde transport of sterols, which is the first step in the sterol esterification pathway. In

order to assess the localization of these proteins we tagged both *AUS1* and *PDR11* with YFP in the chromosome by homologous recombination in a *upc2-1* strain, so that their expression could by monitored aerobically by fluorescence microscopy. Aus1p and Pdr11p localized to the periphery of the cell in a punctate pattern, consistent with a plasma membrane and/or a cortical ER localization (Figure 3A). The plasma membrane localization was further confirmed by a subcellular fractionation (Figure 3B). To assess the possible co-localization of these proteins we performed a simple cellular sub-fractionation and found that both ABC-transporters localize to microsomes, along with Are2p (Fig. 4). This co-localization provides a cellular context for the *in vivo* interaction of these three proteins.

*Aus1p, Pdr11p, and Are2p physically interact.* In order to confirm the physical interaction of Are2p with Aus1p and Pdr11p, we performed co-immunoprecipitation assays (Figure 5). Microsomal fractions were isolated from cells, which contained either an Aus1 or Pdr11 YFP fusion and were transformed with an *ARE2-HA* plasmid or vector control. Proteins were immunoprecipitated with anti-GFP conjugated agarose beads in the presence of an exogenous cross-linker (DSP). Eluted proteins were blotted using an anti-HA antibody. These assays confirm that both Aus1p and Pdr11p physically interact with Are2p. This suggests that sterols may be directly transferred from the ABC transporters to the ACATs, thereby negating the need for an intermediary sterol binding protein.

*Aus1p, Pdr11p, and Are2p co-localize to membrane microdomains*. Cold Detergent Resistant Microdomains (DRMs) are cholesterol and sphingolipid rich membrane foci common to all eukaryotic organisms. DRMs serve as membrane hubs that integrate various pathways, such as lipid influx and efflux, protein trafficking, and signal transduction (23). To assess whether DRMs play a role in the sterol esterification pathway, total membrane proteins were solubilized with ice-cold 1% Triton X-100 detergent and fractionated by an Opti-prep gradient

centrifugation. The isolated DRMs were probed with anti-HA and anti-GFP antibodies to look for expression of Aus1p, Pdr11p, and Are2p (Figure 6A & 7B). In control cells, all three proteins co-localize with the DRM marker Pma1p (Figure 6). This suggests that DRMs may provide a platform, that integrates the sterol influx and esterification pathways in yeast. Interestingly, a deletion of either ABC transporter significantly altered Are2p localization from a DRM to a detergent soluble fraction (Figure 6B). This data suggests that Are2p's physical interaction with the ABC transporters is necessary for its DRM localization. We speculate that this shift in localization may contribute to the decrease in the percent of esterification associated with a deletion of *AUS1* or *PDR11* (Figure 1). Based on these data we propose that sterol transfer in the cholesterol esterification pathway occurs as a consequence of a physical interaction of Aus1p, Pdr11p, and Are2p in a DRM fraction.

*mABCG1 and mACAT1 co-localize with the DRM marker mFlotillin-1 in murine lung.* Aus1p and Pdr11p are members of the ABC-G subfamily and share approximately 29% sequence identity with mammalian ABCG1. The cholesterol esterification pathway in higher eukaryotes, as in yeast, is unaffected by defects in vesicular trafficking and the endosomal/lysosomal pathway. Furthermore, overexpression of ABCG1 in baby hamster kidney cells significantly increased cholesterol esterification (24). ABCG1 may thereby play a role in the transport of cholesterol to the ACATs. In order to investigate whether ABCG1 and ACAT1 co-localize, we isolated DRMs from murine lung and probed these fractions with ABCG1 and ACAT1 antibodies (Figure 7A). We found that both proteins co-localize to DRMs. Furthermore, we observed that in an ABCG1 KO murine lung (Figure 7B), there was more ACAT1 in the detergent soluble fraction than in the control mouse. This data suggests that similar to budding yeast, ACAT1's localization to the DRM is dependent on its interaction with ABCG1.

## DISCUSSION

The esterification of free cholesterol by the ACATs is an evolutionarily conserved component of cholesterol homeostasis that accomplishes a significant change in both physico-chemical and biological properties of this lipid. Prior to esterification, the cholesterol substrate requires solubilization by proteins and /or membranes, in order to be efficiently delivered to the ACAT reaction and yet the manner in which this is achieved, remains elusive. 50% of the ACAT substrate pool originates from the plasma membrane and its esterification is unaffected by energy depletion, inhibition of membrane vesicle trafficking, and defects in the endosomal-lysosomal pathway. The studies presented here offer an attractive mechanism for plasma membrane to ER cholesterol transport. Our studies in yeast show that sterol is transferred from the plasma membrane via the ABC transporters, Aus1p and Pdr11p to the ARE2-encoded esterification reaction at the ER. Furthermore, Are2p, Aus1p, and Pdr11p co-localize to both the plasma membrane and the ER, particularly in DRMs. Deletion of either ABC transporter results in Are2p re-localization from a DRM to a detergent soluble fraction as well as a significant decrease in the percent of cholesterol esterified. Interestingly, this co- localization is conserved; ABCG1 and ACAT1 co-localize with the DRM marker flot-1 in murine lung. Overexpression of human ABCG1 in baby hamster kidney cells redistributes membrane cholesterol to cell-surface domains (accessible to treatment with the enzyme cholesterol oxidase) and increases cholesterol esterification suggesting a physiological role of the interaction between these proteins in mammals (24).

ACAT multimerization is likely required for enzymatic activity and in addition the allosteric regulation of activity by sterols. Interestingly, both Are2p and Acat1 contain putative leucine zipper motifs, which mediate protein-protein interaction. Although the exact role of these motifs has not been elucidated, it is reasonable that these sites may enhance ACAT homomultimerization. However, leucine zipper motifs have also been shown to promote heterodimerization of

proteins. Therefore, the possibility that these motifs may also promote the interaction of the ACATs with other proteins, can not be excluded.

Plasma membrane pools of cholesterol are tightly regulated. Modest alterations in plasma membrane cholesterol induce a rapid and multifaceted homeostatic response. The esterification of cholesterol by the ACATs is the first line defense employed by the cell against increasing cholesterol levels. ACAT activity can increase three fold within an hour as a response to just a 10% increase in cell surface cholesterol. Intrinsic to this acute response by the ACATs is the requirement for rapid cholesterol transport from the plasma membrane to the ER (25). We and others have shown that classical cholesterol transport mechanisms such as vesicular trafficking or movement of cholesterol through the endocytic pathway do not significantly contribute to the transport of cholesterol to the ER. Based on our studies we propose that the interaction between members of the ABC transporter family and the ACATs promotes rapid cholesterol transport from the plasma membrane to the ER. Furthermore, the co-localization of these proteins to cholesterol rich DRMs provides an attractive cellular context for this transport mechanism to occur. Further characterization of this interaction will provide valuable insight as to how these proteins contribute to sterol homeostasis and disease states that occur as a result of sterol dysregulation.

**FOOTNOTES**

Supported by the American Heart Association, the Ara Parseghian Medical Research Foundation, the Hirschl/Weil-Caulier Trust, Pfizer and NIH (DK54320) to SLS. LJW was supported by a fellowship from the Canadian Institutes of Health Research.

**Abbreviations:** ER, endoplasmic reticulum; ACAT: acyl-coenzyme A (Co-A): cholesterol acyl transferase; Co-IP, co-immunoprecipitation; CSM, complete synthetic medium; Cub, C-terminal ubiquitin; DSP, dithiobis succinimidyl ropionate; ER, endoplasmic reticulum; HA, peptide from human hemagglutinin; Nub, N-terminal ubiquitin; X-Gal, 5-bromo-4-chloro-3-indolyl-ß-D-galactoside.

**TABLES.**

| pAD fusion | pLexA fusion | two-hybrid interaction (Miller units) |
|---|---|---|
| Are1 | Are1 | 830.1 ± 58.7 |
| Are1 | Max | 22.8 ± 4.7 |
| Mxi | Are1 | 21.3 ± 2.0 |
| Are2 | Are2 | 309.1 ± 15.9 |
| Are2 | Max | 40.8 ± 5.5 |
| Mxi | Are2 | 15.2 ± 2.3 |
| Are1 | Are2 | 52.9 ± 7.1 |
| Are2 | Are1 | 16.8 ± 3.8 |
| Mxi | Max | 203.5 ± 12.9 |
| None | None | 16.2 ± 2.8 |

**Table 1. Multimerization of sterol esterification enzymes.** The yeast strain was transformed with the reporter plasmid pSH 18-34, pAD fusions and pLexA fusions as indicated. β-galactosidase activity was determined in log phase cultures in SC-Ura-Trp-His galactose-containing medium as described under "Materials and Methods." The values (± standard deviation) are the mean of three determinations. Two viral proteins, Max and Mxi form a complex ???However, if pLexA-*ARE2* was co-transformed with the vector pAD or with pAD-Mxi, b-galactosidase activity was low. This was also true for pAD-*ARE2* when co-transformed with pLexA or with pLexA-Max. The combination of pLexA-Max and pAD-Mxi served as a positive control. Table taken from (11).

**Figure 1**

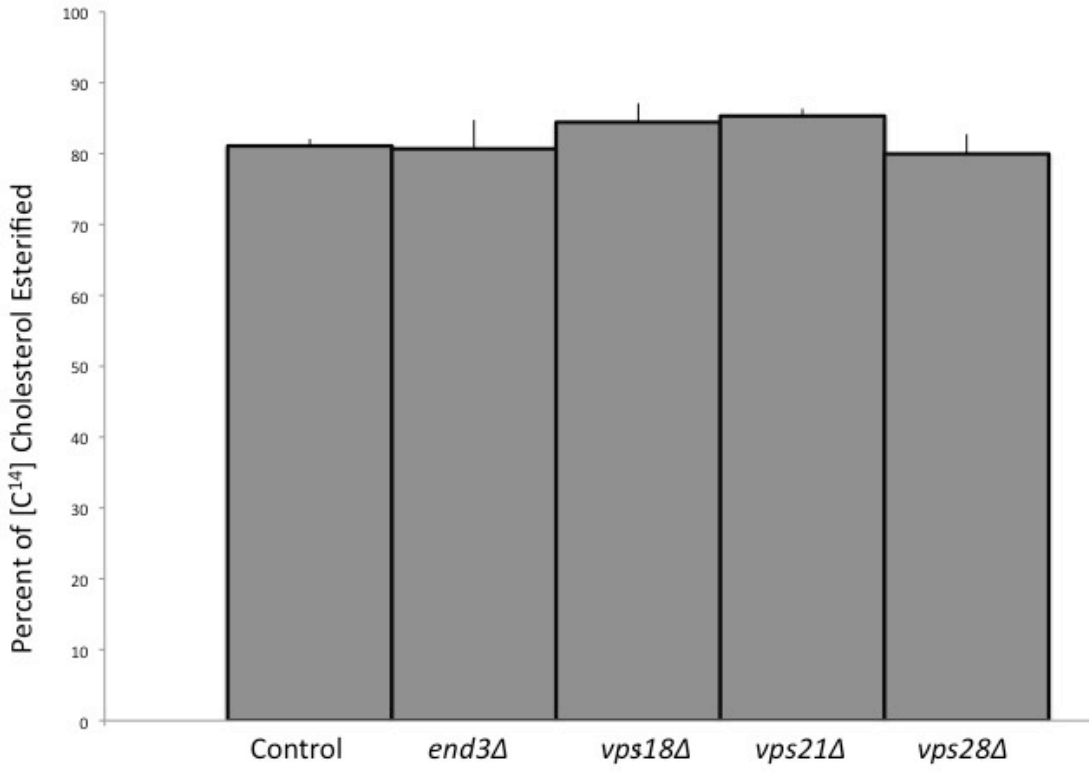


**Figure 1. Sterol esterification is independent of the endosomal and vacuolar protein sorting pathways.** The indicated strains were grown for 18 h to mid-log phase in YEPD media containing 1% tyloxapol/ethanol (1:1), fatty acids (Tween 80), unlabeled cholesterol (20 µg/ml), and 0.01 µCi/ml [4-$^{14}$C]cholesterol. Anaerobic growth was achieved using BD PharMingen, $CO_2$-generating gas packs and jars . Sterol esterification was determined by the inclusion of 0.01 µCi/ml [4-$^{14}$C]cholesterol (as previously described) and reflects the mean ± S.E. from triplicates of each strain. There were no statistically significant difference between strains as assessed by the unpaired t-test.

**Figure 2**

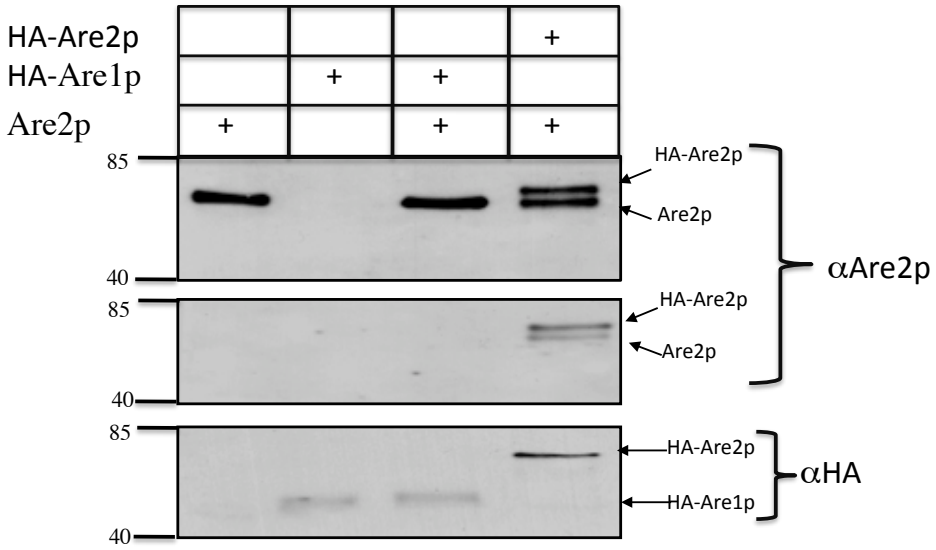


**Figure 2. Are2p complexes with HA-Are2p but not with HA-Are1p by co-immunoprecipitation.** Microsomal proteins were prepared from an *are1Δ are2Δ* strains carrying one or two plasmids as indicated on top of the figure. The strains were solubilized and co-immunoprecipitated with anti-HA antibody. The eluate was immunoblotted with either anti-Are2p antibody or anti-HA antibody. The arrow indicates one of the full-length proteins: HA-Are2p, HA-Are1p, or Are2p. This figure was taken from (11)

**Figure 3**

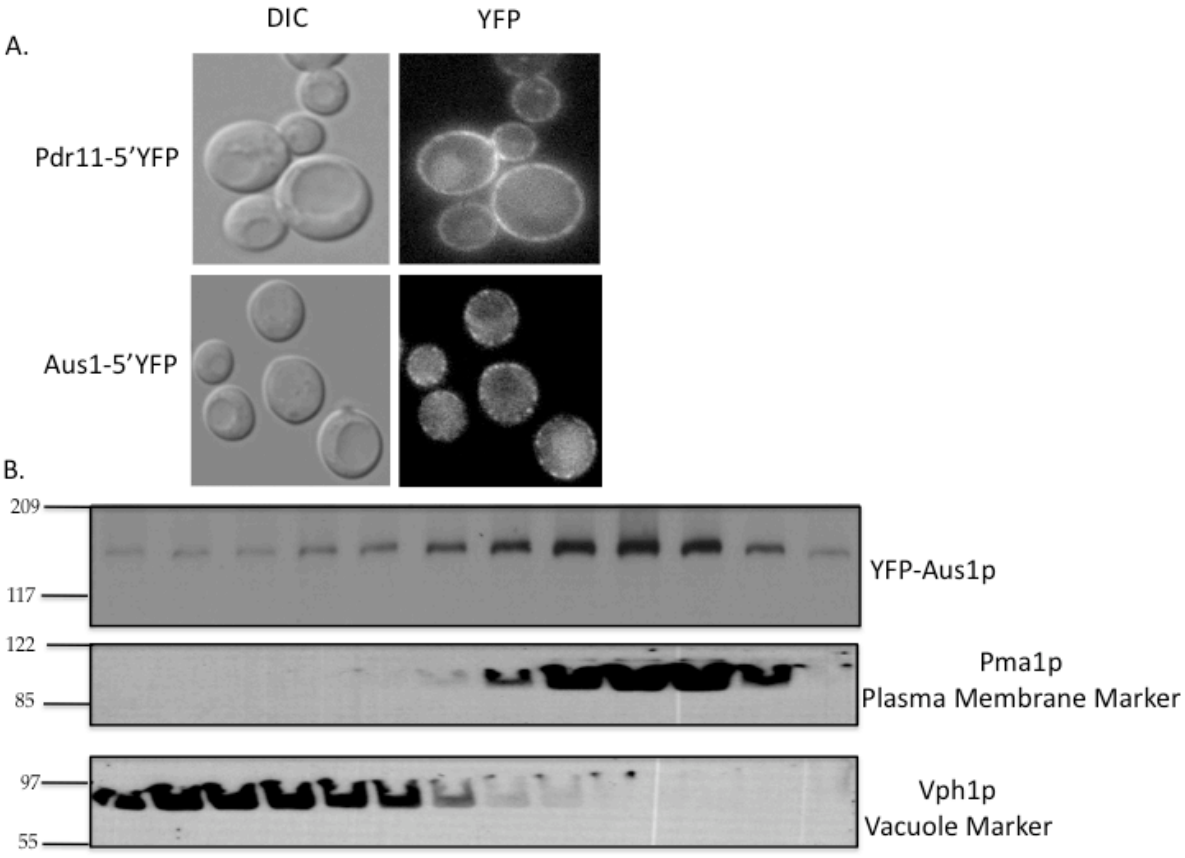


**Figure 3. Aus1p and Pdr11p localize to the plasma membrane. A**, Fluorescence microscopy of Aus1-5'YFP and Pdr11-5'YFP shows a punctate localization to the plasma membrane. **B**, A western blot of membrane proteins seperated by Renografin density gradients. The blot was probed with anti-YFP, anti-PMA1, and anti-VPH1.

**Figure 4**

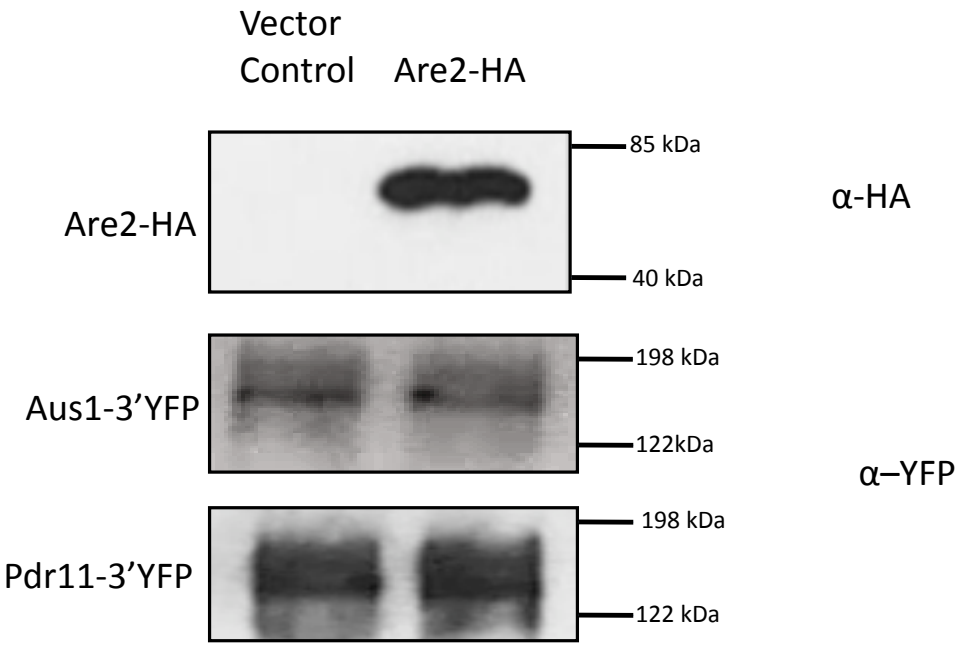


**Figure 4. Are2p, Aus1p, and Pdr11p localize to the microsomal fraction of the ER.** The indicated strains were transformed with pRS424 or pRS424/Are2-HA and microsomes were isolated. The microsomal fractions were subjected to Western blots. Anti-HA was used to detect are2p and anti-YFP was used to detect aus1p and pdr11p.

**Figure 5.**

**A**

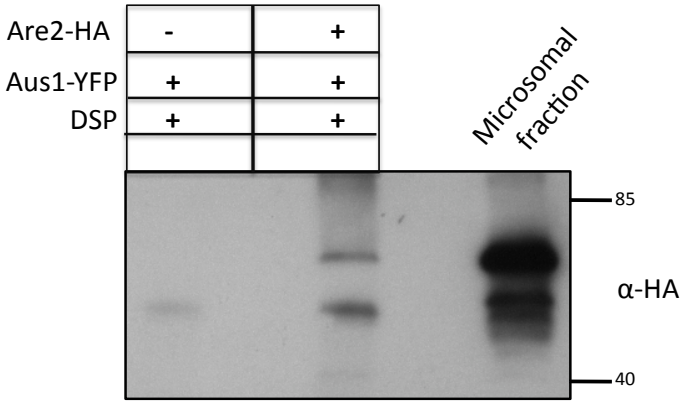


**B**

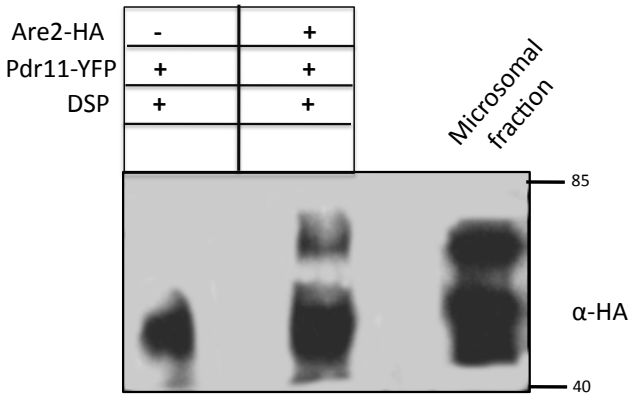


**Figure 5. Multimerization of ABC transporters and sterol esterification enzyme**. A, Co-immunoprecipitation of Aus1-YFP and Are2-HA. Aus1-YFP was transformed with a vector control (pRS424) or pRS424/Are2-HA. Microsomes from these strains were solubilized and co-immunoprecipiated with GFP conjugated agarose beads. The eluate was immunoblotted with anti-HA. B, Co-immunoprecipitation of Pdr11-YFP and Are2-HA. Pdr11-YFP was transformed with a vector control (pRS424) or pRS424/Are2-HA. Microsomes from these strains were solubilized and co-immunoprecipiated with GFP conjugated agarose beads. The eluate was immunoblotted with anti-HA.

**Figure 6**

**A**

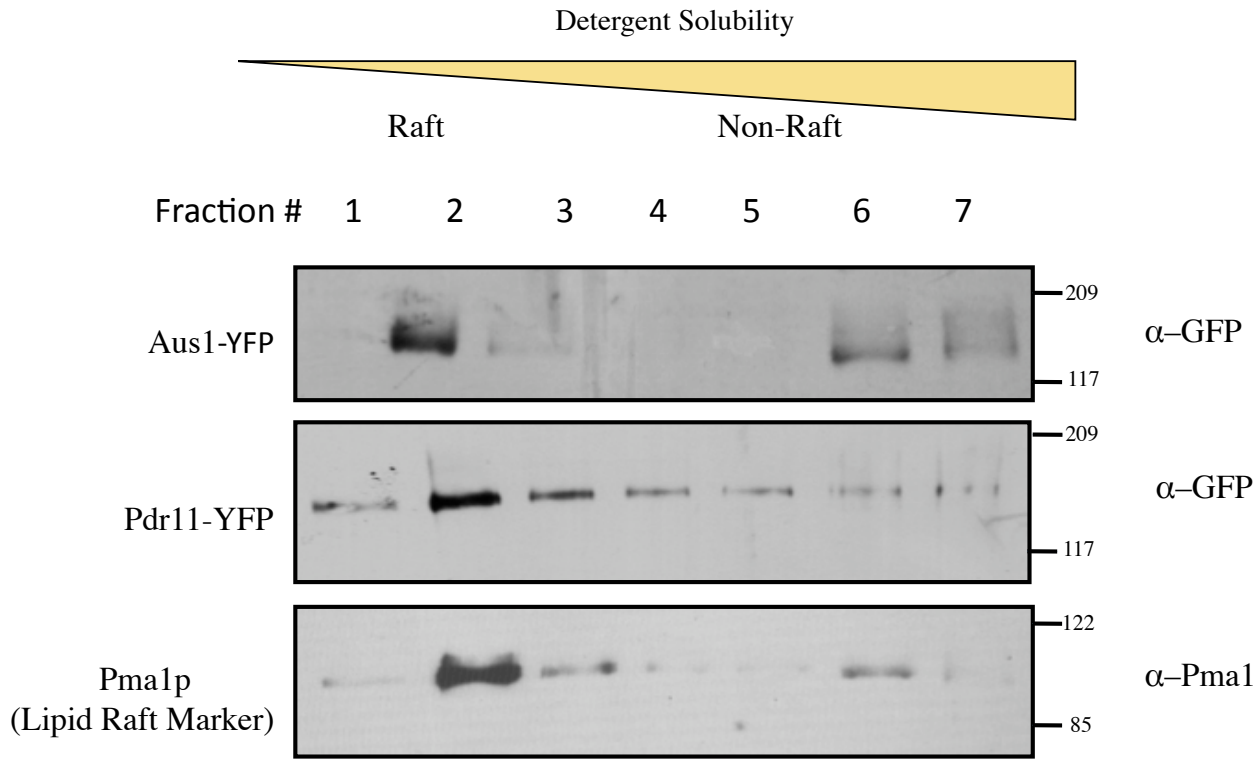


**Figure 6A. ABC-transporters localize to plasma membrane microdomains.** Total membrane protein from the indicated strains were solubilized with ice-cold 1% Triton X-100 and fractionated by an Opti-prep gradient centrifugation. Isolated fractions were run on gradient SDS-PAGE gel and the Western blot membrane was probed with anti-PMA1 and anti-GFP.

**B.**

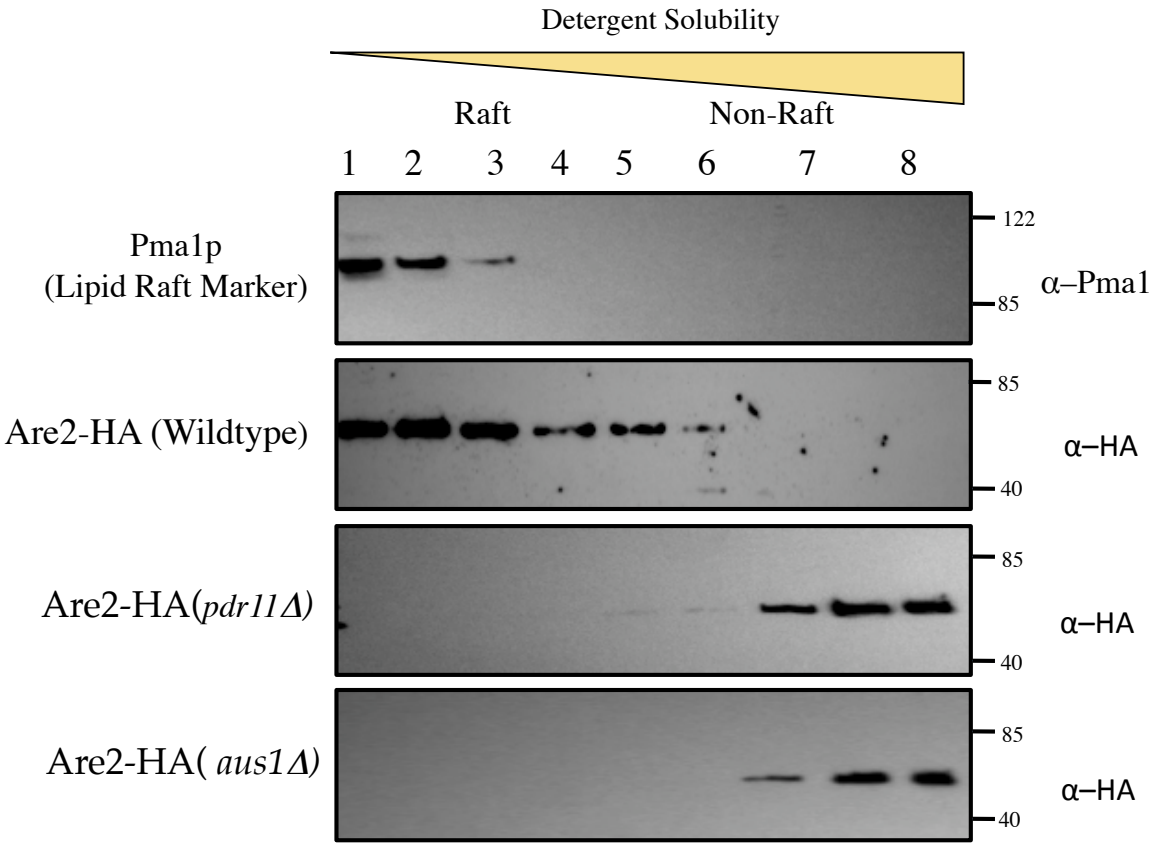


**Figure 6B. ABC-transporters localize to plasma membrane microdomains**. Total membrane protein from the indicated strains were solubilized with ice-cold 1% Triton X-100 and fractionated by an Opti-prep gradient centrifugation. Isolated fractions were run on gradient SDS-PAGE gel and the Western blot membrane was probed with anti-PMA1 and anti-HA. Pma1p localization in mutants is the same as that shown in the wildtype strain (data not shown).

**Figure 7**

**A**

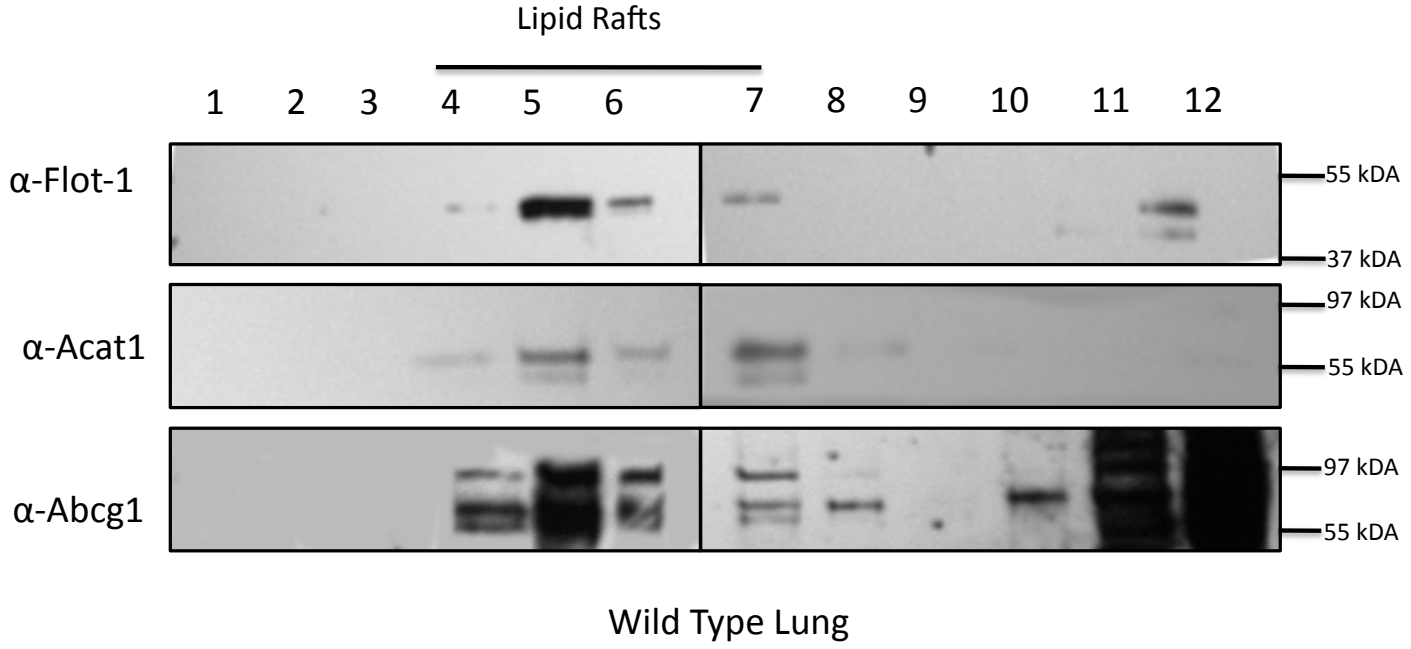


**Figure 7A. ABC-transporters and Sterol esterification enzymes localize to detergent insoluble domains in mammalian cells.** Expression of Flotillin-1, Acat1, and Abcg1 in lipid rafts of wild type murine lung.

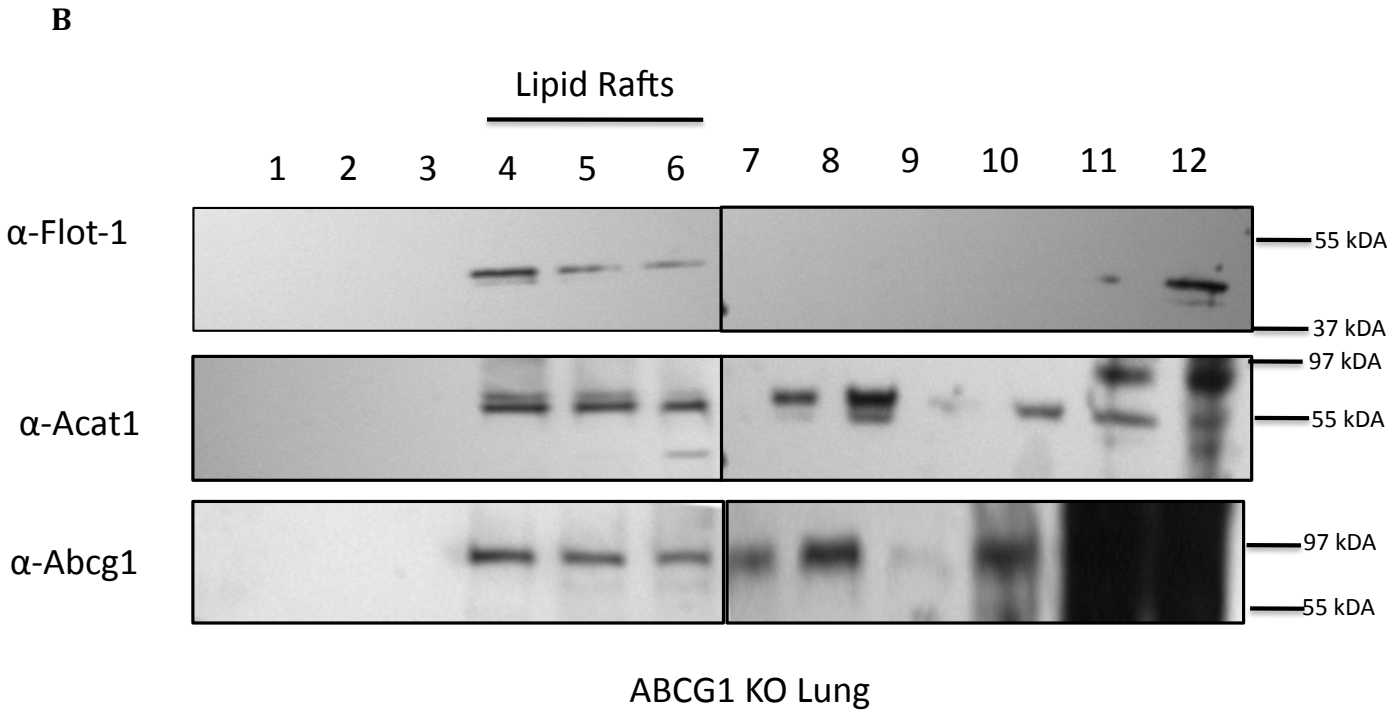


**Figure 7B. ABC-transporters and Sterol esterification enzymes localize to detergent insoluble domains in mammalian cells.** Expression of Flotillin-1, Acat1, and Abcg1 in lipid rafts of an abcg1 KO murine

## REFERENCES.


1. Cheng, D., Chang, C. C., Qu, X., and Chang, T. Y. (1995) *Journal of Biological Chemistry* **270**, 685-695
2. Chang, T.-Y., and Doolittle, G. M. (1983) Acyl Coenzyme A: Cholesterol O-Acyltransferase. in *The Enzymes* (Boyer, P. ed.), Academic Press, New York. pp 523-539
3. Goodman, D. S., Deykin, D., and Shiratori, T. (1964) *J. Biol. Chem.* **239**, 1335-1344
4. Lin, S., Cheng, D., Liu, M. S., Chen, J., and Chang, T. Y. (1999) *J Biol Chem* **274**, 23276-23285
5. Billheimer, J. T., Cromley, D. A., and Kempner, E. S. (1990) *J Biol Chem* **265**, 8632-8635
6. Erickson, S. K., Lear, S. R., and McCreery, M. J. (1994) *J. Lipid Res.* **35**, 763-769
7. Yu, C., Chen, J., Lin, S., Liu, J., Chang, C. C., and Chang, T. Y. (1999) *J Biol Chem* **274**, 36139-36145
8. Tabas, I. (2002) *J Clin Invest* **110**, 905-911
9. Liscum, L., and Underwood, K. W. (1995) *J. Biol. Chem.* **270**, 15443-15446
10. Wilcox, L. J., Balderes, D. A., Wharton, B., Tinkelenberg, A. H., Rao, G., and Sturley, S. L. (2002) *J. Biol. Chem.* **277**, 32466-32472
11. Guo, Z. (2000) Functional Characterization of Sterol Esterification Enzymes in Yeast. in *Human Nutrition*, Columbia University, New York
12. Tinkelenberg, A. H., Liu, Y., Alcantara, F., Khan, S., Guo, Z., Bard, M., and Sturley, S. L. (2000) *J. Biol. Chem.* **275**, 40667 - 40670
13. Guo, Z., Cromley, D., Billheimer, J. T., and Sturley, S. L. (2001) *J Lipid Res* **42**, 1282-1291
14. Turkish, A. R., Henneberry, A. L., Cromley, D., Padamsee, M., Oelkers, P., Bazzi, H., Christiano, A. M., Billheimer, J. T., and Sturley, S. L. (2005) *J Biol Chem* **280**, 14755-14764
15. Jensen-Pergakes, K., Guo, Z., Giattina, M., Sturley, S. L., and Bard, M. (2001) *J. Bacteriol.* **183**, 4950-4957
16. Li, Y., and Prinz, W. A. (2004) *J Biol Chem* **279**, 45226-45234
17. Raths, S., Rohrer, J., Crausaz, F., and Riezman, H. (1993) *J Cell Biol* **120**, 55-65
18. Fields, S., and Song, O. (1989) *Nature* **340**, 245-246
19. Finley, R. L., Jr., and Brent, R. (1995) Interaction trap cloning with yeast. in *Gene Probes - A Practical Approach*, Oxford University Press. pp
20. Yang, H., Bard, M., Bruner, D. A., Gleeson, A., Deckelbaum, R. J., Aljinovic, G., Pohl, T. M., Rothstein, R., and Sturley, S. L. (1996) *Science* **272**, 1353-1356
21. Suter, B., Kittanakom, S., and Stagljar, I. (2008) *Curr Opin Biotechnol* **19**, 316-323
22. Lewis, T. L., Keesler, G. A., Fenner, G. P., and Parks, L. W. (1988) *Yeast* **4**, 93-106
23. Gulati, S., Liu, Y., Munkacsi, A. B., Wilcox, L., and Sturley, S. L. (2010) *Prog Lipid Res* **49**, 353-365

24. Vaughan, A. M., Tang, C., and Oram, J. F. (2009) *J Lipid Res* **50**, 285-292
25. Lange, Y., Strebel, F., and Steck, T. L. (1993) *J Biol Chem* **268**, 13838-13843

# Chapter 5: Conclusions and Future Studies

## Conclusions

ABC transporters comprise one of the largest paralogous protein families (1). In humans, ABC transporters are involved in a vast array of cellular processes such as nutrient uptake, cell division, and resistance to xenobiotics (2). Mutations in ABC transporters cause or contribute to many different Mendelian and complex disorders including Tangier disease, cystic fibrosis, retinal degeneration, and hypercholesterolemia (3). Regardless of their distance in the evolutionary spectrum and diverse substrate specificity, all ABC transporters share one basic biological function-to harness the energy of ATP binding and hydrolysis to transport a diverse set of hydrophobic molecules across membranes (1). However, direction of substrate transport varies within this superfamily. An ABC transporter may function either as a influx or efflux pump, but no transporter has been identified to function physiologically in both directions (3). Despite their preponderance throughout evolution and their significance to human health the mechanisms that regulate direction of transport and its activity remain elusive (2).

In this thesis I have attempted to define the parameters that influence direction of transport for sterol transporting members of the ABCG subfamily. Members of this subfamily (ABCG1 and ABCG4) are recognized as key components in the mammalian reverse cholesterol transport pathway (4). To date, mammalian ABC transporters are exclusively associated with efflux of cholesterol (3). Contrastingly, in *Saccharomyces cerevisiae*, we have demonstrated that the opposite (i.e inward) transport of sterol in yeast is also dependent on two members of the ABCG subfamily (Aus1p and Pdr11p) (5). As such, I exploit these contrasting states (outward v. inward transport of the same substrate) to dissect whether substrate transport from the plasma membrane is defined by the molecule (i.e. the ABC transporter) or by the microenvironment (i.e. the status of other proteins and lipids) in which it resides.

To begin to answer this question, in Chapter 2 we expressed mABCG1 in budding yeast and assessed transporter activity in varying intracellular sterol environments. We found that in strains with diminished sterol uptake (*aus1Δ*, *pdr11Δ*, and *are1Δ are2Δ*) expression of mABCG1 was able to promote sterol influx (Chapter, Figure 2). Conversely, in an environment of sterol excess (*upc2-1*) mABCG1 was able to decrease intracellular levels (Chapter 2, Figure 3) and promote sterol efflux (Chapter 2, Figure 4B). Moreover, we found that in addition to their established role as influx pumps, Aus1p and Pdr11p contribute to the efflux of a sterol derivative, steryl acetate. A deletion of either *AUS1* or *PDR11* results both in a significant intracellular accumulation and a decrease in the extracellular concentration of cholesteryl acetate (Chapter 2, Figure 4A & B).

Our data collectively shows that changes in the surrounding sterol environment of the transporter can elicit a change in direction of substrate transport. Moreover, this data suggests that direction of transport is not a static property of the transporter but rather can adapt in response to environmental cues. Similarly, expression of mABCG1 in baby hamster kidney cells redistributed membrane cholesterol to cholesterol oxidase-accessible surface domains, which could then either be effluxed to $HDL_3$ or influxed to the esterifying enzymes (6). As such we posit that cholesterol transporting ABC transporters do not possess directionality *per se*, but utilize energy from ATP hydrolysis to redistribute membrane cholesterol in order to enhance its rate of projection from the membrane. However, the observation that ABC transporter mediated cholesterol movement does indeed modulate direction in response to the cellular environment can't be ignored. We propose that direction of transport is dictated by cellular cues, specifically, by the balance of extracellular and intracellular protein/lipid acceptors. Interestingly, in baby hamster kidney cells the proportion of free cholesterol imported to the ACATs decreased in the presence of $HDL_3$ (6). This suggests that the presence of $HDL_3$ tipped the direction of transport towards efflux. Identifying the intracellular and extracellular acceptor molecules will be

paramount in understanding how these ABC transporters maintain cholesterol homeostasis.

In *Saccharomyces cerevisiae* and in baby hamster kidney cells, sterols transported by members of the ABCG subfamily serve as a substrate for ACAT1 (6,7). Moreover, studies presented in Chapter 2 demonstrated that the absence of the esterifying enzymes affects transport activity of both mABCG1 and its budding yeast orthologs. Therefore, we propose that ACAT1 may act as a putative intracellular acceptor molecule for these ABC transporters. In order to further expound on this hypothesis, in Chapter 3 we performed a membrane split ubiquitin yeast two hybrid to identify protein interactors of Are2p. As a result of our screen and subsequent viability assays we discovered nine putative Are2p interacting proteins (Chapter 3, Table 2) and established a previously uncharacterized role for them in mediating sterol homeostasis. Interestingly, amongst these hits we identified Pdr11p, as a putative interactor of Are2p (Chapter 3, Table 2). This suggested that the plasma membrane ABC transporter participates in a protein complex that directly transfers sterols to the ACAT enzymes.

In chapter 4, we performed a series of assays to confirm the physical interaction of Are2p and Pdr11p, as well as explore its physiological implications. By crosslinking and co-immunoprecipitation assays, we confirmed that that both Aus1p and Pdr1p physically interact with the esterifying enzyme, Are2p (Chapter 4, Figure 6). We also demonstrated that Are2p, Aus1p, and Pdr11p co-localized to the endoplasmic reticulum (Chapter 4, Figure 5) and the plasma membrane (Chapter 4, Figure 4) in cold detergent resistant membrane microdomains (DRMs) (Chapter 4, Figure 7A). This therefore suggests that DRMs may provide a platform that integrates the sterol influx and esterification pathways in yeast. Interestingly, a deletion of either ABC transporter significantly altered Are2p localization from a DRM to a detergent soluble fraction (Chapter 4, Figure 7B), suggesting that Are2p's physical interaction with the ABC transporters is necessary for its DRM localization. We speculate that this shift in localization

may contribute to the decrease in the percent of esterification associated with a deletion of *AUS1* or *PDR11* (Chapter 3, Figure 3). Based on these data we propose that sterol transfer in the cholesterol esterification pathway occurs as a consequence of a physical interaction of Aus1p, Pdr11p, and Are2p in a DRM fraction.

The studies presented in this thesis attempt to elucidate the role of ABCG1 and its budding yeast orthologs in maintaining sterol homeostasis. Collectively, these studies demonstrate that direction of ABC mediated transport is not a inherent property of the transporter, but rather it is modulated by the presence of lipid and protein acceptors. The data provided here offers further insight as to how ABC transporters move cholesterol from the membrane and therefore may provide a platform for innovative strategies to combat atherosclerosis.

**Future Studies**

In Chapter 2, we demonstrated that direction of ABC mediated transport is not an inherent property of the transporter but rather dictated by cues in the microenvironment. Studies in baby hamster kidney cells showed that sterols transported by ABCG1 can be shuttled intracellularly to the ACATs or extracellularly to $HDL_{3(6)}$. Furthermore, the presence of the extracellular acceptor promoted efflux of sterols and diminished sterol transfer to the ACATs(6). To firmly establish if direction of transport is dictated by the presence of acceptor molecules, I propose to express mABCG1 in budding yeast and supply various exogenous acceptors ($HDL_3$ or BSA) in increasing doses and measure esterification of sterols. If acceptor molecules dictate direction I hypothesize that as we increase the concentration of exogenous acceptors we should see a concurrent decrease in sterol esterification. By being able to define how ABC transporter mediated cholesterol flux is modulated, we may be able provide insight as to how to prevent and treat such diseases as atherosclerosis.

Another key finding of this chapter was that Aus1p and Pdr11p contribute to the export of cholesteryl acetate. However, the mechanism by which sterols

reach the acetylating enzyme, Atf2p at the ER remains elusive. Cholesterol acetylation and its subsequent export represents an alternate cholesterol detoxification pathway (8). In order to assess if Aus1p and Pdr11p also directly transfer sterol to this detoxification pathway, I propose a cross-linking and co-immunoprecipitation assay. If we are able to demonstrate a physical interaction between these proteins, I would then assess if this interaction occurs in DRMs. This finding would further demonstrate the DRMs play a key role in sterol transport and its homeostasis.

In chapter 3, we identified nine putative Are2p interacting proteins. Interestingly, two of these genes, *COS8* and *MFB1* produced synthetic lethal phenotypes with *are1Δ are2Δ* in myriocin and tunicamycin respectively. As a result, these proteins in particular warrant follow up experiments to confirm their physical interaction and investigate the physiological implications of these interactions. Therefore, initially I would propose performing a co-immunoprecipitation assay with both of these interactors.

In chapter 4, we confirmed that Aus1p and Pdr11p physically interact in with Are2p in DRMs and that loss of this interaction has a significant impact on sterol homeostasis. Furthermore, we were able to demonstrate that this phenomenon is evolutionarily conserved, by showing that mABCG1 and mACAT1 also co-localizat to DRMs in murine lung. However, in order to prove that mABCG1 and mACAT1 form a complex in an analogous fashion to their budding yeast orthologs, a co-immunoprecipiation assay will be done. It would also be interesting to assess if ACAT interaction is specific to ABCG1 or extends to other sterol transporting ABC transporters, such as ABCA1 or ABCG5/G8. Studies such as these will further our understanding of the mechanisms underlying sterol homeostasis and the pathophysiologies that occur as a result of its disruption.

**References:**


1. Moitra, K., and Dean, M. (2011) *Biol Chem* **392**, 29-37
2. Gottesman, M. M., and Ambudkar, S. V. (2001) *J Bioenerg Biomembr* **33**, 453-458
3. Rees, D. C., Johnson, E., and Lewinson, O. (2009) *Nat Rev Mol Cell Biol* **10**, 218-227
4. van der Velde, A. E. (2010) *World J Gastroenterol* **16**, 5908-5915
5. Gulati, S., Liu, Y., Munkacsi, A. B., Wilcox, L., and Sturley, S. L. (2010) *Prog Lipid Res* **49**, 353-365
6. Vaughan, A. M., and Oram, J. F. (2005) *J Biol Chem* **280**, 30150-30157
7. Li, Y., and Prinz, W. A. (2004) *J Biol Chem* **279**, 45226-45234
8. Tiwari, R., Koffel, R., and Schneiter, R. (2007) *EMBO J* **26**, 5109-5119